AJUR

American Journal of *Undergraduate Research*

Volume 16 | Issue 3 | December 2019

www.ajuronline.org

Print Edition ISSN 1536-4585
Online Edition ISSN 2375-8732

AJUR
American Journal of
Undergraduate Research

Volume 16 | Issue 3 | December 2019 *www.ajuronline.org*

American Journal of Undergraduate Research (AJUR) *is a national, independent, peer-reviewed, open-source, quarterly, multidisciplinary student research journal. Each manuscript of AJUR receives a DOI number. AJUR is archived by the US Library of Congress. AJUR was established in 2002, incorporated as an NFP in 2018. AJUR is indexed internationally by EBSCO and Crossref with ISSNs of 1536-4585 (print) and 2375-8732 (web).*

SPECIAL THANKS

AJUR is made possible through the volunteer efforts of our editorial team and assistance of our sponsors.

We thank our sponsors:

OSWEGO
STATE UNIVERSITY OF NEW YORK

Please support undergraduate research
Request sponsorship information from *editor@ajuronline.org*

Women in Higher Educational Leadership: Representation, Career Progression, and Compensation

Carla Cañas, Caitlyn Keeve, Carmen Ramos, Jocelyn Rivera, & Michelle L. Samuel

Department of Psychology, Mount Saint Mary's University, Los Angeles, CA

https://doi.org/10.33697/ajur.2019.026

Students: carlcana6012@msmu.edu, caitkeev@msmu.edu, carmramo7577@msmu.edu, jocerive5909@msmu.edu*
Mentor: msamuel@msmu.edu

ABSTRACT

Men in university administration repeatedly outnumber women in leadership positions. The problem under investigation is that this gender gap exists due to barriers to advancement and discrimination in both the hiring process and in the workplace. With less representation of women in higher education leadership, there is a higher risk of bias for women in this field. This study used an ex-post facto methodology and gathered public data from the University of California (UC) Annual Payroll Compensation database. Three separate studies were run to determine the level of gender differences in the representation of educational leaders, compensation, and career progression. Significant differences in gender equity existed, with more men represented at several levels of educational leadership. Significant differences were also found in compensation levels, where men earned more money than women in the same position. Lastly, a small effect, although not significant, was observed when comparing early career gender representation to non-early career gender representation. There are more women recent graduates than men in leadership positions. Together these results suggest that while there are gender gaps in representation and compensation, there may be slow progress towards better representation in early career leadership positions in the UC system. The implication of this research supports further research into factors which impact the compensation of women leaders in academia. Higher education hiring professionals and candidates for leadership positions could benefit from further development of theories around gender equity and representation.

KEYWORDS

Gender Representation; Gender Equity; Higher Educational Leadership; Women; Higher Education; Psychology; Wage Gap; Higher Education Administration

INTRODUCTION

Today, there are a variety of obstacles that stop women from achieving parity in the workforce. Occupational sex segregation paired with a male dominated work environment are two key barriers that affect women's advancement vertically and horizontally in the corporate arena.[1] As a result, research has shown that women in fields where they are the minority, demonstrate higher levels of resilience as it relates to their careers including within the field of higher education leadership.[2] That is, women progress in the field even though they lack representation. This study uses three analyses to further explore this idea. The problems under investigation are how women in higher educational leadership are represented, how this affects compensation, and how they progress in their careers. The method of study is an ex-post facto design that uses the UC Annual Wage database to identify inequities between women and men leaders within the UC System.[3]

While 58.2% of the United States workforce are women, they are still unequally represented in most fields.[3] In 2016, more than 40% of women in the labor force obtained college degrees.[4] As of 2017, 30% of university presidents in the United States were women.[5] Given the national disparity of women's representation in the higher educational leadership, one study sought to see how their university stacked up. Researchers initiated an audit for their large university to assess the representation of women and men in their senior decision-making committees.[6] A base line measurement was taken across committee groups, followed by a proposed initiative to implement parity between men and women leaders on the committee. After one year, the effectiveness of the initiative was measured. The study found some improvements towards gender equity in faculty-based groups however, other groups remained the same. A greater proportion of women were found at the lower academic staff levels and a greater proportion of men were staffed at the higher levels within the faculty of Medicine, Dentistry and Health Science

school leadership committees. Within this professional staffing sample, the findings indicated greater proportions of women in all categories except at the highest levels.

Just why does this gender representation gap exist? The shortage of women in higher education leadership roles has been problematized in literature, suggesting that women lacked characteristics which led to advancement.[7] However, some believe that universities are the issue instead.[8] Higher education scholars in a qualitative study found that the work environments women were in, did not encourage them to become leaders or to build up their careers. Several women discussed that they had to adapt to the "entrenched masculine culture" within a department that was not accommodating to all genders.[8] Current research shows that men and women do not differ in their desire to advance their careers in higher education administration, but that there are a variety of barriers that prevent women from advancing towards senior leadership.[8] Factors that affect women's advancement include work relationships, environment, invisible rules, proactivity, and personal circumstances.[9] These factors show that women face more external than internal hurdles that prevent them from advancing within their careers.

Consequentially, women's advancement to higher positions within universities are hindered despite more women receiving post-secondary degrees.[8] This suggests that while there are many qualified women to progress into leadership positions, the larger issue is systemic. A 2015 study found that there was a higher proportion of women in lower-level administration when compared to higher levels.[6] While there are women who rank higher than their male colleagues, the study found that this was not often the case in higher education administration.

To combat this phenomenon the University of California (UC) System has made strides to maintain and increase faculty equity among its ten campuses, such as raising funding to expand and create programs which increase faculty diversity. The UC President delivered a press release stating that 44.1% of new ladder-rank hires were women and 17.1% came from minority groups.[10] These advances are good, but do not eliminate the overall issue of gender and wage disparities. In California, the average salary for women in 2017 was $45,489, while the average for men was $58,225, which supports the claim for a gender pay gap of $12,736.92 between women and men.[3] In comparison to other states, California ranked #1 for the narrowest gender wage gap in 2018.[11] This may be due to the strength of equal pay laws within the state. New York, a state with a similar infrastructure was also ranked highly in third place, whereas states with weak equal pay laws such as Texas ranked lower in twenty-second place. Because women are amongst all high-ranking positions in academia, including Chancellor, Provost, and Dean in the University of California school system, compensation is an important aspect of their experience to explore.

To investigate how women in higher education leadership roles are represented, how they progress in their career, and how they are compensated, three studies were conducted by the authors. Each study had its own unique hypothesis.

Study 1- Gender Representation in UC Higher Educational Leadership: Is there a significant difference in representation between men and women in higher education leadership roles? It was hypothesized that a significant difference in representation between men and women in higher education leadership roles would occur.

Study 2- Gender Differences in UC Higher Educational Leadership Compensation: Are women leaders at UC institutions compensated the same as their male colleagues in a comparable position? It was hypothesized that women leaders at the University of California (UC) institutions were compensated less than their male colleagues in the same position.

Study 3- Gender Differences in Early Career and Non-early Career Professionals: Is there a significant difference in the proportion of early-career professionals versus non-early career professionals between men and women in higher educational leadership? It was hypothesized that women who recently began their career hold a majority of higher education leadership positions when compared to men in early-career professions.

METHODS AND PROCEDURES

The study utilized an ex-post facto design where publicly available data were analyzed to identify gender differences in representation, compensation, and career trajectories of leaders in the UC system.[12] The method for the study applied the UC Annual Payroll Compensation public database to collect and analyze data from a sample size of 424 chancellors, vice chancellors, provosts, associate, assistant and divisional deans. Participants were from ten public four-year institutions within the UC system. These positions were selected from organizational charts found on the University of California Office of the President website which is maintained by the President's Executive Office. The website offered a link to each school's organizational chart. The authors included the positions mentioned above as they were found in all ten universities and listed based on role importance and size. The role of the president was omitted because one woman fulfills this role, therefore making dichotomous gender comparisons impossible. After gathering data from the public database, the data were split among the researchers, who looked for missing variable information in online school biography statements. Data was compiled, coded, and analyzed using SPSS. Each study had no significant missing data, however, the total sample sizes of all three studies vary slightly.

Gender Representation in UC Higher Educational Leadership

A quantitative study with one dichotomous variable, gender, and one nominal variable with ten levels (chancellors, executive vice chancellor and provost, vice chancellor, assistant vice chancellor, college provost, vice provost, dean, associate dean, assistant dean, Senior VP and Senior VC) was done.

Gender Differences in UC Higher Educational Leadership Compensation

A 2x7 design was used in this quantitative study. The two independent variables examined were gender (men and women) and leadership position (chancellor, vice chancellor, divisional dean, vice provost, associate dean, assistance vice chancellor, and assistant dean). One hundred and eighty-two women respondents (*M*= $232,692.82, *SD*= $124,271.48) and 233 men respondents (*M*= $277,656, *SD*= $154,805.87) comprised the sample. Please see **Figure 1** for a graph of the average salaries by gender in higher educational leadership positions within the UC system.

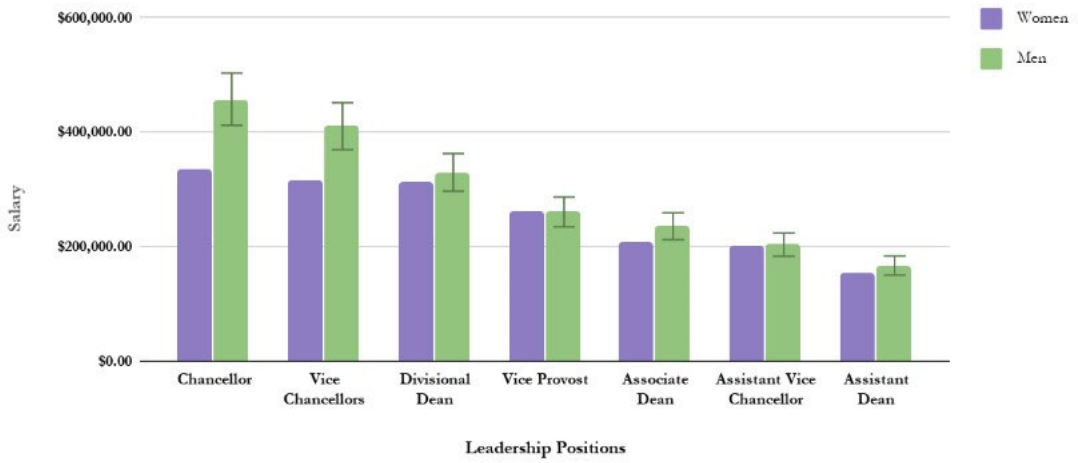

Figure 1. The graph above depicts average salaries by gender in higher education leadership: UC System

Gender Differences in Early Career and Non-early Career Professionals

This study followed a quantitative design with two dichotomous variables: gender and years since terminal degree. Terminal degree year determined whether a participant was an early career or non-early career professional. The year 2007 was set as the cut-off for consideration as an early career professional, requiring professionals in the sample to have 10 years or less since their terminal degree.[13] Participants who received their terminal degree before 2007 were considered non-early career professionals. A total of 330 participants were used in this study. There were 194 men and 136 women in this study, where 307 were non-early career professionals and 23 were early career professionals. See **Figure 2** for additional demographic details.

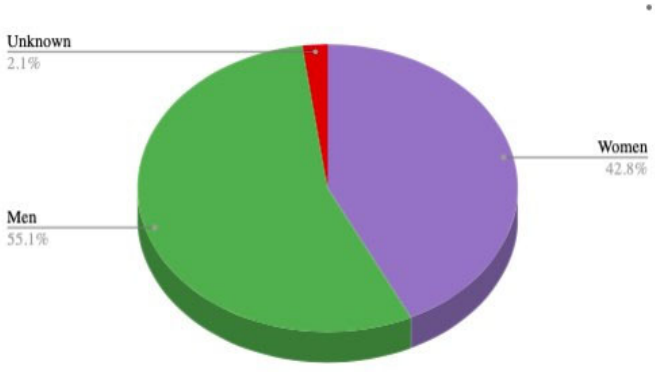

Figure 2. Pie chart of women and men participants

RESULTS

Gender Representation in UC Higher Educational Leadership

To summarize the data, a frequency analysis was performed. This resulted in 181 women and 233 men for a total of 414 participants. For the frequency of how many men and women were in each corresponding leadership position, refer to **Figure 3**. A chi-squared analysis was performed to examine the relationship between gender and leadership position. Analyses revealed there was a statistically significant difference between the representation of men and women in higher education leadership roles, chi-squared (9, *N*=414, p=.002) suggesting that men are frequently more represented in these positions than women are. A phi coefficient was calculated to assess the strength of this relationship: phi=.253. This corresponds to a medium-size effect. The analyses resulted in rejecting the null hypothesis.

Gender Differences in UC Higher Educational Leadership Compensation

A two-way ANOVA was used to compare mean salaries of men and women in the same position. The simple main effect of gender on salary was statistically significant (F (1, 412) = 6.839, p=.009). The main effect of leadership title on salary was also statistically significant, (F (7, 412) = 14.921, p=.000) and these null hypotheses were rejected. The interaction between the effect of both gender and leadership title on salary was not statistically significant, (F (7, 412) = .91, p=.503), but a partial eta-squared statistic did indicate a small effect size (partial eta-squared=0.018). In a power analysis, the interaction had a power less than .80, which suggested that the sample size was too small to detect real differences if they existed.[14] According to the data, out of the seven ranks, six of them had mean differences where men earned more. For example, women chancellors (*M* =$336,774.50, *SD*=$103,457) made less than chancellors who were men (*M*=$457,761.00, *SD*= $177,828.73), while women divisional deans (*M*=$314,377.04, *SD*=$155,239.90) on average were compensated $15,279 less than division deans who were men (*M*= $329,656.92, *SD*=$126,373.58). Please see **Figure 1** for additional gender wage disparities.

Gender Differences in Early Career and Non-Early Career Professionals

A chi-square analysis was used to see if there was a significant relationship in the frequencies within gender and early versus non-early career professionals. There was a significant relationship between early career professionals and non- early career

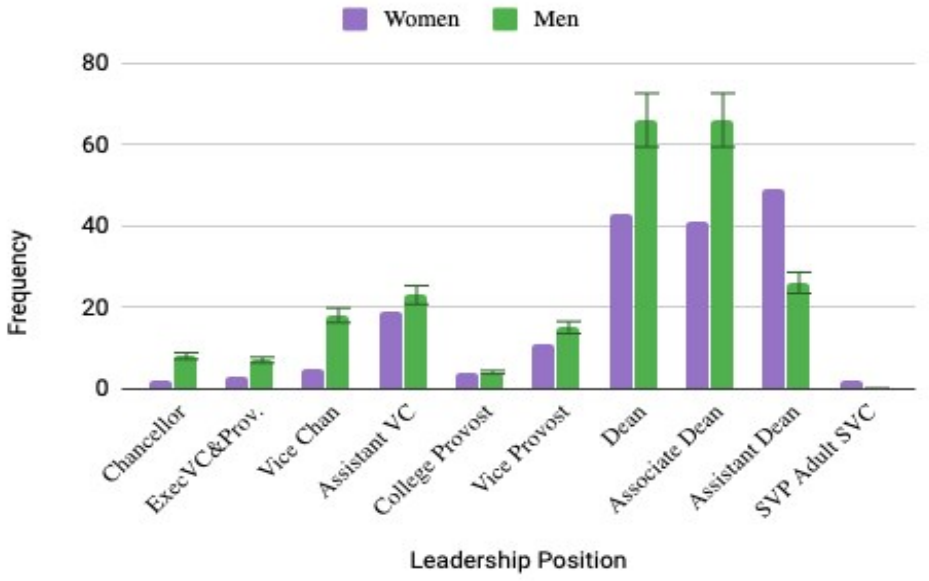

Figure 3. Frequency of men and women in each position

professionals, chi squared (1, *N* = 330) = 272.7, p = .000, phi = 0.90, therefore rejecting the null hypothesis, with a large effect size. There was also a significant relationship within gender, chi squared (1, *N* = 415) = 6.27, p = .012, therefore rejecting the null hypothesis, with a small effect size. However, there was not a significant difference in frequency when these two variables were combined, chi squared (2, *N* = 330) = 2.39, p = .122, phi = .085, showing a small effect size. This suggests that while there are significant differences in the frequency of gender and career level, there is not one for men and women at the non-early career level nor between men and women at the early career level. There are slightly more women at the early career level and more men at the non-early career level. Although this is non-significant, the percentage of women being hired at the early career level is higher than at the non-early career level. Please see **Figure 4** for the frequency of career levels and gender.

DISCUSSION

Together these three studies suggest that gender disparities still exist in the leadership of the UC system. These differences under investigation exist in California, the state that holds the narrowest gender wage gap.[11]

Gender Representation in UC Higher Educational Leadership

There are a wide variety of factors that contribute to the lack of gender parity within higher educational leadership. For starters, researchers argued that the structure of higher education institutions often reflect gendered values and trends.[15] It was also found that many women fail to progress through the academic hierarchy when compared to their male counterparts over time. Analysis of women in higher education leadership roles in Australia demonstrate a higher proportion of women in lower ranks, estimating about only 11% of women in the country being full professors.[16] This suggests that women want to be in higher education leadership roles, however they face hurdles when advancing in their careers. Additionally, researchers found that the women they interviewed felt they had to navigate a "masculine context" in which their university leadership operated and therefore adapt to overcome obstacles to excel and fit into leadership positions.[7] This means that for women leaders to succeed in university administration, they often have to conform to the masculine norms already in place.

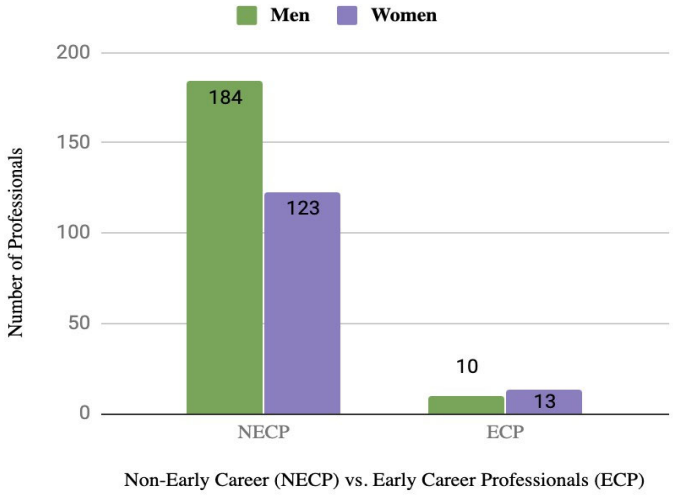

Figure 4. Distributions of Non-Early and Early Career Professionals by Gender

Along with patriarchal and structural conditions, another common obstacle identified was a lack of women mentors during women's ascension to higher leadership positions.[17] In a study analyzing the gender differences in perceptions of STEM workplace climates, it was found that 18% of the total participants indicated having a mentor, while 58% of those were men and 38% were women.[18] Without access to representative mentorship, women in higher education administration are often left to navigate through the academic hierarchy on their own.

Although progress has been made, obstacles still exist for women leaders in university administration today. For example, gender impacts the perception of leadership abilities, professional relationships, and personal relationships in women college presidents.[19] The results of this study indicated that 61% of participants felt that their gender contributed to feelings of isolation within the institutional setting and 53% of participants agreed that perceptions of gender affected their ability to influence or "restructure" the institution overall. This shows that issues arise due to gender even for those women who can make it to the top of their field. Additionally, personal obstacles have been found to affect women more than men. A study done by the Department of Political Science at the University of Colorado argued that women in managerial positions have higher levels of work-family conflict that can be associated with health issues, problems with drinking, and high stress levels.[20] The results from this four-year study determined that women leaders in managerial positions experienced more work-family conflict and health risks as compared to men in the same positions.

The results from the current study are in alignment with several other research studies on the gender gap in professional leadership roles. Another recent study aimed at finding the reasons behind the gender gap created three models to explain women's under representation.[21] The individual, or meritocracy model, explained that women were the cause for their under representation; that the university's perspective was that women were not assertive enough or did not possess enough desire for higher positions, causing the gender gap. The second model is the organizational or discrimination model, which detailed that

the educational system and its practices that discriminated against women in higher positions were to blame for the under representation. Lastly, the "women's place or social model" detailed society's norms and the socialization patterns of women and men; thus, seeing more men hold higher roles than women.

An additional study identified social constructs as barriers to women in higher education leadership. The author argued that the representation of women at senior academic levels have not yet achieved the same numbers as male colleagues in these positions despite the existence of various equity programs in universities.[22] A solution for this issue is that academic women need to challenge these hierarchical relations. This could be done by addressing the societal opposition between work and family, passing the challenge on to the next generation, and exposing gendered career structures.

Gender inequity is a prevalent issue in higher education administration today. Although some progress has been made, much more needs to be achieved to level out the playing field between men and women in university administration leadership. This research can be used to help public and private colleges and institutions develop policies to combat this issue and help address the systemic barriers that exist for women looking to advance in higher education careers.

Gender Differences in UC Higher Educational Leadership Compensation

These findings are consistent with recent research on California's compensation of women and men across industries. In 2017 there was an average wage gap between employed men and women in California of over $12,000; the results of our study indicate an average disparity of over $50,000 where men are the higher earners, supporting the argument that income is largely dependent on industry and sample size.[23] While some argue that pay discrimination between genders is decreasing, it has been found that education as a career field in the public sector allows for greater "bureaucratic regulation" or systematic and formalized criterion for compensation than the private sector.[24] This could also be due to a perceived superior level of transparency that public education models as an employer, where private sectors report compensation less often.

Compensation as a tool for a better quality of life can be used to assess the lasting effects of the gender wage gap. According to the National Institute of Retirement Security, women are 80% more likely than men to live in poverty at the age of 65 and three times more likely once they reach 75.[25] In careers where women earn less than men, a cycle of saving less while living longer persists. It's important to see the pattern of wage distribution over the lifespan and between genders because of its effects on wellbeing and ability to reach retirement. Women over the age of thirty report the highest difference in salary from men over thirty, with absence from the workforce due to childbearing and less years of experience as two contributing factors.[23] Theoretically, all people should earn more as they advance in their careers, however, there is evidence to support that women's salaries often stagnate in competitive environments while men's continue to increase.[26, 27] The effects of salary on women in higher education leadership reinforce economic and cultural insecurities about money and financial independence.

There are consequences of a gender wage gap that reach beyond the seven administrative positions analyzed in this study. Inequities in compensation between men and women in leadership positions are also shown to have adverse effects on the salaries and experiences of women in lower level teaching positions as well.[28] While location and academic discipline were not reviewed in this study, in support of the hypothesis, some factors that influence salary include years of experience and administrative positions. The data indicated that women occupied both the highest, the president, and the least compensated administrative position, assistant dean, in the UC system. As a result, the gender wage gap was identified as a structural element that impacted all leadership levels differently. This public data can be used as a key source for candidates of leadership positions in higher education to participate in salary negotiations and continue to be informed individuals. Similarly in other industries like politics and public service, where women face unfair biases in campaigns and distorted media coverage, scientific approaches to the disparity could lead to changing perceptions of women leaders.[29] The implication of this research supports further research into various factors that impact the compensation of women leaders in academia across the country and to women leaders beyond education.

Hiring professionals and candidates for leadership positions could benefit from further development of theories around gender equity in the workplace. One limitation to this study was that there were more men (56%) than women (44%) in the sample size, which contributed to the increased mean representing men's salaries in the UC system.

Gender Differences in Early Career and Non-Early Career Professionals

The results suggest that more early career professional women were hired than early career professional men, although this difference was not statistically significant. While this study did not test the effectiveness of programs structured to increase faculty equity, there are several possible factors that explain why more women are present among early career professionals than men.[30] One possible factor, is the President's Postdoctoral Fellowship Program which was initiated by the UC president to help women get into tenure-track positions at any of the general UC campuses.

The cornerstone of the President's Postdoctoral Fellowship Program is the accessibility to mentorship it provides to participants. Having a mentor gives women a push in climbing up the academic ladder since having an individual with power who can vouch for a rising academic professional can make a difference.[25] A mentor can direct their mentees to leadership development opportunities and other professionals in the field. Studies show that women leaders are viewed as more authentic by women peers.[31] This suggests that in some cases a woman having a mentor of the same sex can be more beneficial than having a mentor of the opposite sex. As part of the President's Postdoctoral Fellowship Program, UC President Janet Napolitano gave five million dollars to continue a salary hiring incentive and to begin an incentive to hire current and former UC President's and Chancellor's postdoctoral fellows. The office of the UC President released statements on the program stating that sixteen out of fifty-eight fellows have been hired in the same campus in which they were fellows.[10] This initiative shows that programs can help reach faculty gender-equity, by giving women academic professionals somewhere to start.

Leadership development programs in partnership with women's centers can help women build a professional network and self-confidence.[9] Participants stated that the program gave them a space to develop their identities as professionals and normalize concerns about the workforce. Programs directed toward developing leadership skills in women are essential because they provide a shared space to talk about the experience's women face as potential academic professionals.

CONCLUSIONS

Limitations of this study include missing information concerning age, ethnicity, and academic discipline that were examined. It is essential to acknowledge that despite the progress that has been made in addressing the gender gap that exists in the workplace, there are still many fields in which men disproportionately outnumber women. This study only considers whether individuals are a non-early career or early career, versus looking at their entire progression up the administrative ladder, due to the data being from a single year. Future studies should follow professionals throughout their academic career to clarify the difference, if any, of the patterns of advancement and the amount of time it takes to advance between the genders.

The study also used the year in which individuals attained their terminal degree rather than the year they were hired. Future studies should address this limitation and look at gender disparity in hires among different departments. Additionally, the hiring practices different departments within the UC System use should also be taken into consideration.

The purpose for this study was to gain a better understanding of gender representation, compensation, and career progression in higher education leadership positions within 10 schools in the UC system. This study contributed to the existing research on women in higher educational leadership and provided an understanding of the gender gap within one of the largest higher education systems in the state of California. Logical extensions of this research could include investigating other higher education systems in other states; particularly in states with wider gender wage gaps than California. Results from this study suggest that gender inequity in higher education leadership is still a pervasive issue.

REFERENCES

1. Kalev, A., and Deutsch, G. (2018) Gender inequality and workplace organizations: Understanding reproduction and change, in *Handbook of Sociology and Gender*, (Risman B., Froyum C., and Scarborough W. Eds.) 2nd ed., 257–269. Springer Cham, New York. *https://doi.org/10.1007/978-3-319-763330_19*
2. Isaacs, A. J. (2014) Gender differences in resilience of academic deans, *Journal of Research in Education*, 24(1), 112–119. *https://files.eric.ed.gov/fulltext/EJ1098305.pdf* (accessed Feb 2019)
3. U.S. Census Bureau, American community survey 5 year-estimate, *https://datausa.io/profile/geo/california/* (accessed Feb 2019)
4. Bureau of Labor Statistics, Labor Force Statistics from the Current Population Survey, *https://www.bls.gov/cps/demographics.htm* (accessed Jan 2019)
5. American Council on Education's Center for Policy Research and Strategy, Women Presidents Profile, *https://www.aceacps.org/women-presidents/* (accessed Mar 2019)
6. Johnson, K. A., Warr, D. J., Hegarty, K., and Guillemin, M. (2015) Small wins: An initiative to promote gender equity in higher education, *Journal of Higher Education and Management* 37, 689–701. *https://doi.org/10.1080/1360080X.2015.1102820*

7. Burkinshaw, P., and White, K. (2017) Fixing the women or fixing universities: Women in higher education leadership, *Administrative Sciences*, 7(30), 1–14. *https://EconPapers.repec.org/RePEc:gam:jadmsc:v:7:y:2017:i:3:p:30-:d:109122* (accessed Feb 2019)

8. Lepkowski, C. (2009) Gender and the career aspirations, professional assets, and personal variables of higher education administrators, *Advancing Women in Leadership Journal*, 27(6), 1–15. *https://doi.org/10.18738/awl.v29i0.284*

9. Bonebright, D. A., Cottledge, A. D., and Lonnquist, P. (2012) Developing women leaders on campus: A human resources-women's center partnership at the University of Minnesota, *Advances in Developing Human Resources*, 14(1), 79–95. *https://doi.org/10.1177/1523422311429733*

10. University of California, About President's Postdoctoral Fellowship Program, *https://ppfp.ucop.edu/info/about-ppfp/index.html* (accessed Feb 2019)

11. American Association of University Women (AAUW), The gender pay gap by state: An interactive map, *https://www.aauw.org/resource/gender-pay-gap-by-state-and-congressional-district/* (accessed Jan 2019)

12. UC Office of the President, University of California employee pay, *https://ucannualwage.ucop.edu/wage/(*accessed Jan 2019)

13. American Geophysical Union, Career stages and other terms definitions, *https://honors.agu.org/career-stages-andother-terms-definitions/*(accessed Feb 2019)

14. Cohen, J. (1992) Statistical Power Analysis, *Current Directions in Psychological Science*, 1(3), 98–101. *http://www.jstor.org/stable/20182143* (accessed Feb 2019)

15. Maphalala, M., and C. Mpofu, N. (2017) Are we there yet? A literature study of the challenges of women academics in institutions of higher education, *Gender Behavior*, 9245–9253. *https://www.researchgate.net/publication/318455987_Are_we_there_yet_A_literature_study_of_the_challenges_of_women_academic_in_institutions_of_higher_education*

16. White, K. (2004) The leaking pipeline: Women postgraduate and early career researchers in Australia, *Tertiary Education and Management*, 10(3), 227–241, *https://doi.org/10.1080/13583883.2004.9967129*

17. Ballenger, J., and Stephen, F. (2010) Women's access to higher education leadership: Cultural and structural barriers, *Forum on Public Policy Online: A Journal of the Oxford Round Table* 5, 1–20. *https://files.eric.ed.gov/fulltext/EJ913023.pdf* (accessed Mar 2019)

18. Riffle, R., Schneider, T., Hillard, A., Polander, E., Jackson, S., Des Autels, P., and Wheatly, M. (2013) A mixed methods study of gender, STEM department climate, and workplace outcomes, *Journal of Women and Minorities in Science and Engineering,* 19(3), 227–243. *https://doi.org/10.1615/JWomenMinorScienEng.2013005743*

19. Caton, M. T. (2007) Common trends in U.S. women college president issues, *Forum on Public Policy* 3, 1–26. *https://www.semanticscholar.org/paper/Common-Trends-in-U.S.-Women-College-President-Caton/7b3933b2b66f5692b6080973edbd40091c74b8db#citing-papers* (accessed Feb 2019)

20. Apperson, M., Schmidt, H., and Moore, S., Grunberg, L. (2002) Women managers and the experience of work-family conflict, *American Journal of Undergraduate Research*, 1(3), 9–16. *https://doi.org/10.33697/ajur.2002.020*

21. Growe, R., and Montgomery P. (1999) Women and the leadership paradigm: Bridging the gender gap, *National Forum Journal* 17, 1–21. *https://www.researchgate.net/publication/242783132_Women_and_the_leadership_paradigm_bridging_the_gender_gap* (accessed Feb 2019)

22. White, K. (2003) Women and leadership in higher education in Australia, *Tertiary Education and Management*, 9(1), 45–60. *https://doi.org/10.1080/13583883.2003.9967092*

23. Archer, E. (2018) A closer look: Establishing the gender pay gap, *The Report on the Status of Women and Girls in California*, 16–17, *https://www.msmu.edu/media/website/content-assets/msmuedu/home/academics/financial-aid/documents/StatusOfWomenCA2018_WEBFINAL[5].pdf* (accessed Feb 2019)

24. Mandel, H., and Semyonov, M. (2014) Gender pay gap and employment sector: Sources of earnings disparities in the United States 1970–2010, *Demography*, 51(5), 1597–1618. *https://doi.org/10.1007/s13524-014-0320-y*

25. Brown, T. M. (2005) Mentorship and the female college president, *Sex Roles*, 52(9), 659–666. *https://doi.org/10.1007/s11199-005-3733-7*

26. Gneezy, U., and Rustichini, A. (2004) Gender and Competition at a Young Age, *American Economic Review*, 94 (2), 377–381. *https://doi.org/10.1257/0002828041301821*

27. Niederle, M., Vesterlund, L. (2008) Gender differences in competition, *Negotiation Journal*, 24(4), 447–463. *https://doi.org/10.3386/w13727*

28. Cohen, P. N., and Huffman, M. L. (2007) Working for the woman? Female managers and the gender wage gap, *American Sociological Review*, 72(5), 681–704. *https://doi.org/10.1177/000312240707200502*

29. Bjerre, K. (2018) The role of gender stereotypes in gubernatorial campaign coverage. *American Journal of Undergraduate Research*, 15(1), 55–69. *https://doi.org/10.33697/ajur.2018.012*

30. UC Office of the President, UC launches major push to increase faculty diversity. *https://www.universityofcalifornia.edu/press-room/uc-launches-major-push-increase-faculty-diversity* (accessed Jan 2019)
31. Tibbs, S., Green, M. T., Gergen, E., and Montoya, J. A. (2016) If you are like me, I think you are more authentic: An analysis of the interaction of follower and leader gender, *Administrative Issues Journal: Connecting Education, Practice, and Research*, 6(1), 118–133. *https://eric.ed.gov/?id=EJ1104359*

ABOUT THE AUTHORS

Carla Cañas graduated from Mount Saint Mary's University, Los Angeles in May 2019 with her B.A. in Psychology. She is currently working as a research assistant at the Keck School of Medicine of USC in a preventive study for Alzheimer's disease. She wishes to pursue her Ph.D. in neuropsychology and become a University professor and researcher in the future.

Caitlyn Keeve completed this manuscript as a junior at Mount Saint Mary's University, Los Angeles. She will graduate with a B.A. in Psychology with an emphasis in research Fall 2019. After graduation, she plans to pursue a Ph.D. in Social Psychology. Her goal is to become a published author and a University professor in the future.

Carmen Ramos completed this manuscript as a junior at Mount Saint Mary's University. She will graduate with a B.A. in Psychology in the spring of 2020. Her future education plans include obtaining a graduate degree in industrial/organizational psychology.

Jocelyn Rivera graduated from Mount Saint Mary's University in December 2018 with her B.A. in Psychology. She is currently working as a Registered Behavior Technician to help children with autism and other developmental delays. She plans to obtain a graduate degree in Behavior Analysis and become a Board-Certified Behavior Analyst.

Michelle L. Samuel is an Assistant Professor of Psychology at Mount Saint Mary's University. She has an M.A. in General Experimental Psychology and is pursuing a Ph.D. in Higher Education Administration. She will investigate gender differences in academic leadership for her dissertation.

PRESS SUMMARY

This research investigates the representation, career progression, and compensation disparities of women in higher education leadership when compared to men. Significant differences in gender equity among deans, chancellors, and provosts in the University of California system were found in this analysis. With more men represented at several levels of educational leadership, a gender wage gap also revealed that men earned more money than women in the same administrative position. When comparing early-career women to non-early career, the percentage of women being hired at the early-career level is higher than later in their careers. This study contributes to the existing research on women in higher education leadership and provides an understanding of the gender gap within one of the largest higher education systems in the state of California.

Anisotropic Behavior of Ultrasonic Waves in 3D Printed Materials

Edward Alexander[a] & Gordon D. Hoople[b]*

[a]Department of Mechanical Engineering, Shiley-Marcos School of Engineering, University of San Diego, San Diego, CA
[b]Department of Integrated Engineering, Shiley-Marcos School of Engineering, University of San Diego, San Diego, CA

https://doi.org/10.33697/ajur.2019.027

*Student: ealexander@sandiego.edu**
Mentor: ghoople@sandiego.edu

ABSTRACT
This study quantifies the anisotropic behavior of ultrasonic wave transmission for materials printed with three different 3D printers. As 3D printed materials become more prevalent in manufactured products, fully characterizing the physical properties of these materials become more important. This paper examines the longitudinal velocity of sound and acoustic impedance in two directions: orthogonal and parallel to the printed layers. Each of the 3D printed materials displayed slightly different transmission results. For PMMA like samples printed on a SLA printer waves travelled more quickly in the orthogonal direction than the parallel direction. For samples printed on an industrial FDM printer using ABS the opposite was true: the parallel direction was faster than the orthogonal. For samples printed on an entry level FDM printer with PLA there was no consistent pattern, instead there was a tight clustering of ultrasonic velocity in the parallel direction but substantial variation in the orthogonal direction. Overall the variation between the orthogonal and parallel directions was found to be less than 2% in all cases.

KEYWORDS
3D Printing; Additive Manufacturing; Ultrasonic Waves; Anisotropic Material Properties; ABS; PLA

INTRODUCTION
In recent years 3D printing has fundamentally changed the ways that parts are manufactured. Gone are the days when 3D printing was only used for prototyping. From dental implants[1] to aircraft components,[2] 3D printed parts are now being used in a wide range of permanent applications. With this shift towards permanent usage, understanding the material properties of 3D printed parts has become more important than ever. Previous studies have reported on properties like tensile strength and young's modulus.[3–11] To date, however, we are unaware of any studies on the manner in which 3D printed materials transmit ultrasonic waves.

3D printing refers to a collection of additive manufacturing techniques where material is joined in a variety of layer by layer approaches. The desired part is created using Computer Aided Design (CAD) software and then converted to a series of thin layers by the 3D printing software. Perhaps the most common type of 3D printing technology is fused deposition modeling (FDM). FDM printers operate by rapidly extruding a heated polymer filament into the desired layer geometry.[12] The printers typically achieve this by incorporating a nozzle mounted to an X-Y stage. This nozzle moves across a build platform, extruding the filament in thin layers at the desired locations. A Z-stage, either mounted to the nozzle or to the build platform, then moves fractions of millimeters to enable the deposition of material at the next layer. Recently stereolithography (SLA) based printers, which traditionally were much more expensive than FDM printers, have become more affordable and can be found in university makerspaces. SLA, in contrast to FDM, operates by using a laser to selectively cure liquid polymer precursors.[19] Material is still deposited in a layer by layer approach, but due the challenges of accurately moving the focal plane of the laser, the work piece itself is typically repositioned using a Z-stage between layers. There are dozens of other technologies for 3D printing, including direct metal laser sintering, selective laser sintering, and selective laser melting. [12] In this study we report the ultrasonic properties of materials printed using an entry level FDM printer (Ultimaker 2®), an industrial FDM (Stratasys uPrint SE®), and an entry level SLA (Formlabs Form2®). These printers were chosen because they provided a range of material types and were local to the University of San Diego, where this research took place.

Ultrasonic waves have proven to be a powerful and non-invasive method for a wide range of sensing applications including pregnancy screening, proximity sensors, and crack detection.[13] One of the unique features of many 3D printed materials, due to their layer by layer fabrication, is their mechanical anisotropic behavior.[14] Due to the individual layer stacking the properties are variable depending upon the direction that specimens are tested. This happens because of environmental conditions present while cooling, and is inherent to the 3D printing process. We hypothesized, and confirmed in this study, that this anisotropy can have an effect on the way in which ultrasonic waves are transmitted through 3D printed materials.

Ultrasonic waves are sound waves above 20 kHz – the ultra- prefix refers to the fact that waves at these frequencies are above the limit of human hearing.[15] While the mathematical models for ultrasonic waves are quite complex, the fundamental concept is relatively straightforward: when a propagating wave encounters a discontinuity, such as a fetal tissue surrounded by fluid in the womb, reflections are generated that can be measured by an ultrasonic sensor. These waves, like all sound waves, propagate through solids, liquids, and gasses. The mechanism of this propagation is through molecular collisions – hence these waves travel considerably more quickly through solids than through air. When there are no molecules to transmit these vibrations, such as in the vacuum of outer space, there is no sound.

By carefully generating, measuring, and modeling the way these waves move through materials a huge range of technologies has been enabled.[16] Within engineering one of the most common applications for ultrasonics is known as ultrasonic nondestructive evaluation.[15, 17] By measuring the velocity and attenuation of ultrasonic waves it is possible to determine a great deal of information about an unknown specimen, including geometry (including hidden cracks), elastic modulus, or density. This testing technique has been used for decades across a wide range of industries.[13] For example, ultrasonics provides a way to check for hidden defects in composite materials for aerospace applications as well as structural health monitoring for large concrete structures in civil applications.[18, 19] Ultrasonic information can be collected in two ways: either using two transducers – one to create the signal and one to receive it - or a single transducer that serves both functions.

In this study we focus on measuring the properties of longitudinal ultrasonic waves, where molecular motion is parallel to the direction of wave travel, as this type of wave is commonly found in engineering applications. This is the ultrasonic velocity that is used in applications such as ultrasonic distance measurements and flaw detection. Longitudinal ultrasonic wave transmission through a material is typically reported as either the velocity of sound v or the acoustic impedance $Z = \rho v$, where ρ is density.[15] In this paper we report both values and comment on the differences found between the 3D printed materials.

Materials and Methods

For this study we characterize the material properties for samples printed using three different 3D printers. In this section we describe the sample manufacturing process, how we collected and processed our data, and the statistical approach we took to analyzing our results. These printers were selected primarily due to their availability on our campus, but cover a varied range of possible 3D printing approaches. All printers were configured and calibrated as per manufacturer specifications. As a test specimen we chose to print a 25.4 mm (1 inch) solid cube with a small locating feature on one corner to identify the print orientation. This size was selected primarily as it was the smallest specimen with enough surface to mount our ultrasonic transducers. We printed four copies of each part on each 3D printer for a total of 12 samples. Each sample was then measured in two directions for a total of 24 measurements.

Test part manufacturing

We manufactured parts in three ways: polylactic acid (PLA) printed with an Ultimaker 2, acrylonitrile butadiene styrene (ABS) printed with a Stratasys uPrint, and "clear resin" - similar to poly(methyl methacrylate) (PMMA) - printed with the Form 2 (**Figure 1**). The first printer, the uPrint Stratasys SE, is an industrial fused deposition modeling (FDM) 3D printer. Our model includes a temperature controlled build volume and is capable of printing both ABS filament and a dissolvable support material. We printed parts using a layer height of 100 μm and 100% fill density. (The user is not able to set the extrusion or build volume temperatures for this printer, they are proprietary to the manufacturer.) The second printer in this study, the Ultimaker 2, is an entry level FDM 3D printer. We elected to use a polylactic acid (PLA) filament and printed our part using the standard settings in our makerspace: 268 °C nozzle temperature, 60 °C bed temperature, a layer height of 100 μm, nozzle diameter of 0.6 mm. The only non-standard setting used was a fill density of 100%. The final printer in this study, the Form2, is a stereolithographic (SLA) 3D printer that uses proprietary UV curing resins. We used the "clear resin", similar to PMMA, for our material and selected a layer height of 50 μm. For all printers we chose to print directly on the build platform whenever possible to eliminate the need for support materials that would later need to be removed.

(A)

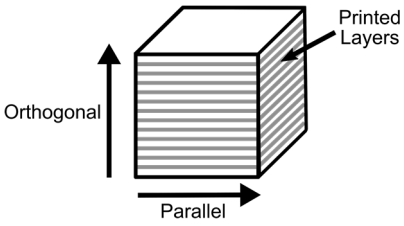

(B)

Figure 1. (A) The four types of samples, with the ultrasonic transducers installed, tested in this study. From left to right Acrylic (control), Form 2 Clear Resin, uPrint ABS, and Ultimaker PLA. Coordinate systems indicate wave travel directions parallel or orthogonal to the printed layers, and were drawn on the cubes after printing. **(B)** The convention used in this study to define the orthogonal and parallel directions of wave travel. The grey lines indicate the 3D printed layers of the sample. When waves travel parallel to the layers they move along the path of a printed layer. When waves travel orthogonally they move through multiple layers.

Test setup and data collection

We measured the ultrasonic properties of our test samples using a "pitch and catch" configuration with two ultrasonic transducers, (**Figure 2)**. Transducer pairs were installed to measure the ultrasonic properties in two directions – parallel to and orthogonal to the printed layers, (**Figure 1)**. We hypothesized the anisotropic nature of 3D printed parts would lead to variations in ultrasonic velocities.

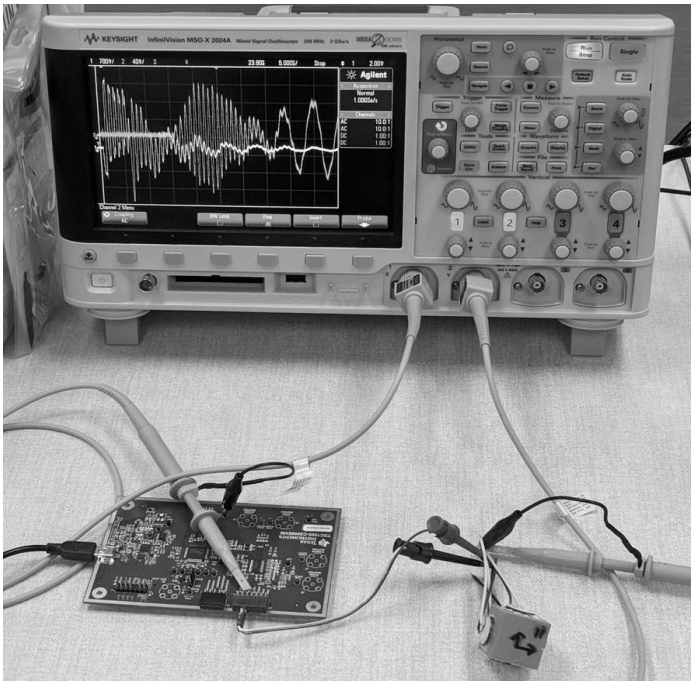

Figure 2. The test setup used in this study. The PCB in the foreground is the Texas Instruments development board we used to generate the 1 MHz ultrasonic pulses, it is connected to the "pitch transducer". The "catch" transducer is connected directly to the oscilloscope which we used to both visualize the signals and store the data. Note that the block shows 4 sensors installed – pitch and catch transducers for both orthogonal and parallel directions.

We selected a 1 MHz Ultrasonic transducer (Steminc® SMD10T2R111) as it is commonly used in engineering applications, including automotive and medical markets. One important note: frequency selection for ultrasonic transducers is highly

application dependent. In general, higher frequency waves offer higher spatial resolution, but the signal attenuates more quickly. The 1 MHz wave we selected offers a resolution on distance measurements of approximately ±1 mm. For liquids and solids transducers that produce waves in the MHz range are practical, for transmission through air excitations in the kHz range are preferred. [20]

Following manufacturer recommendations, we cleaned the surfaces of the cubes and then lightly sanded them with 400 grit sandpaper to improve transducer adhesion.[20] We then applied Bob Smith Industries Insta-flex glue™ to the transducers, activated with Bob Smith Industries activator, and pressed them into the center of the cube face. After holding the sensor in place for 60 seconds, we removed the pressure and applied glue around the edges of the transducers to ensure maximum adherence to the block surface.

We used a Texas Instruments TDC-1000 C2000EVM development board to generate the 1 MHz ultrasonic pulse input signal. After some initial testing with one, five, and seven excitation pulses, we settled on a five pulse configuration for our data collection as it provided the optimal balance between signal and noise. We recorded data from both transducers using an InfiniVision ® MSO-X 2024A oscilloscope. We started by setting the sampling frequency to 2 Gsa/s, we then adjusted the settings for each signal to capture as much of the waveform as possible without clipping the data.

Signal processing

The ultrasonic transducer data were processed using MATLAB®. The raw signals were smoothed using a moving average filter. After some experimentation we concluded 100 data points (0.2 μs) was sufficient to remove the noise in the data without substantially reducing the magnitudes of the peaks. We also removed the DC bias in the signal. We used data taken from acrylic blocks, with known ultrasonic properties, to calibrate our system. Acrylic blocks were chosen as a control because they cast blocks lacked the layered properties of the other samples. This property meant the time of flight was similar in any direction through the block for our control, allowing us to find a good detection threshold. We found that a threshold of 25% of the magnitude of the first peak in the received signal correlated with the expected time of flight for an ultrasonic wave through acrylic. We opted to normalize each data set to the magnitude of this first peak, rather than a common voltage threshold, as the material properties for each block resulted in substantially different signal amplitudes. We used this 25% threshold to compute ultrasonic times of flight times for all of the blocks we tested. (**Figure 3** in results shows an example of this threshold and signal.) We then calculated an ultrasonic velocity by dividing the width of the block by the ultrasonic time of flight.

Statistical analysis

As with any material characterization study, it is critical to consider the statistical power of the study. Not enough data and your conclusions are meaningless – too much and you have wasted time and resources. In this case we found that a small sample size (N=4) was sufficient to discern the relevant behavior at each of our measurement conditions. We used a standard single factor analysis of variance (ANOVA)[21] to demonstrate the differences we observed between the three types of printed blocks were statistically meaningful. Within each sample group, we used a paired t-test to compare the parallel and orthogonal velocities for each sample.[21] We selected a paired t-test as our data points were coupled – each block had both an orthogonal and parallel velocity. Using this approach we discovered statistically meaningful conclusions about the differences (or lack thereof) in velocity between the parallel and orthogonal directions.

Results and Discussion

For each of the three printers we tested the ultrasonic properties of four test specimens. Properties were measured in two directions for each specimen: parallel and orthogonal to the printed layers. An example of the data from a specimen printed with the Form 2 is shown in **Figure 3**, note that this figure shows the post-processed data. The top panel shows the excitation signal. The five pulse ultrasonic excitation can be seen clearly between 0 and 5 μs, the remaining signal shows a typical ultrasonic transducer ring down. The lower panel shows the received signal (solid) and the threshold for computing time of flight (dashed). As discussed in the methods section, we established a threshold for computing time of flight at 25% of the magnitude of the first peak in the received signal.

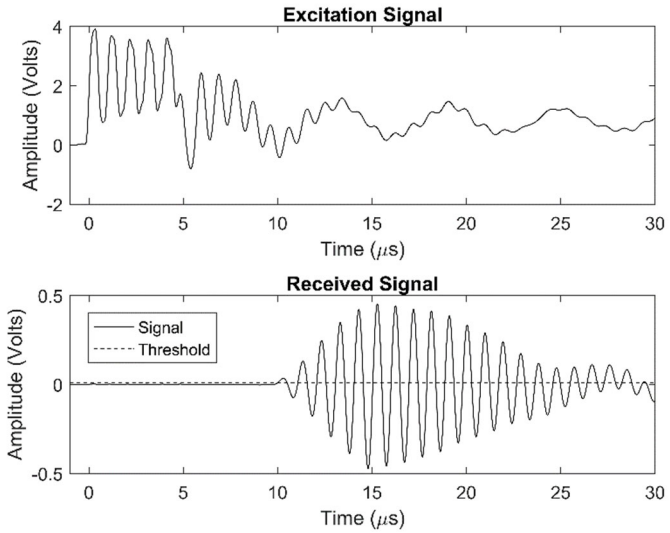

Figure 3. A representative example of the pitch and catch ultrasonic signals collected for this study. Data shown were collected from a Form 2 block in the parallel direction.

The results for the ultrasonic velocities for the twelve specimens are shown in **Figure 4** and summarized in Table 1. Each subplot of **Figure 4** shows the data collected for all of the specimens from a particular type of 3D printer.

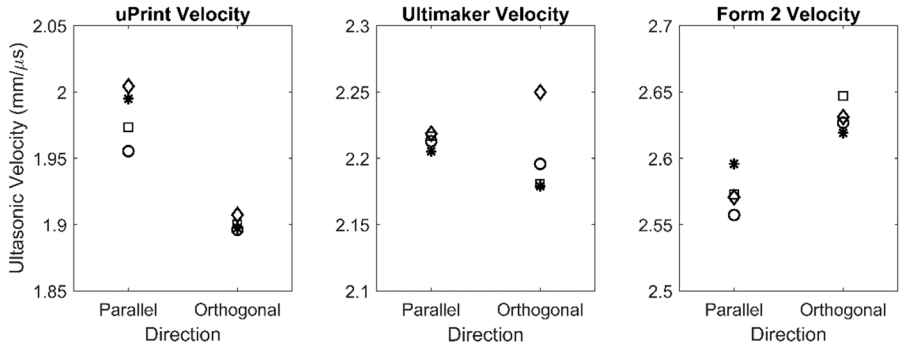

Figure 4. Ultrasonic velocities in the parallel and orthogonal directions for each of the 3D Printers examined in this study. Within each subplot the four samples tested are represented by a unique character (diamond, star, square, or circle).

3D Printed Material	Density g/cm³	Travel Direction Relative to Layers	Longitudinal Velocity of Sound (υ) mm / μs	Acoustic Impedance Z = ϱ υ 10^6 kg / m²s	Deviation Relative to Parallel %	Standard Material Velocity mm / μs
uPrint – ABS	0.97	Parallel	1.70	1.65	-1.8%	2.25
		Orthogonal	1.67	1.62		
Ultimaker - PLA	1.19	Parallel	2.20*	2.62*	n/a*	2.22
		Orthogonal	2.18*	2.59*		
Form2 – Clear Resin	1.14	Parallel	2.58	2.94	2.0%	2.75
		Orthogonal	2.63	3.00		
* We found no statistical difference between these values						

Table 1. Density, Velocity of Sound, and Acoustic Impedance for the samples tested as a part of this work. Reference values are provided for the speed of sound in standard (non 3D printed) materials.[22-23]

Within each subplot a unique marker is used to represent each specimen. This is most cleanly seen in the parallel direction for the uPrint (left most panel) where the velocities are spread out amongst each of the four samples that were tested. In the orthogonal

direction, however, these four data points are collapsed on each other. For each specimen we collected a single measurement, represented by the single point on the plot. (During the validation phase of this study we collected multiple measurements for several specimens and found them to be identical. We therefore concluded a single measurement to be sufficient for the full data set.) We computed a one-way analysis of variance (ANOVA) on the time of flight data between the different types of 3D printers and found the differences between each material in our testing to be statistically different ($F=550$, $p=0$). This came as no surprise as each of these printers used a different material. For reference we have included the velocity of ABS, PLA, and PMMA manufactured using traditional means.[22,23] The Ultimaker and Form 2 specimens have ultrasonic speeds similar to those of standard materials, while the ABS printed on the uPrint is substantially lower than the "traditional" stock material.

Within each sample type we computed a paired t-test to determine if the differences between ultrasonic velocities for the two directions (orthogonal and parallel) were statistically meaningful. Both the uPrint ($t= -9.155$, $p= 0.003$) and Form 2 ($t = 4.935$, $p= 0.016$) showed statistical differences as the ultrasonic velocities were quite repeatable. For the Ultimaker, however, there was no quantifiable difference between the two directions as there was wider variations in the velocity between the samples ($t=-0.836$, $p=0.464$). Using the density and longitudinal velocity for ultrasonic waves we calculated an acoustic impedance. These values are shown in **Table 1**.

Interestingly there is a lack of clear trends between the three printers. Coming into the study we hypothesized that ultrasonic waves traveling orthogonal to the print direction would be slightly slower than those waves traveling parallel to the printed layers. We speculated that when traveling parallel to the printed layers, the layers would act as wave guides resulting in higher longitudinal velocities of the ultrasonic waves. While we observed this trend for parts created with the uPrint, the opposite was true for the parts created with the Form 2. An unexpected result was the tight clustering of velocities for a particular direction in the uPrint (orthogonal) and Ultimaker (parallel). This lack of consistent behavior suggests that some other property of these printers changes the transmission of ultrasonic waves. One theory for this could be that the bonds between the layers could be harder than the plastic substrate, making the orthogonal permeability less than the parallel direction. This suggests that for each of these printers the manufacturing process is more consistent with respect to a particular direction. In contrast the Form2 showed similar variations between the data points for a given travel direction.

The major outlier in this group is the Ultimaker. It shows a tight grouping of ultrasonic velocities in the parallel direction, but the samples do not reveal a consistent pattern for the orthogonal direction. Sometimes the orthogonal direction is faster than the parallel, sometimes it is slower. This suggests that something about the layer by layer fabrication process is not always repeatable. This tracks with our broader experience with this printer – of the three printers we find our prints fail the most often on the Ultimaker, producing non-uniform blocks, not finishing prints, or layers separating on removal. More broadly speaking, our results confirm that the anisotropic nature of 3D printed materials does have an impact on ultrasonic velocities. An important note here: 3D printed parts are often printed with lower fill densities (20% – 80%) to speed up printing time and reduce the amount of material needed. For ultrasonic applications we do not recommended this approach: it creates air gaps inside of parts that cause unwanted reflections and substantially attenuate signals. We did test some parts with incomplete infill and found that we could not collect reliable data due to this increased scattering. For applications where ultrasonics will be employed with 3D printing we strongly recommend using 100% infill.

Conclusions

3D printing is an incredibly powerful technology that has fundamentally shifted the way we think about manufacturing. As 3D printed parts move from prototyping to production, designers must consider the unique material properties of parts made using this approach. While the anisotropic behavior of these materials has been well documented, this study is the first to examine this anisotropy in the realm of ultrasonics. While we have shown clear, repeatable differences in ultrasonic velocities, the variations are relatively small (< 2%). For some applications these variations will be irrelevant, for others, such as the project that motivated this study, a well-developed understanding of ultrasonic behavior in 3D printed parts is critical.

This study is just a first step in investigating the ultrasonic properties of 3D printed materials. There is more work to be done to investigate the specific mechanisms that cause these variations. Future studies would benefit from correlating this ultrasonic data with measurements of Young's modulus and fracture strain using an Instron machine. Similarly, sectioned SEM imaging of specimens in the parallel and orthogonal directions might provide insight into the causes of these variations. It is also possible that there are variations between the two parallel directions of the specimens. (Some 3D printers have been known to create parts that show anisotropic behavior in three directions rather than just two.) Future researchers could also investigate other 3D printing

methods or examine the impact of varying specific printing parameters, such as layer height or extrusion temperature, within a particular printer. As designers continue to use 3D printers in innovative ways, we hope the research presented here lays a foundation that will serve them well.

ACKNOWLEDGMENTS

The authors thank Sam Burt, Steve Saxer, and Khoa Vu for their help printing samples for this study. This work was supported by funding from the Shiley-Marcos School of Engineering at the University of San Diego.

AUTHOR DISCLOSURE STATEMENT

The authors have no competing financial interests.

AUTHOR CONTRIBUTIONS

EA and GH collaboratively conceived of the study, analyzed the data, and wrote the manuscript. EA conducted all experiments.

REFERENCES

1. Ventola, C. L. (2014). Medical Applications for 3D Printing: Current and Projected Uses. *P T* 39, 704–711.
2. Huang, W. and Lin, X. (2014). Research Progress in Laser Solid Forming of High-Performance Metallic Components at the State Key Laboratory of Solidification Processing of China. *3D Print. Addit. Manuf.* 1, 156–165. *doi.org/10.1089/3dp.2014.0016*
3. Dizon, J. R. C., Espera, A. H., Chen, Q. and Advincula, R. C. (2018). Mechanical characterization of 3D-printed polymers. *Addit. Manuf.* 20, 44–67. *doi.org/10.1016/j.addma.2017.12.002*
4. Wittbrodt, B. and Pearce, J. M. (2015). The effects of PLA color on material properties of 3-D printed components. *Addit. Manuf.* 8, 110–116. *doi.org/10.1016/j.addma.2015.09.006*
5. Park, S., Rosen, D. W., Choi, S. and Duty, C. E. (2014). Effective mechanical properties of lattice material fabricated by material extrusion additive manufacturing. *Addit. Manuf.* 1–4, 12–23. *doi.org/10.1016/j.addma.2014.07.002*
6. Anderson, I. (2017). Mechanical Properties of Specimens 3D Printed with Virgin and Recycled Polylactic Acid. *3D Print. Addit. Manuf.* 4, 110–115. *doi.org/10.1089/3dp.2016.0054*
7. Ahmed, M., Islam, M., Vanhoose, J. and Rahman, M. (2017). Comparisons of Elasticity Moduli of Different Specimens Made Through Three Dimensional Printing. *3D Print. Addit. Manuf.* 4, 105–109. *doi.org/10.1089/3dp.2016.0057*
8. Domingo-Espin, M., Borros, S., Agullo, N., Garcia-Granada, A.-A. and Reyes, G. (2014). Influence of Building Parameters on the Dynamic Mechanical Properties of Polycarbonate Fused Deposition Modeling Parts. *3D Print. Addit. Manuf.* 1, 70–77. *doi.org/10.1089/3dp.2013.0007*
9. Bible, M., Sefa, M., Fedchak, J. A., Scherschligt, J., Natarajan, B., Ahmed, Z. and Hartings, M. R. (2018). 3D-Printed Acrylonitrile Butadiene Styrene-Metal Organic Framework Composite Materials and Their Gas Storage Properties. *3D Print. Addit. Manuf.* 5, 63–72. *doi.org/10.1089/3dp.2017.0067*
10. Mueller, J., Courty, D., Spielhofer, M., Spolenak, R. and Shea, K. (2017). Mechanical Properties of Interfaces in Inkjet 3D Printed Single- and Multi-Material Parts. *3D Print. Addit. Manuf.* 4, 193–199. *doi.org/10.1089/3dp.2017.0038*
11. Bikas, H., Stavropoulos, P. and Chryssolouris, G. (2016). Additive manufacturing methods and modelling approaches: a critical review. *Int. J. Adv. Manuf. Technol.* 83, 389–405. *doi.org/10.1007/s00170-015-7576-2*
12. Ahn, S., Montero, M., Odell, D., Roundy, S. and Wright, P. K. (2002). Anisotropic material properties of fused deposition modeling ABS. *Rapid Prototyp. J.* 8, 248–257. *doi.org/10.1108/13552540210441166*
13. Rose, J. L. (2014). *Ultrasonic guided waves in solid media*, Cambridge University Press, Cambridge, UK.
14. Lee, C. S., Kim, S. G., Kim, H. J. and Ahn, S. H. (2007). Measurement of anisotropic compressive strength of rapid prototyping parts. *J. Mater. Process. Technol.* 187–188, 627–630. *doi.org/10.1016/j.jmatprotec.2006.11.095*
15. Shull, P. J. (2002). Introduction to NDE. *Nondestructive Evaluation: Theory, Techniques, and Applications*, Marcel Dekker, New York, NY.
16. Cheeke, J. D. N. (2012). *Fundamentals and Applications of Ultrasonic Waves*, CRC Press, Boca Raton, FL.
17. Rose, J. L. (2014). Ultrasonic Nondestructive Testing Principles, Analysis, and Display Technology. *Ultrasonic guided waves in solid media*, 421–444, Cambridge University Press, Cambridge, UK.
18. Katunin, A., Dragan, K. and Dziendzikowski, M. (2015). Damage identification in aircraft composite structures: A case study using various non-destructive testing techniques. *Compos. Struct.* 127, 1–9. *doi.org/10.1016/j.compstruct.2015.02.080*
19. Shiotani, T., Aggelis, D. G. and Makishima, O. (2009). Global Monitoring of Large Concrete Structures Using Acoustic Emission and Ultrasonic Techniques: Case Study. *J. Bridg. Eng.* 14, 188–192. *doi.org/10.1061/(ASCE)1084-0702(2009)14:3(188)*
20. Minasi, M. (2015). How to Select and Mount Transducers in Ultrasonic Sensing for Level Sensing and Fluid ID. *http://www.ti.com/lit/an/snaa266a/snaa266a.pdf* (accessed May 2018)

21. Devore, J. L. (2012). *Probability and statistics for engineering and the sciences* 6 ed., Thompson, Belmont, CA.
22. Tarrazó-Serrano, D., Castiñeira-Ibáñez, S., Sánchez-Aparisi, E., Uris, A. and Rubio, C. (2018). MRI compatible planar material acoustic lenses. *Appl. Sci.* 8, 1–9. *doi.org/10.3390/app8122634*
24. Carlson, J. E., Van Deventer, J., Scolan, A. and Carlander, C. (2003). Frequency and temperature dependence of acoustic properties of polymers used in pulse-echo systems. *Proc. IEEE Ultrason. Symp.* 1, 885–888. *doi.org/10.1109/ULTSYM.2003.1293541*

ABOUT STUDENT AUTHOR

Edward Alexander recently graduated with a BS/BA in Mechanical Engineering from the University of San Diego. Originally from Denver, CO, he gained an interest in engineering from his experience working with his parents. He currently lives in Denver, Colorado, working for Ricoh Global and studying for the Fundamentals of Engineering exam. He plans to move towards acquiring a professional engineering license.

PRESS SUMMARY

This study describes the non-uniform behavior of ultrasonic wave transmission for materials printed with three different 3D printers. The ultrasonic velocity of samples was measured in two directions: orthogonal to and parallel to the printed layers. Each of the 3D printed materials displayed unique behavior. Overall the variation between the two directions was found to be less than 2% in all cases, however these variations could be important in sensitive engineering applications. This fundamental materials research will be useful to engineers designing 3D printed parts for use with ultrasonic waves.

Why Regimes Repress: The Factors that Lead to Censorship of Social Media

Ezhan Hasan
Department of Political Science, Texas Christian University, Fort Worth, TX

https://doi.org/10.33697/ajur.2019.028

Student: azhan.hasan@tcu.edu
Mentors: j.scott@tcu.edu, j.riddlesperger@tcu.edu, grant.ferguson@tcu.edu*

ABSTRACT
Social media have made it easier to create mass political action. Prominent examples include the Arab Spring movements, which took place in regions where information was previously tightly controlled by authoritarian regimes. Fearing radical change, several regimes have repressed social media use, but not all authoritarian regimes have taken the same measures. Previous research suggests that regime leadership is motivated to ensure its own survival but also influenced by a strong independent media and the need for citizens to vent grievances. To understand the relationship of these factors to social media repression, this research conducts a comparative process-tracing case study of Iran, Turkey, and Venezuela from 2004 to 2017, using a hypothesis-testing approach. It concludes with discussion of the findings for the nature of regime response to the role of social media in protest.

KEYWORDS
Internet; Media; Protest; Authoritarian; Iran; Turkey; Venezuela; Comparative; Case-Study

INTRODUCTION

In April 2018, the Sri Lankan government confronted mob violence targeting the Muslim minority in the nation. The primary response by the government was to completely shut down Facebook, claiming that it had amplified hate speech that incited the attacks. Officials ordered internet service providers in the region to stop allowing Sri Lankan users to send or receive any messages from the platform.[1] The same tactic of shutting down social media had been used before this. About a year prior, the Jammu and Kashmir government blocked access to several social media sites, much like the Iranian government had done in 2008, because the platforms were being used to advance anti-government propaganda.[2] When countries do not want particular messages being seen, they ban particular users from social media or rely on the social media platform to censor for them. Similar to Turkish restriction of particular users' access in early 2014, Myanmar has blocked Arshin Wirathu, a Buddhist monk who preached intolerance of the refugee Rohingya population.[3] Each of these countries has recognized social media's power to influence the information that people receive, along with the people's willingness to believe and act on the information. Social media, due to their ability to easily reach a vast number of people, have a special power to persuade that other forms of public discourse do not have.

Many cases of persuasion through social media involve the spread of untrue information. In Cambodia, several untrue claims about opposition party leader Kem Monovithya went viral on Facebook in 2017. Published dishonestly by those aligned with Prime Minister Hun Sen, the untrue allegations influenced public opinion to the point that opposition leaders were arrested and given sentences—all simply because of a few social media posts.[4] Further, in the 2016 United States presidential election, Russian firms interested in stirring discord used social media to accomplish their goal. In the two years leading up to the election, these groups spread false information by garnering American followers and spreading digital ads. Through their spread of misinformation, they were able to organize rallies and events—from thousands of miles away via social media.[5] The prospect of untrue messages on social media gives rise to a government's inclination to combat what it considers false, as in Iran, Turkey, Venezuela, and numerous other nations.

The use of social media has become a common factor in the spreading of information regardless of truth and regardless of government sanctioning of the information. In some cases, it leads to political action, both peaceful and violent. Several states have made decisions on banning social media platforms at least temporarily following one of these uprisings, but others have made no such decision despite the involvement of social media in harmful activities for the state. This research seeks to identify the factors that cause a state to censor social media, including the type of message, strength of the mainstream media, and wealth of citizens. It also seeks to identify the motivating causes behind particular cases of censorship in Iran, Turkey, and Venezuela. To

understand the relationship of these factors to social media repression, previous research is used to generate three hypotheses, which are then tested using cases from Iran, Turkey, and Venezuela from 2004-2017.

PROTEST AND SOCIAL MEDIA

The Power of Social Media

The dispersion of information that sparks political change has quite obviously existed well before the advent of social media. Lohmann discusses one notable example of the power of information—a series of political protests in Eastern Germany beginning in 1989 and ending in 1991. In protests that occurred every consecutive Monday for thirteen weeks, "demonstrators expressed their demands for political liberalization, open borders, and, toward the end of the cycle, German unification." Lohmann attributes the speed with which the several protests grew to the concept of informational cascading—in simple terms, a process which involves a critically affected population passing information at high rates. In the case of political action, a more ideologically extreme portion of the population triggers the dispersion of negative assessment of the state, and as more moderate parts of the population slowly continue to spread the information, the government loses support from the public. Initially, members of society develop assessments of the nature of the state based on a private interaction with their government. Because each experience is different, these private assessments can either be positive or negative. It is likely that those with negative views will want political change, but "an individual receiver cannot unilaterally decide to overthrow the status quo regime; this is the collective decision of a large number of people." Through protest, those without the negative assessment are made aware of the views of those with the negative assessment and can then choose whether or not to adopt the views. Once the protests reach a certain threshold of support, they have enough power to overthrow the government. In the case of Eastern Germany at the time, there was no free press or other means of information dispersion. The onset of the demonstrations led to swift change because it spread information about negative experiences quicker than other media.[6]

It took a special set of circumstances to circumvent traditional mass communication channels in the Eastern Germany demonstrations. The advent of social media has made mass political mobilization much less difficult. The most prominent example is the Arab Spring—a series of protests that began in Tunisia and quickly spread to several nations in the Middle East. The wave of mass action was unprecedented for a region dominated by authoritarian regimes. The correct mix of factors was once again necessary for mass political action, and Bellin identified emotional triggers, impunity of state officials, and social media as the essential backdrop to the Arab Spring. Of these three, social media presence was the only factor that explained why these protests could not have occurred a decade prior to when they did. In several of these nations, the citizens' ability to do what Eastern Germans did two decades before them was hampered in the past by an "authoritarian bargain":

> They exchanged political quiescence for stability as well as for economic growth. But even those citizens who rejected the authoritarian bargain found their capacity to organize politically blocked. The Tunisian and Egyptian regimes did everything in their power to suppress opposition and atomize society. Political activists were arrested and brutalized. Public gatherings were controlled, if not forbidden. Speech was censored and publications (especially in Tunisia) were often shut down.

Social media not only made up for the repressed communication channels but also proved to be more powerful than the alternate methods of uprising. Social media avoided authoritarian control through its "anonymity and spontaneity" and allowed for "coordinating and synchronizing thousands of people, making mass gatherings possible even in the absence of formal organizational infrastructure."[7] This is the power of social media. Social media make it much more difficult for dictators to atomize society. Any regime that exercises control over other types of media would quite understandably be frightened by the prospect of immense power in the hands of the people granted by social media.

Government Censorship Decisions

Just as information dispersal had existed prior to social media, states had adopted techniques to control information that are now being applied to social media. Through a mathematical model, Edmond explains that if a regime's most important concern is survival, then its preferred state is to have a strong state-controlled centralized source of information. The state can then easily establish economies of scale to block or control all other sources of information. With more decentralized sources of information as is the case with social media, there is likely to be a larger number of information signals to each individual in the population, making establishing economies of scale much more difficult for the regime, which is unfavorable to its survival.[8]

If a state's interest is in controlling information, it is important for the state to acknowledge the scope of its power. Shadmehr and Bernhardt consider the regime's decisions under a model in which a strong independent media already exists, where it is not possible to completely control (as is the case with social media). They once again assert that censorship is beneficial to cementing power over the people, but that if it is overdone, it may be counterproductive. In these cases where no precedent exists for a completely state controlled media, rulers will censor existing media to the point that some negative stories may be released while still censoring the most negative stories. The rulers do this to maintain believability of the news: both the rulers and citizens realize that no government is perfect, and thus a media that only reports positive stories is not credible. Rulers recognize that

complete censorship means that a single leaked negative story will have a huge impact on the regime's survival.[9] Hassid's characterization of microblogs as safety valves and pressure cookers supports this idea. In China, social media criticism relieves social pressure when it simply comments on that which the mainstream media have already reported. This is referred to as the safety valve, which allows citizens to vent their frustrations without posing significant threat to the regime. It is also beneficial to a government that wishes to take feedback from citizens to improve and solve social problems. The other iteration of social media commentary is the pressure cooker, where citizens' commentary increases social tension. A pressure cooker occurs when bloggers express evaluations on issues the mainstream media are not discussing and therefore on which the government already has an established stance. The Chinese government has dealt with these more harshly because they are more likely to induce protest movements.[10] Ultimately, decisions on censorship come down to governments controlling what they can but strategically allowing information dispersion when it least harms the regime.

Much of the existing understanding of social media censorship patterns comes from China, which has a complete ban on large social media outlets like Facebook and also has human enforcement that monitors the general internet. King, Pan, and Roberts conducted a study in which they automated several posts on various Chinese-controlled websites to examine patterns in what was censored and what was left on the web. Interestingly, Chinese officials did not censor everything that was oppositional to the government. In several cases, they allowed information with negative evaluations of Chinese leadership, with the exception of negative evaluations of the internet police. However, they consistently censored any information that encouraged collective political action.[11] This is consistent with the idea that a regime's primary interest in censorship is cementing its own power, not necessarily having only positive public evaluation. The Chinese seemingly recognize what Aday and colleagues found: the unique power of new media, including social media, was organizing political action.[12] Citizens would otherwise identify common interests and goals, but without social media, as in the cases preceding the Arab Spring, there would be no movement. Collective action has been more influential in controlling corruption than the presence of an electoral democracy.[13] The Chinese government's motives for censorship give light to motives behind censorship in other nations.

Research into the Chinese model of censorship reveals the meticulous nature by which decisions are made on social media allowance. As Sullivan explains, the use of microblogging platforms in China can cause political change with the cooperation of the Chinese government. One of the primary platforms is Twitter, which is not technically allowed in China, but can still be accessed by some citizens using a Virtual Private Network (VPN). Although criticism of the government is generally not allowed in China, some Chinese social activists on Twitter or other microblogs are not stopped by the Chinese government, which actually uses some of the feedback to make changes in its governing. Chinese leaders allow this feedback loop primarily because they know the vast majority of citizens do not have access to Twitter, meaning that it cannot be used for inducing collective action. In this way, the microblogging platforms allow citizens to express their negative assessments of the government, but instead of primarily making others aware by triggering protest, the Chinese government uses the assessments to make positive changes. Essentially, Chinese officials overlook this loophole because the informational cascade doesn't reach the masses—it allows them to gain valuable feedback but does not threaten any sort of uprising.[14]

THEORY AND HYPOTHESES

The power of social media to encourage political action is of primary interest to this study. Political action that expresses negative assessment of an authoritarian government puts regime survival at risk. Repressive reactions (i.e. censorship) to that risk under different circumstances are the subject of this study. While recent research has been theoretical or focused on single countries as case studies, empirical cross-national research remains necessary to advancing knowledge on regime response to social media use. The regimes of interest to this study must be selective in determination of what to censor and not censor. In many strong democratic governments, there will be no repressive reaction by the regime to social media posts encouraging action because the government has strongly held values of press and speech freedom. For this reason, any nation with an average Polity score[A] of 8 or higher over the timeframe of this study has been excluded from the study and its implications. Some governments, such as the North Korean regime, repress all media indiscriminately, and are therefore also excluded from the study. For all other autocratic states, theoretical research suggests that avoiding mass political action is the primary reason that authoritarian regimes repress social media, and this study tests that idea cross-nationally. This study tests the **Mass Political Action Hypothesis**:

Mass Political Action Hypothesis: When social media use encourages mass political action, authoritarian regimes respond with censorship.

Existing research suggests refinements to this hypothesis based on other factors, which form the foundation for the remaining hypotheses. The example of Chinese Twitter use shows how when mass action is encouraged, but extremely unlikely to come into fruition, the regime will not repress the media.[14] By extension, there may be cases in which mass action is encouraged by social media users but the general public either lacks access to the posts or is not receptive to the messages they see. In these cases, the

[A] Polity scores are a measure of the democratization of a nation, typically ranging from 0 to 10.

regime's primary concern is to prevent the pressure-cooker phenomenon, in which extreme negative sentiment builds up because citizens cannot express frustrations.[10] The primary concern shifts only because mass political action is encouraged but unlikely to be realized. Regime survival is best achieved by allowing social media to serve as the safety valve by which citizens vent and relieve pressure. Therefore, this research tests the **Unlikely Action Hypothesis**:

Unlikely Action Hypothesis: When social media use encourages mass political action that is unlikely to be realized, regimes do not respond with censorship.

An important factor to consider is the amount of information that citizens can already access, prior to social media. In the case of a nation with existing strong independent mainstream media, a decision to censor social media messages will most likely backfire because the mainstream media will report on such censorship. Regimes will allow at least some negative stories to circulate in order to maintain the believability of the news.[9] If there are no preexisting strong mainstream media, then it is easier for a regime to censor social media without consequences. Additionally, without strong independent mainstream media, the primary news source a citizen would have about events occurring in a different part of the country would be social media, outside of state media. In a nation that already controls the mainstream broadcast of events, maintaining control over national dialogue would require controlling social media. The **Mainstream Media Hypothesis** follows:

Mainstream Media Hypothesis: A regime in a nation with a strong independent mainstream media is less likely to repress social media than a regime in a nation with a weak mainstream media.

RESEARCH DESIGN AND METHODS

The cases of Iran, Turkey, and Venezuela are used from the period of 2004, the year when Facebook was launched, to 2017 to test the hypotheses. Consistent with Mill's method of agreement, this research uses different cases with the similar outcomes of having instances where social media are repressed and instances where it is not repressed. As such, two criteria were considered when choosing cases. First, the cases each have a known presence of protest movements and censorship. Second, the chosen cases are dissimilar in a number of relevant ways: level of democratization, ethnic fractionalization,[B] natural resource wealth, types of mainstream media, and GDP per capita. Each of these differences contribute to ensuring that similar censorship patterns are not simply indicative of overwhelming similarity between the cases. **Table 1** summarizes the variation, with italicized values indicating lower levels, underlined values indicating median levels, and bold values indicating higher levels. **Table 1** includes the average, as well as the minimum and maximum for the time period where available. A full table of the value for every available year is included in the appendix.

Country	AVG Polity Score (Minimum, Maximum)	Ethnic Fractionalization	AVG Natural Resource Wealth (Minimum, Maximum)	Mainstream Media Description	AVG GDP per Capita (Minimum, Maximum)
Iran	*-6 (-7, -6)*	**0.669**	**24.4 (13.5, 33.8)**	*Only state-run media*	*5350 (2729, 7833)*
Turkey	**5 (-4, 9)**	*0.229*	*0.442 (0.28, 0.71)*	**Several privately owned media sources**	10132 (6040, 12542)
Venezuela	2 (-3, 6)	0.483	**17.1 (7.68, 25.4)**	A mixture of state-run and private media	10226 (4271, 15692)

Table 1. Summary of Variation on Independent Variables

The average polity score was calculated as the average from the Polity IV Project's data from 2004 to 2017. Polity scores typically run from 0 to 10, but in some cases (like Iran) there are negative values.[15] Ethnic fractionalization scores were taken from Fearon and run from 0 to 1, with higher scores indicating more fractionalization.[16] Average natural resource wealth is a percentage of the nation's GDP taken as the average from 2004 to 2017 data from World Bank estimates.[17] The description of mainstream media is based on descriptions from *The World Factbook* published by the CIA.[18] Average GDP per capita is taken as the average of World Bank and OECD data from 2004 to 2017.[19]

For the analysis, CountryWatch reports are used to compile a list of all of the major political developments in each country. The list was not comprehensive but aimed to provide a representation of major events that would incite political discussion. These events were divided into Domestic Affairs, Elections, and International Relations. Domestic Affairs include changes in domestic

[B] Ethnic fractionalization is a measure of the number and prevalence of different ethnic groups in a country.

policy, actions taken by the government within its own borders, and citizen-generated political action. Elections are specifically related to the occurrence of any election, a change in election rules, or a change in political parties. International Relations include any diplomatic or contentious dealings with other nations or international organizations (including terror organizations). Because the background research for this project does not discuss citizen response to international relations, those were excluded from the case study. From there, each domestic and election-related event is investigated to find evidence of social media discussion through the Nexus Uni database. In many cases, no evidence was found, either because it was unavailable (i.e. social media discussion did not happen or was not noteworthy enough to be included in reports) or evasive of key search terms. Those cases were excluded from further analysis. Also systematically discarded from analysis were terror attacks, which were prevalent in Iran and Turkey, because while these may be encouraged by social media, they do not fall under the same citizen-generated political discussion as the other cases. The exception to this, which is noted below, is in the case that discussion of terror attacks dominates discussions surrounding an otherwise domestic affair or election related event. While the remaining cases may not comprehensively cover every occurrence in each region, they still provide an accurate picture of different types of events that could lead to repressive response by the regime. The full list, as well as indications of which cases were excluded, is available in the appendix.

The goal of the analysis is to trace the process by which each regime makes a decision on whether or not to repress social media use. Relevant context surrounding each social media, protest, and/or censorship event is included for the purpose of highlighting factors that the regime may take under consideration in its response. Based on factors that consistently draw regimes in a particular direction, the hypotheses are evaluated.

RESULTS

Each case consists of a general background on the nation's varying natural resource wealth and GDP per capita. Following that are a summary of the proceedings of the events and discussion of the evidence of social media presence and/or censorship.

IRAN

The government of the Islamic Republic of Iran consists of a Parliament and a President, but also consists of an Ayatollah, or Supreme Leader, and a number of councils that serve as religious and constitutional checks on the government. Iran has a generally high level of ethnic fractionalization, measured at 0.669. Its average natural resource wealth is consistently high, and negotiations over oil production are ongoing international topics. Iranian citizens have extremely limited access to mainstream media, and the government also has attempted to restrict international broadcasts of the news. The range of GDP per capita is generally lower than the other two nations in this analysis. Iran begins as a very autocratic state and becomes slightly more autocratic over the course of this study.[20]

Iran Social Media, Protest, and Censorship Events

Table 2 provides a summary of the timeline, social media events, and government response for Iran. The full description of events follows below.

Approximate Time Period	Description of Social Media Use	Government Response
February-June 2004	Calls for boycott of parliamentary elections	No censorship
June 2005	Calls for boycott of presidential election; Online election polling and discussion	No censorship
March 2008	Promotion of government reform leading up to parliamentary elections	Selective censorship of particular sites/messages and brief internet blackout
2009	Organization of mass protests and communication with international organizations in the aftermath of the presidential election	Selective censorship of particular sites/messages
September 2010	General messages on a pro-government group attacking Karroubi's home	Continued selective censorship from 2009
February 2011	Mousavi and Karroubi call for protests in the streets	Continued selective censorship from 2009
February 2011	Organization of anti-government marches	Continued selective censorship from 2009
Mid-2011	General messages on the reportedly missing Karroubi	Continued selective censorship from 2009
February 2012	General messages on parliamentary elections	Continued selective censorship from 2009

2012	Videos of protests against high prices	No censorship
May 2013	General messages on presidential elections.	Continued selective censorship from 2009
February 2016	Protests of the disqualification of candidates in parliamentary elections	Continued selective censorship from 2009
November 2017	Updates on earthquake and criticism of government for wasting resources	No censorship

Table 2. Summary of Iran Events over 2004-2017

Over the period of February - June 2004, Iran was finalizing candidates for the parliamentary elections to be held in June. After the Council of Guardians disqualified thousands of reformist candidates from consideration, leading intellectuals and journalists called for a boycott of the election as a form of protest. Because they could not penetrate mainstream media, they used e-mails and mobile phone messages instead. While the government did not censor these messages, it did engage in its own campaign to encourage people to vote through the state-run news media.[21]

The June 2005 presidential election once again featured calls to boycott in response to the disqualification of several candidates. Around this time, internet interactions were becoming more common, as Iranian citizens had online contact with personal religious leaders.[22] The internet was also used more heavily in the election to gauge public interest in candidates through polling, including a poll by the Iranian Students Polling Agency. In general, the government did not repress these opinion polls or the discussions on them, with the exception of polling done by individuals in contact with foreign officials.[23]

Preceding the March 2008 parliamentary elections, Parliament was reviewing proposals to cut the term of conservative President Mahmoud Ahmadinejad from four years to two-and-a-half years. At the time, Parliament was controlled by the conservative party, so the election of a majority opposition in Parliament was vital to the success of the proposed limits. Several pro-reform websites and chat services existed at the time of this election and were used in political conversation about the elections. Just before the election, the government restricted access to the Yahoo messenger service and Yahoo email sites, as well as SMS text messages found to be "destructive."[24] On Election Day, the Iranian government reportedly shut down Internet access countrywide.[25] After the election, Ahmadinejad's party maintained control of Parliament.

The primary candidates in the 2009 presidential election were former Prime Minister Mir Hossein Mousavi and incumbent Mahmoud Ahmadinejad. Election turnout in June 2009 was so high that polling stations had to extend operations for several hours due to long lines of voters. After polls closed, both Ahmadinejad and Mousavi claimed victory, with no official word on the matter. Soon after, Mousavi's website was shut off, his mobile messaging cut off, social networking curtailed, and headquarters reportedly raided. Iranian state media then declared Ahmadinejad the winner. What followed was the largest series of protests in Iran since 1979, which were called the "Green Revolution" by supporters of the reformists Mousavi and Mehdi Karroubi. Millions of protestors filled the streets, responding to calls by Mousavi and Karroubi to peacefully demonstrate. At that time, the hashtag "#iranelection" was the most popular in the world and, along with pop star Michael Jackson's death, inspired Twitter's "trending" feature. Social media were used by Iranians to communicate to international news outlets, who were not allowed to report in the country. The government quickly took steps to curtail internet use and has held tight control over social media use since 2009. The mode of censorship from 2009 until the latest records have been very similar to Chinese censorship; several websites and social media websites have been blocked entirely but are still illegally accessible to Iranian citizens via Virtual Private Networks (VPNs). The Iranian government is selective in its censorship of the illegal social media posts from citizens but tends to exercise tightest censorship around elections.[26-39] Based on this knowledge of general censorship patterns, messages surrounding major events in the ongoing social revolution are included as examples of continued selective censorship in **Table 2** above.

In 2012, Iranian citizens had difficulty purchasing staples, such as rice and cooking oil, due to the harsh economic sanctions by the international community in response to disagreements over Iran's possession of nuclear capabilities. Scarcity resulted in a series of protests by citizens. Videos of protests were recorded and posted on social media, in which protestors are heard chanting "Death to High Prices."[30] No evidence of censorship of these particular messages was found, but existing censorship laws remained in effect.

In November 2017, Iran experienced a 7.3 magnitude earthquake that killed hundreds of people and injured thousands more. Twitter users posted updates as the earthquake was happening and as they witnessed the devastation afterwards.[31] Additionally, several users criticized the government for "wasting resources" in other countries, as a reference to Iran's ongoing aid in Syria.[32] No evidence of censorship of these messages was found.

Summary of Findings from Iran

Iran's government allowed unrestricted social media use for only a short time. The 2008 elections marked the first time the government experimented with social media censorship, and repressive measures were taken to full scale following the protests of the 2009 election. In accordance with the **Mass Political Action Hypothesis**, Iran censored social media use following mass political action, the largest example of which is the protests sparked by the 2009 election and anticipated mass action surrounding other elections. In these cases, the government likely wanted to avoid challenges to the regime that mass protest could have caused. Early lack of censorship may provide weak support for the **Unlikely Action Hypothesis** because political action was less likely to be realized before social media use became more widespread, but it may also be the case that the regime was also not yet well-versed in censorship methods. Because the internet is generally blocked but still accessible via VPN, social media posts that were not specifically blocked by the government after 2009, such as the 2012 difficulty in purchasing staples and the 2017 earthquake, also provide support for the **Unlikely Action Hypothesis**. As opposed to posts encouraging protests of the government's corruption, these messages generally contain weaker calls to action. The identifiable adversaries were the sanctioning nations in the 2012 case and an earthquake in the 2017 case. As a result, the government had less interest in censoring those messages. In accordance with the **Mainstream Media Hypothesis**, Iran was the only nation to feature a tightly state-controlled mainstream media from the beginning of the time period of the study and began censoring social media relatively sooner than the other nations in the study. This suggests that the lack of available information via strong mainstream media enabled Iran to make information via social media also unavailable.

TURKEY

Turkey's government operates on a parliamentary representative system, where a Prime Minister heads the government and a president elected by Parliament heads the state. Turkey's ethnic fractionalization is measured at 0.229, which is the lowest among the three cases in this study. Its natural resource wealth is consistently much lower than the other two cases at less than one percent of the country's GDP for the entire time period. Turkish citizens initially had access to "multiple privately owned national television stations and up to 300 private regional and local television stations, multi-channel cable TV subscriptions, [and] more than 1,000 private radio broadcast stations."[18] Over the time period of this study, however, the government took measures to limit access to mainstream media. The GDP per capita in Turkey is very much comparable to the average GDP per capita for all nations in the world over the time period. Turkey begins as the most democratized nation in the study but becomes drastically more autocratic over the course of the study; it exhibits the widest range in Polity scores.[33]

Turkey Social Media, Protest, and Censorship Events

Table 3 provides a summary of the timeline, social media events, and government response for Turkey. The full description of events follows below.

Approximate Time Period	Description of Social Media Use	Government Response
August 2011- April 2012	Criticism of government for restricting journalist access.	No censorship
June-July 2013	Organization and coverage of mass protests of Gezi Park repurposing.	Brief internet blackouts
December 2013- March 2014	Spread of tapes of Erdogan alluding to corrupt dealings in conversation.	Selective restriction of particular users
March 2014	General messages on the release of Basbug.	Continued selective restriction
August 2014	General messages on presidential election.	Continued selective restriction
June- November 2015	General messages on parliamentary election and subsequent snap election, including messages on terror attacks and journalist arrests.	No censorship (although general selective restriction continued)
July 2016	General messages on attempted military coup.	Continued selective restriction, with less enforcement
April 2017	General messages on the referendum to increase presidential power	Arrests of social media users

Table 3. Summary of Turkey Events over 2004-2007

From the period of August 2011 to April 2012, top military officials were arrested on charges of conspiring against the government. Early in 2012, the former head of Turkish armed forces General Ilker Basbug was arrested and other top officials were removed from their roles. Journalists were also arrested and were restricted access to covering military-related events.

Leaders of news agencies criticized the government on social media for one of these events, the funeral of twelve Turkish soldiers who fought in Afghanistan, where reporters were denied entry to report on the event.[34] Despite the attempted repression of mainstream news, there was no reported repression of social media.

In June and July 2013, protests surged in Gezi Park after the government announced its plans to repurpose the park. Initially, protests were peaceful in nature, but they soon became violent due to clashes with pro-government forces. Social media was key in organizing the protests, with over 20 trending hashtags including "#occupygezi". Use of Twitter surged from 1.8 million uses per day at the end of May 2013 to 10 million uses per day in June. Photos depicting police violence circulated Facebook and Twitter to encourage more protest. Of those who participated in demonstrations, 69% received their news from social media, while only 7% received news from mainstream media, over which the government had tightened its grip. Prime Minister Recip Tayyip Erdogan made several anti-social media statements. For a short period of time during the protests, Internet access was cut off in Istanbul.[35, 36]

In December 2013, tapes of Prime Minister Erdogan talking to his son, alluding to corrupt dealings, were released. Protests, in which many labeled Erdogan a "thief" and called for him to resign, ensued in the beginning of 2014. Erdogan blamed social media, including Facebook, Twitter, and YouTube, for spreading false information on the subject. Erdogan took steps to regain control over the narrative in the nation, perhaps to keep the scandal from affecting his presidential campaign later that year. In March 2014, Erdogan pushed new legislation through parliament to increase his control over the internet and especially Twitter. Interestingly, while President Abdullah Gul and other members of the government maintained their Twitter accounts, all other Turkish users were banned.[37]

In March 2014, General Ilker Basbug was released from his life sentence in prison, as a court ruled that his rights were violated in the investigation process. This came as a blow to Erdogan, who had imprisoned Basbug for conspiring against him. At the time, bans on social media were still in place.[33]

In August 2014, Turkey held its first direct presidential elections and Prime Minister Erdogan of the AKP party was elected. On the campaign trail, internet restrictions were still in place from previous events, but many users were able to easily circumvent the obstacles. Erdogan's AKP party employed its own internet force to spread positive messages about the government on social media for the users that could still access it.[37]

Parliamentary elections were held in June 2015, and the AKP party won a plurality of seats but not a majority. Parliament found itself at an impasse in electing a prime minister until August, when it decided to hold another snap election in November. The second election in November 2015 resulted in AKP earning a majority of seats, and Ahmet Davutoglu was elected prime minister. Much of the national conversation surrounding the second election had to do with a series of attacks by the Kurdistan Worker's Party (PKK).[C] Turkish security concerns led to an increased trust in the government to handle the violence, which allowed the AKP to win the seats they needed. While Erdogan continued his campaign against media outlets in other respects, no social media censorship was found in connection to messages regarding these elections, possibly because most messages being spread were in favor of the ruling party gaining the majority they needed.[33]

In July 2016, after an attempted coup d'état, President Erdogan cracked down on several thousand soldiers and media outlets. Restrictions on social media from previous events continued, but with less enforcement.[33]

In April 2017, a referendum was held to increase the executive power of the president. The government repressed both mainstream media and social media opposition to the measures increasing Erdogan's power. Over 150 journalists were imprisoned, and over 170 media outlets were closed. While social media played a vital role in spreading the oppositional messages, more than 2500 individuals had been arrested for insulting the president on social media over the six months leading up to the referendum.[38] The motion to increase executive power passed with 51.4 percent of the vote, and further protests ensued over what was considered a rigged election.[39]

Summary of Findings from Turkey

Turkey's history with social media censorship began in 2013, following the Gezi Park demonstrations, and continued intermittently over the course of the time period. In accordance with the **Mass Political Action Hypothesis**, Turkey censored social media following mass political action in the Gezi Park demonstrations and anticipated political action in Erdogan's 2014 scandal and the 2017 referendum. Interestingly, there was no specific social media censorship of discussion on the 2014 or 2015 elections, even though general restrictions are in place. Weak support is provided for the **Unlikely Action Hypothesis**. The only

[C] This reference of terror attacks is included because it dominates discussion of the November 2015 election.

events with social media discussion that did not lead to mass political action concern the imprisonment of military leaders in 2011 and 2012 and the release of General Basbug in 2014. For the former, there was no evidence of social media censorship, and for the latter, general social media restrictions were still in place following the 2014 Erdogan scandal. The **Mainstream Media Hypothesis** is strongly supported, as crackdowns on mainstream media preceded social media censorship in every case. This suggests the government's steps to curtail information available via mainstream media opened the door to restriction of social media.

VENEZUELA

Venezuela's government initially operated as a federal presidential republic, although more power becomes concentrated in the hands of the executive over the course of this study. The president acts as both head of government and head of state. Legislative power is vested in a national assembly. The level of ethnic fractionalization is between that of the other two countries, measured at 0.483. The natural resource wealth is high in this oil-rich nation throughout the time period of the study and is slightly under the resource wealth of Iran. Venezuelans have access to a mixture of state-run and private media in television and radio. While the government has always exercised heavy control on some stations, the control over private news sources varies throughout the time period of the study. The GDP per capita is about the same as the average of all other nations in the world over the time period and is very much comparable with the GDP per capita of Turkey. Venezuela experiences waves of severe and moderate levels of autocracy over the time period, with Polity scores that generally become lower over the course of the study.[40]

Venezuela Social Media, Protest, and Censorship Events

Table 4 provides a summary of the timeline, social media events, and government response for Venezuela. The full description of events follows below.

Approximate Time Period	Description of Social Media Use	Government Response
August-December 2006	Claims of government financial mismanagement during presidential election season	No censorship
June 2011-March 2013	Messages in support of Chavez throughout his battle with cancer, including during presidential election in October 2012	No censorship
April 2013	General messages on snap presidential election	Brief internet blackout
2014	Organization of mass protest and heavy criticism of government; general news about protest movement	Selective censorship of messages
February 2015	Messages about the death of teenager Kluiver Roa Nunez	Continued selective censorship from 2014
December 2015	Messages in support of opposition party in legislative election	Localized internet blackouts
Late 2016	Anti-Maduro messages	Continued selective censorship from 2014
July 2017	Opposition to Maduro's referendum to increase his power by dissolving parliament	Continued selective censorship from 2014

Table 4. Summary of Venezuela Events over 2004-2017

In the 2006 presidential election, incumbent Hugo Chavez accused his opponents of spreading false rumors of a failing financial system via the Internet and cell phones. While Chavez rebuked the claims, there was no censorship of the messages.[40]

Concerns about President Hugo Chavez's health arose in June 2011 when the leader was reportedly taken to a hospital in Cuba to be treated. This came one year before the 2012 election season. Chavez addressed the Venezuelan people on several occasions, assuring them that he was recovering well and highly optimistic about his condition. Throughout the election, Chavez actively used his Twitter account to "garnish support as well as criticize his opponent."[41] As Chavez was taken back to the hospital after the election, his supporters both rallied in the streets and "lit up social media" to show their appreciation for the leader.[42] Throughout the period from June 2011 to Chavez's death in March 2013, Chavez had high approval ratings amongst the population. No evidence of social media censorship was found.

After the death of Chavez in March 2013, a snap election was organized for April 2013, in which Chavez's successor would be decided. Throughout the election process, interim president Nicolas Maduro was in power. Social media was heavily used as a means of political conversation about the candidates, as there were over six million references of the election by over 800 thousand different users on social media.[43] With Maduro and his opponent in a close race, internet access was completely blocked for a brief period of time just before the election.[44] Maduro narrowly claimed victory, leading to small-scale oppositional protests.

In 2014, protests ensued over economic mismanagement, high inflation, rising crime rates, and electricity shortages. Only one television network, NTN24, showed coverage of the protests that took place in primarily middle-class areas, until Maduro blocked the news channel broadcast. Twitter, Facebook, and YouTube were used to fill in the gaps of information left by NTN24. The hashtag #LaSalida was used to unify protestors and call for "the exit" of Maduro from power. The government countered with the hashtag #VzlaUnidaContraElFascismo (Venezuela United Against Fascism), which labeled protestors as fascists and affirmed Maduro's power. Months before the protests began, Maduro was given permission to act without consultation of parliament in response to national crises. Using this power as protests gained strength in February 2014, Maduro began to block anti-government messages on Twitter. As early as March 2014, the regime began arresting leaders of the opposition party.[45-47]
In the December 2015 legislative elections, the opposition party was expected to gain the majority of seats. The opposition was very much active on social media, using Twitter, YouTube, and Periscope to garner support. While there was no repeat of the countrywide internet blackout of 2013, there were local internet outages in 12 of the 24 states in Venezuela at some point during the campaign process. Issues with internet access on election weekend were more prevalent in states with anti-Maduro tendencies like Zulia and Tachíra.[44]

Summary of Findings from Venezuela
Venezuela began censoring social media just before the 2013 snap presidential election and continued throughout the 2014 nationwide protests, with selective censorship in the 2015 elections. In accordance with the **Mass Political Action Hypothesis**, the Venezuelan government restricted social media following mass political action in 2014 and in anticipation of election-related action in 2013 and 2014. Interestingly, the government made no move toward censoring social media calls for pro-Chavez rallies between 2011 and 2013, which suggests that the regime strategically censored messages that were antithetical to its survival while allowing pro-regime messages to circulate. Weak support for the **Unlikely Action Hypothesis** comes from the lack of censorship in the 2006 election, when social media use was less public and less likely to lead to lead to mass political action, especially while President Chavez rebuked any claims against him on the more accessible mainstream media. However, it may also be the case that the government was simply not well-versed in social media censorship methods at the time. Strong support for the **Mainstream Media Hypothesis** comes from the government curtailing mainstream media coverage prior to the largest social media censorship occurrences in 2014. This suggests that the weakening of mainstream media was a necessary precursor to curbing social media access.

DISCUSSION

Table 5 provides a summary of the results for each case. A full discussion for each hypothesis is below.

Hypothesis	Iran	Turkey	Venezuela
Mass Political Action	Strong Support	Strong Support	Strong Support
Unlikely Action	Weak Support	Weak Support	Weak Support
Mainstream Media	Strong Support	Strong Support	Strong Support

Table 5. Summary of Results for Each Country/Hypothesis

Mass Political Action Hypothesis: When social media use encourages mass political action, regimes respond with censorship.

The evidence presented in all three cases provides strong support for the first hypothesis. The governments of all three countries repress when mass protest follows a change in landscape on social media. The examples for this are censorship in Iran following protests of the 2009 election, in Turkey during the Gezi Park demonstrations in 2013, and in the Venezuelan mass protests beginning in 2014. In contrast, social media use that did not necessarily encourage mass political action was not censored. The examples for this include criticism of the Iranian government after the 2017 earthquake and dissent on the arrests of Turkish military leaders in 2011 and 2012.

Each of the nations, in at least one case, censored social media during an election campaign. Casting a ballot is very different from participating in a rally, but it is still a political action that has an impact on whether a regime remains in power. Even without the presence of mass rallies, governments repressed social media use when they anticipated that the party in opposition was gaining leverage in a campaign. This was the case in all three nations at some point, but the 2015 elections in Venezuela lend great

support to the idea that a regime wanted to control voting outcomes, as specific states with tendencies toward anti-Maduro beliefs experienced Internet outages the most.

One qualification that should be made is that governments tend to censor social media interactions that encourage political action only when it is not in their favor. Turkey did not add to censorship of social media during the 2015 election because the social media users that expressed security concerns generally placed trust in the current government to handle threats and thus favored the regime's continuation of power. In Venezuela, social media users organized mass rallies to show support for Chavez following concerns about his health, and these were understandably favored by the government and not censored. Even though these are citizen-generated and not government-initiated activities, the government will not repress actions that are advantageous to its maintenance of power.

Unlikely Action Hypothesis: When social media use encourages mass political action that is unlikely to be realized, regimes do not respond with censorship.

Weak support for the **Unlikely Action Hypothesis** comes from the lack of censorship on calls for political action in early social media. The examples for this include the 2004 and 2005 elections in Iran and the 2006 election in Venezuela. In these early cases, social media use was not as widespread, and the government used its own platform of mainstream media to combat the calls for political action. Because the political action was unlikely to be realized, there was no push to censor the messages. While this provides support for the hypothesis, it is also possible that government officials were not yet skilled in censorship methods that would take some time to establish after new social media technology was developed. A lack of effective censorship methods may have alternately disabled them from repressing the messages.

Stronger support for this hypothesis comes from the lack of specific censorship of certain messages after a general mode of censorship is established. Because social media messages are less accessible except for by the few citizens with VPNs, governments may allow messages to circulate if they relieve pressure without rallying mass action. The allowed messages contain calls to action that are typically weaker, such as the 2012 difficulty in purchasing staples in Iran. In that case, the identifiable adversary was not a corrupt Iranian government, but it was the outside nations that sanctioned Iran and caused the high prices. Since outside nations could not be directly reproached, it is less likely that the already few people with access to social media would join the protests. As a result of a combination of these factors, the Iranian government allowed the messages. This proposed causal chain should be examined further in future studies, as there are not enough examples in this study to strongly affirm its validity.

Further analysis of this hypothesis might involve a smaller scale study of specific social media posts. Since this study examines larger social media movements, only posts that become viral are analyzed. Future studies may analyze posts that encourage action but do not become viral and compare them to viral posts for rates of censorship.

Mainstream Media Hypothesis: A regime in a nation with a strong independent mainstream media is less likely to repress social media than a regime in a nation with a weak mainstream media.

The **Mainstream Media Hypothesis** is strongly supported. Iran had a tightly state-controlled mainstream media throughout the time period of the study and also contains the earliest example of social media repression of the three nations. Iran began censoring social media in the 2008 elections, which is much earlier than Turkey and Venezuela's first instances in 2013. In both Turkey and Venezuela, the regime took measures to restrict the mainstream media before censoring social media. In fact, the rise in prevalence of social media came as a result of Erdogan censoring mainstream broadcasts of the 2013 protests in Turkey and Maduro's blocking of NTN24's coverage of the 2014 protests in Venezuela. Further, Erdogan imprisoned journalists and shut down media outlets before arresting social media users leading up to the 2017 referendum. In all of the cases examined, limitations on the mainstream media's ability to report precede and enable social media censorship, consistent with Shadmehr and Bernhardt's theoretical research.

In each case, as the regime increased control of mainstream media and social media, the nation also generally lowered in its level of democratization. A closely related subject of this research is the process by which governments become more autocratic through their responses to social media use over time. Waldner and Lust refer to this gradual decrease in the democratic qualities of a nation as "democratic backsliding."[48] Theories describing how regimes create uneven playing fields that induce democratic backsliding include control of mainstream media, but have not yet included social media.[49] Based on the findings of the third hypothesis, future theories on democratic backsliding should include thorough discussion of social media, including examining its relationship to the status of mainstream media.

CONCLUSION

The new analysis of data from Iran, Turkey, and Venezuela confirms many of the reasons for censorship of social media generated from other cases and theoretical research. The findings also shed light on specific instances in which authoritarian regimes generally repress social media use and the types of preconditions that make a regime more likely to repress.

The major proposed reason for censorship by a regime was to reduce the likelihood of mass political action triggered by social media communication. Not only was this confirmed by all cases, it was further qualified by considering elections as opportunities for political action that may trigger temporary censorship. Selective censorship by each regime confirmed and furthered Hassid's characterization of social media use as a safety valve or pressure cooker, in which regimes only censor messages that are likely to lead to their removal from power.

The evidence provided strong support for the notion that countries with strong independent mainstream media are less likely to repress social media than countries with weak mainstream media. In fact, these cases present a bright-line scenario in which limitations on mainstream media must precede social media repression.

One major limitation of this research is that it attempts to understand a process that cannot be directly observed. Decisions about censorship are made by a combination of the thought processes of the regime leader and those acting on the leader's behalf. A more complete understanding would require that Rouhani, Erdogan, and Maduro answer questions honestly in an interview, which was well beyond the scope of the available resources. Instead, this research approximates the regime's reasoning by detailing the background information behind the censorship events and attempting to connect the dots. The resulting conclusions may not be perfect, but they are indicative of patterns common to different nations.

Future research should contextualize social media censorship in terms of general decreases in democratization. Social media censorship and control of mainstream media are likely two pieces in a much larger puzzle of the process by which democratic nations backslide. Future studies should also empirically consider factors, such as the nation's natural resource wealth and citizen's individual wealth, that were used to denote differences between cases in this paper. Previous theoretical research has found that nations with higher natural resource wealth have a higher tendency to repress social media;[50] comparative study of new cases may help evaluate this hypothesis. Levels of individual wealth, indicated by GDP per capita, may also have an impact on government tendencies to repress social media.

All of these findings are significant to our understanding of when authoritarian regimes begin to repress. Social media organizations should be interested in which populations may lose access to their service based on the predictive power of the theories advanced by this research. Media freedom activists should also be interested in identifying susceptible societies and empowering citizens to maintain freedoms. The findings are pertinent to many nations in different parts of the world. Even in the nations that were studied, cases of potential social media activism and repression are ongoing—Venezuela, for example, is undergoing an economic crisis and is reportedly experiencing a resulting battle between citizens and the government over access to social media.[51] The results from these case studies have strong predictive power for similar authoritarian regimes. Analysts of social media, protest, and censorship patterns benefit from the advanced understanding of what causes regimes to repress.

REFERENCES

1. Goel, V., Kumar, H., and Frenkel, S. (2018). In Sri Lanka, Facebook contends with shutdown after mob violence. *The New York Times. www.nytimes.com/2018/03/08/technology/sri-lanka-facebook-shutdown.html.*
2. Das, S. (2017) Kashmir: govt bans Facebook, Whatsapp, Twitter and other 19 social media sites. *Livemint. www.livemint.com/Politics/VJEGyOaZ0YHhfdxzH5F0oM/JK-govt-orders-suspension-of-Internet-services.html.*
3. Specia, M., and Mozur, P. (2017) A war of words puts Facebook at the center of Myanmar's Rohingya crisis. *The New York Times. www.nytimes.com/2017/10/27/world/asia/myanmar-government-facebook-rohingya.html.*
4. Rajagopalan, M. (2018) This country's leader shut down democracy – with a little help from Facebook. *BuzzFeed. www.buzzfeed.com/meghara/facebook-cambodia-democracy?utm_term=.fnVwDr7AQK#.ohYpMDrZxm.*
5. Frenkel, S., and Benner, K. (2018) To stir discord in 2016, Russians turned most often to Facebook." *The New York Times. www.nytimes.com/2018/02/17/technology/indictment-russian-tech-facebook.html.*
6. Lohmann, S. (1994) The dynamics of informational cascades: The Monday demonstrations in Leipzig, East Germany, 1989–91. *World Politics, 47*(1), 42-101. *doi:10.2307/2950679*
7. Bellin, E. (2012) Reconsidering the robustness of authoritarianism in the Middle East: Lessons from the Arab spring. *Comparative Politics, 44*(2), 127-149. *doi:10.5129/001041512798838021*
8. Edmond, C. (2013) Information manipulation, coordination, and regime change. *The Review of Economic Studies, 80*(4 (285)), 1422-1458. *doi:10.1093/restud/rdt020*

9. Shadmehr, M., and Bernhardt, D. (2015). State censorship. *American Economic Journal: Microeconomics, 7*(2), 280-307. *doi:10.1257/mic.20130221*

10. Hassid, J. (2012). Safety valve or pressure cooker? Blogs in Chinese political life. *Journal of Communication, 62*(2), 212-230. *doi:10.1111/j.1460-2466.2012.01634.x*

11. King, G., Pan, J., and Roberts, M. E. (2013) How censorship in China allows government criticism but silences collective expression. *The American Political Science Review, 107*(2), 326-343. *doi:10.1017/S0003055413000014*

12. Aday, S., and United States Institute of Peace. (2012) Blogs and bullets II: New media and conflict after the Arab spring. (No. 80). *Washington, DC: United States Institute of Peace.*

13. Mungiu-Pippidi, A. (2013) Controlling corruption through collective action. *Journal of Democracy, 24*(1), 101-115. *doi:10.1353/jod.2013.0020*

14. Sullivan, J. (2012) A tale of two microblogs in China. *Media, Culture & Society, 34*(6), 773-783. *doi:10.1177/0163443712448951*

15. Polity IV Project, Political Regime Characteristics and Transitions, 1800-2017.

16. Fearon, J. (2003) Ethnic and cultural diversity by country. *Journal of Economic Growth, 8*(2), 195-222. Retrieved from *http://www.jstor.org/stable/40215943*

17. World Bank, and OECD. (2019). World development indicators: GDP per capita (constant 2010 US$). *World Bank. https://databank.worldbank.org/source/world-development-indicators*

18. The World Factbook. (2018). Washington, DC: Central Intelligence Agency, 2018. *https://www.cia.gov/library/publications/the-world-factbook/index.html*

19. World Bank. (2019). World development indicators: Total natural resource rents. *World Bank. https://databank.worldbank.org/source/world-development-indicators*

20. Country Watch Reviews. (2018) Political conditions Iran. *Syndigate Media Inc.* Retrieved from Lexis Nexis database at *https://advance-lexis-com.ezproxy.tcu.edu/api/document?collection=news&id=urn:contentItem:5WYG-RFC1-F11P-X163-00000-00&context=1516831*

21. Murphy, B. (2004). Poll weapons: e-mail and TV: Protagonists in Iran's election duel on Internet and in media [News Report]. *The Gazette (Montreal, Quebec).* Retrieved from Lexis Nexis database at *https://advance-lexis-com.ezproxy.tcu.edu/api/permalink/51f0f179-c55e-4e1d-b3d1-21d68897112a/?context=1516831*

22. Agence France Presse. (2005) Iranian presidential election [Newswire]. Retrieved from Lexis Nexis database at *https://advance-lexis-com.ezproxy.tcu.edu/api/permalink/d1cda89b-6e9b-41d6-a953-611e86ba91ea/?context=1516831*

23. BBC Monitoring Middle East. (2005) Iran media watch: Opinion polls on presidential election move to the Internet [News]. Retrieved from Lexis Nexis database at *https://advance-lexis-com.ezproxy.tcu.edu/api/permalink/95395b91-ffde-4be7-bcef-241f3db564b8/?context=1516831*

24. BBC Monitoring World Media. (2008) Internet messaging limited on eve of Iran elections [News]. Retrieved from Lexis Nexis database at *https://advance-lexis-com.ezproxy.tcu.edu/api/permalink/e03d619d-ca84-4504-aad1-0a68f58552bf/?context=1516831*

25. The New York Times. (2008) Iran may block internet for election [News]. Retrieved from Lexis Nexis database at *https://advance-lexis-com.ezproxy.tcu.edu/api/permalink/261d51d0-dd6e-483e-ad64-298e23599685/?context=1516831*

26. Mueller, P. S., and van Huellen, S. (2012) A revolution in 140 characters? Reflecting on the role of social networking technologies in the 2009 Iranian post-election protests: The role of social networking technologies. *Policy & Internet, 4*(3-4), 184-205. *doi:10.1002/poi3.16*

27. Berman, I. (2015) Iranian devolution: Tehran fights the digital future. *World Affairs, 178*(3), 51-57.

28. Alimardani, M. (2014) The story behind Iran's censorship redirect page. *Global Voices.* Retrieved from Lexis Nexis database at *https://advance-lexis-com.ezproxy.tcu.edu/api/permalink/97e610e2-ead0-4f78-ac14-8ebc5a013582/?context=1516831*

29. Rahimi, B. (2015) Internet censorship in Rouhani's Iran: The "Wooden sword": Media reviews. *Asian Politics & Policy, 7*(2), 336-341. *doi:10.1111/aspp.12182*

30. States News Service. (2012) Iranians reportedly protest against high food prices [Newswire]. Retrieved from Lexis Nexis database at *https://advance-lexis-com.ezproxy.tcu.edu/api/permalink/5ef7f7b9-1574-42d6-9f75-b3bc6ef4c856/?context=1516831*

31. EuroNews. (2017) Iran-Iraq earthquake: Social media images show tragic aftermath. Retrieved from Lexis Nexis database at *https://advance-lexis-com.ezproxy.tcu.edu/api/permalink/d2e6b7e4-571e-4b7e-81e8-976389297acb/?context=1516831*

32. BBC Monitoring Middle East. (2017) Iran quake triggers grief, criticism among social media users [Transcript]. Retrieved from Lexis Nexis database at *https://advance-lexis-com.ezproxy.tcu.edu/api/permalink/092e2ba9-9b72-4e55-8a49-51314b2ec32e/?context=1516831*

33. Country Watch Reviews. (2018) Political conditions Turkey. *Syndigate Media Inc.* Retrieved from Lexis Nexis database at *https://advance-lexis-com.ezproxy.tcu.edu/api/permalink/a5fde426-56ce-44c5-90a6-83e1c6fe056b/?context=1516831*

34. BBC Monitoring Europe. (2012) Paper says media faced discrimination at Turkish troops' funeral [News]. Retrieved from Lexis Nexis database at *https://advance-lexis-com.ezproxy.tcu.edu/api/permalink/6d5d5d06-7cc0-4207-be1a-83f719d7b366/?context=1516831*

35. Vatikiotis, P., and Yörük, Z. F. (2016) Gezi movement and the networked public sphere: A comparative analysis in global context. *Social Media + Society, 2*(3), 205630511666218. *doi:10.1177/2056305116662184*

36. Arda, B (2014) The Medium of the Gezi Movement in Turkey: Viral Pictures as a Tool of Resistance. APSA 2014 Annual Meeting Paper. Available at SSRN: *https://ssrn.com/abstract=2453044*

37. Saka, E. (2014) The AK party's social media strategy: Controlling the uncontrollable. *Turkish Review, 4*(4), 418.

38. Jones, D. (2017) Turkey targets social media before tight referendum. *Voice of America News*. Retrieved from Lexis Nexis database at *https://advance-lexis-com.ezproxy.tcu.edu/api/permalink/952a4d0a-7a2f-46c8-9d96-0aff76cc355b/?context=1516831*

39. Kingsley, P. (2017) Turkey arrests dozens over referendum protests. *The New York Times*. Retrieved from Lexis Nexis database at *https://advance-lexis-com.ezproxy.tcu.edu/api/permalink/e5ae3433-1e5d-461a-b483-5e9672165fc6/?context=1516831*

40. Country Watch Reviews. (2018) Political conditions Venezuela. *Syndigate Media Inc.* Retrieved from Lexis Nexis database at *https://advance-lexis-com.ezproxy.tcu.edu/api/permalink/c870b2a8-bace-4240-bf55-b97f4f9b8ef9/?context=1516831*

41. Dominguez, C. (2013) Leveraging social media: a communications tool for heads of state in Latin America. *Diplomatic Courier. https://www.diplomaticourier.com/posts/leveraging-social-media-a-communications-tool-for-heads-of-state-in-latin-america-2#.Xf-DHa9OtbI.link*

42. Agence France Presse. (2012) Venezuela's Chavez needs more cancer surgery [Newswire]. Retrieved from Lexis Nexis database at *https://advance-lexis-com.ezproxy.tcu.edu/api/permalink/46649f8d-c08a-4407-ab4f-b5b611bf8f88/?context=1516831*

43. Russia and CIS General Newswire. (2013) Maduro, Capriles have almost equal chances to win presidency in Venezuela [Newswire]. Retrieved from Lexis Nexis database at *https://advance-lexis-com.ezproxy.tcu.edu/api/permalink/06ffc18a-e9a0-4f04-a128-c2b588f7f42b/?context=1516831*

44. Hernández, M. (2015) Low bandwidth, high hopes: digital participation in Venezuelan elections. *Global Voices*. Retrieved from Lexis Nexis database at *https://advance-lexis-com.ezproxy.tcu.edu/api/permalink/f521cfc6-f0a5-497c-844b-c4368f2114e6/?context=1516831*

45. Ciccariello-Maher, G. (2014) LaSalida for Venezuela? *New York: The Nation Company L.P. https://www.thenation.com/article/lasalida-venezuela/*

46. Robertson, V. (2014) Reflections amid protests and chaos in Venezuela. *Global Voices*. Retrieved from Lexis Nexis database at *https://advance-lexis-com.ezproxy.tcu.edu/api/permalink/f255fdc0-059f-488b-9ea4-56cbb2cd0840/?context=1516831*

47. Trinkunas, H. (2014) Toward a peaceful solution for Venezuela's crisis. *States News Service*. Retrieved from Lexis Nexis database at *https://advance-lexis-com.ezproxy.tcu.edu/api/permalink/cabbfe7e-e3f1-4297-b2c9-16e425be2925/?context=1516831*

48. Waldner, D., and Lust, E. (2018) Unwelcome change: Coming to terms with democratic backsliding. *Annual Review of Political Science, 21*(1), 93-113. *doi:10.1146/annurev-polisci-050517-114628*

49. Levitsky, S., and Way, L. (2010) Democracy's past and future: Why democracy needs a level playing field. *Journal of Democracy, 21*(1), 57-68. *doi:10.1353/jod.0.0148*

50. Egorov, G., Guriev, S., and Sonin, K. (2009) Why resource-poor dictators allow freer media: A theory and evidence from panel data. *American Political Science Review, 103*(4), 645-668. *doi:10.1017/S0003055409990219*

51. Gilbert, D. (2018) Venezuela just took a huge step towards controlling all access to the internet. *VICE News. https://www.vice.com/en_us/article/59qvwz/venezuela-maduro-tor-network-censorship*

ABOUT STUDENT AUTHOR

Ezhan Hasan is a senior Political Science student at Texas Christian University, graduating in May 2020. Ezhan completed this project in Summer 2018 as part of TCU Political Science's Student Summer Research Program and has since presented at the International Studies Association- Midwest and Pi Sigma Alpha National conferences. Ezhan is currently working on his senior thesis concerning U.S. tribal law.

PRESS RELEASE

In the past 15 years, access to internet and social media has increased worldwide, making it easier to organize mass political action against the government. In response, several leaders have decided to restrict access to social media. However, very few countries restrict total access; rather, countries are selective on when, where, and how they block social media access. Combining the heavily studied case of China with knowledge of media purposes and authoritarian regime objectives, this research organizes theories of what types of factors cause regimes to censor social media. The theories are then applied to Iran, Turkey, and Venezuela over 2004 to 2017 to test and improve understandings of why regimes repress.

APPENDIX

Table of All Country Specific Data

Country/Year	Ethnic Fractionalization	Natural Resource Wealth	GDP per capita	Polity Score
Iran 2004	0.669	25.03669466	2729.838416	-6
Iran 2005		32.16971023	3215.653433	-6
Iran 2006		33.84830641	3738.689284	-6
Iran 2007		28.62496832	4857.368371	-6
Iran 2008		32.76251483	5574.410436	-6
Iran 2009		18.72480243	5619.117621	-6
Iran 2010		21.70051707	6531.92743	-6
Iran 2011		26.58457236	7729.343353	-6
Iran 2012		20.02654936	7832.902635	-6
Iran 2013		24.63678444	6036.192088	-7
Iran 2014		23.84069966	5540.984136	-7
Iran 2015		13.47160625	4862.299729	-7
Iran 2016		15.95320975	5219.109805	-7
Iran 2017		..	5415.209635	-7
Turkey 2004	0.229	0.280923761	6040.88491	7
Turkey 2005		0.283251363	7384.258482	7
Turkey 2006		0.376265044	8034.606676	7
Turkey 2007		0.42492435	9709.720022	7
Turkey 2008		0.640387247	10850.87039	7
Turkey 2009		0.383412265	9036.266711	7
Turkey 2010		0.53836334	10672.40016	7
Turkey 2011		0.706372609	11340.82362	9
Turkey 2012		0.570303282	11720.31386	9
Turkey 2013		0.48874526	12542.72153	9
Turkey 2014		0.423737215	12127.46072	3
Turkey 2015		0.295994769	10984.8052	3
Turkey 2016		0.327203284	10862.72538	-4
Turkey 2017		..	10540.618	-4
Venezuela 2004	0.483	21.79830993	4271.372404	6
Venezuela 2005		25.42053621	5432.688675	6
Venezuela 2006		23.09964189	6735.797588	5
Venezuela 2007		18.97014099	8318.803399	5
Venezuela 2008		19.00754272	11227.23138	5
Venezuela 2009		7.675022522	11536.14939	-3
Venezuela 2010		10.22749148	13545.26345	-3
Venezuela 2011		20.06330853	10741.57638	-3

Venezuela 2012		15.74842153	12755.00008	-3
Venezuela 2013		15.2813507	12237.19374	4
Venezuela 2014		10.10276639	15692.41288	4
Venezuela 2015		..	..	4
Venezuela 2016		..	..	4
Venezuela 2017		..	..	-3

Table A1. All Country Specific Data

List of Events by Country and Type

The following is a list of major political events, derived from each nation's Country Watch report, over the period of 2004 to 2017. The list is not comprehensive, but it aims to provide a representation of major events that would incite political discussion. The events are divided into categories of Domestic Affairs, International Affairs, and Elections. Domestic Affairs include changes in domestic policy, actions taken by the government within its own borders, and citizen-generated political action. International Affairs include any diplomatic or contentious dealings with other nations or international organizations (including terror organizations). Elections are specifically related to the occurrence of any election, a change in election rules, or a change in political parties. For Turkey's ongoing Kurdish conflict, all instances have been placed under the International Relations category for consistency. The reasoning for this is that although many Kurds live in Turkey, the ongoing conflict often involves neighboring countries, like Iraq, and members of the Kurdistan Worker's Party (PKK) engage with the Turkish government as a foreign entity would.

This lists of Domestic Affairs and Election Related events are annotated. All terror attacks are preceded by the letter T. Instances where social media use was not detected are preceded by the letter N. Instances that will be included within an ongoing event elsewhere are preceded by the letter E. Instances that were directly included in the case study analysis are preceded by the letter I. Since International Relations events are systematically excluded, the lists of International Relations events are generally not annotated, except for if the event was included elsewhere or it is a terror attack.

Iran—Domestic Affairs

- (N) May 2006: Members of the Azeri ethnic minority group protest a newspaper cartoon that compares them to an insect.
- (T) February 2007: Sunni Muslim group claims responsibility for attack on Iran's Revolutionary Guard, leading to 11 deaths and several subsequent clashes between militants and armed forces.
- (T) May 2009: A mosque in Zahedan, a province of primarily Sunni Muslims, was bombed, leaving around 80 casualties.
- (T) July 2010: Suicide Bomb attacks leave around 130 casualties at mosque in Zahedan.
- (E) September 2010: The pro-government Basij militia attacked the home of opposition leader Mehdi Karroubi. (part of ongoing 2009 protests)
- (T) December 2010: A suicide bombing targets the Ashura celebrations in Chabahar.
- (E) February 2011: Opposition leaders Mir Hossein Mousavi and Mehdi Karroubi are arrested after calling on Iranians to protest in the streets. (part of ongoing 2009 protests)
- (E) February 2011: Thousands of protestors march against the government in Tehran, Ishfahan, Mashhad, and Shiraz. The government deploys security forces in response. In the protest, the daughter of former president Rafsanjani was arrested. (part of ongoing 2009 protests)
- (E) Mid-2011: Well-known activist Mehdi Karroubi was reported missing, as his family and close friends had not seen him for as many as six weeks. (part of ongoing 2009 protests)
- (I) 2012: Iran reportedly has difficulty purchasing staples, such as rice and cooking oil, due to economic sanctions.
- (I) November 2017: Iran experiences earthquake.

Iran—Election Related

- (I) February - June 2004: The Council of Guardians disqualified thousands of reformist candidates from parliamentary elections. Leading intellectuals and journalists called for a boycott of the election to protest but could not penetrate mainstream media, so they used e-mails and mobile phone messages instead. Conservatives gained control of the largest portions of public office.
- (I) June 2005: Despite calls to boycott the presidential election due to disqualification of reformist and female candidates, large numbers of Iranians show at the polls to elect the conservative Mahmoud Ahmadinejad.

- (N) December 2006: Along with several moderates gaining public office, former president and moderate Akbar Hashemi Rafsanjani was elected to the Assembly of Experts.
- (I) March 2008: Conservatives maintain control of parliament after elections in March 2008.
- (I) 2009: The primary candidates in the 2009 presidential election were former Prime Minister Mir Hossein Mousavi and incumbent Mahmoud Ahmadinejad. Election turnout in June 2009 was so high that polling stations had to extend operations for several hours due to long lines of voters. After polls closed, both Ahmadinejad and Mousavi claimed victory, with no official word on the matter. Soon after, Mousavi's website was shut off, his mobile messaging cut off, social networking curtailed, and headquarters reportedly raided. Iranian state media then declared Ahmadinejad the winner. What followed was the largest series of protests in Iran since 1979, which were called the "Green Revolution" by supporters of the reformists Mousavi and Mehdi Karroubi.
- (E) February 2012: Parliamentary elections (part of ongoing response to 2009)
- (E) May 2013: Presidential elections. Hassan Rouhani is elected, and many in Iran rejoice the exit of Ahmadinejad. (part of ongoing response to 2009)
- (E) February 2016: In the parliamentary elections, several candidates are initially disqualified, but following protests, they are reinstated. (part of ongoing response to 2009)
- (N) May 2017: Presidential elections. Rouhani is re-elected.

Iran—International Relations

- February 2007: The UN deadline for Iran to suspend all nuclear activities passes, as Iran is in noncompliance.
- March 2007: 15 members of the British Navy were captured by Iranian forces.
- January 2008: The U.S. claims that 5 of its Navy ships were threatened in the Strait of Hormuz by Iranian ships.
- July 2008: U.S. begins first diplomatic talks with Iran since 1979.
- October 2009: Tensions increase with Pakistan, as Pakistan detains members of Iran's Revolutionary Guard.
- November 2011: Demonstrations against embassies of Western nations ensue, as the UK degrades its ties with Iran.
- February 2012: Israeli leadership threatens military action in response to Iran nuclear situation.
- July 2012: Israeli leadership blames Iran and Hezbollah for an attack in a Bulgarian airport.
- April-July 2015: Iran backs the rebel Houthis in Yemeni conflict.
- May-July 2015: The final round of talks on the Iran Nuclear Issue with the United States lead to the finalization of a Joint Comprehensive Plan of Action.
- October 2015: The President of Yemen cuts all diplomatic ties with Iran.
- January 2016: Saudi Arabia executes an Iranian cleric
- January 2016: 10 U.S. sailors detained by Iranian forces.
- October 2017: U.S. president decertifies the Iran nuclear deal reached in 2015.

Venezuela—Domestic Affairs

- (N) March 2006: President Hugo Chavez announces a new flag that will be gradually incorporated over the next 5 years.
- (N) January 2007: The National Assembly approves legislation that grants Chavez a bypass of parliament for executive action.
- (N) May 2007: Chavez shuts down the oldest public television station in the country. (no social media activity detected)
- (N) December 2010: An "Enabling law" is passed, granting Chavez more executive power in the face of crisis.
- (I) June 2011-March 2013: Chavez battles cancer and is taken to a hospital in Cuba. The Venezuelan leader makes several visits to and from his country during this time and continues to hold that he is not sick. Chavez is also re-elected during this time. He dies in March 2013 and is succeeded by interim replacement Nicolas Maduro.
- (E) November 2013: Maduro is given permission to act without consultation of parliament in response to national crises. (will be included in forthcoming Maduro protest)
- (I) 2014: Protests ensue over economic mismanagement, high inflation, rising crime rates, and electricity shortage. In February, social media access is blocked by Maduro. In March, mayors of the opposing party are arrested and put on trial. Protest leaders Leopoldo Lopez and Maria Corina are arrested in July and December, respectively.
- (E) February 2015: As protests of Maduro continue, teenager Kluiver Roa Nunez is killed by a police officer. Maduro condemns the death of Nunez. (included in ongoing 2014 protests)
- (E) Late 2016: Protests of the Maduro regime continue. (included as ongoing 2014 protests)

Venezuela—Election Related

- (N) February-August 2004: A petition to remove President Hugo Chavez from office by referendum vote comes to fruition. In the referendum vote, Chavez is able to maintain his position.
- (N) August 2005: Venezuelans march for electoral reform.
- (N) December 2005: Legislative elections. Voter turnout is lower than usual.
- (I) August – December 2006: Presidential election season leads to re-election of Chavez.
- (N) November – December 2007: The National Assembly moves to consolidate presidential power, including ending term limits. The move is pending approval by referendum vote in December, at which time it does not pass.
- (N) November 2008: Municipal elections. Chavez claims victory when several of his own party assume offices.
- (N) February 2009: Another referendum on ending term limits results in passing of the new policy.
- (N) September 2010: Legislative elections
- (E) October 2012: Presidential elections. Several rallies begin in September 2012. Chavez is re-elected, despite health concerns. (included in Chavez health concerns)
- (I) April 2013: Snap presidential elections. Interim president Nicolas Maduro is elected.
- (I) December 2015: Legislative elections. The opposition party gains the most seats.
- (E) July 2017: Maduro announces a referendum to dissolve parliament and give himself full control over the nation. An unofficial referendum is announced by the opposition party to rebuke Maduro's referendum. At the end of the month, Maduro's referendum gives him ultimate power to dismiss anyone from any office in the country. (included in ongoing protests since 2014)

Venezuela—International Relations

- Early 2005: Colombia allegedly encroaches onto Venezuelan territory, leading to protest.
- April – November 2005: A series of events lead to worse relations with the United States. In April, the U.S. secretary of state called Venezuela a negative influence in South America and began to monitor arms sales to the country. In May, Venezuelans demonstrated against the U.S. not returning alleged terrorist Luis Posa Carriles to Venezuelan custody. In July, Venezuela began to investigate the U.S. Drug Enforcement Agency's involvement in the country as an alleged spy operation. In August, U.S. citizen Pat Robertson called for Chavez's assassination, and Venezuela charged him with a terror threat, but the U.S. did not turn him over. In September, Chavez spoke against the U.S. at the UN assembly. In November, Chavez led an anti-U.S. rally in Argentina.
- April 2006: U.S. ambassador is pelted with fruit in Caracas.
- July 2006: Venezuela applies to join South American Mercosur trade bloc
- September 2006: Chavez once again bashes the U.S. in front of the UN.
- November 2006: A bid for Venezuela to gain a non-permanent seat on the UN Security Counsel ends in failure.
- November 2007: Chavez freezes bilateral ties with Colombia and stops negotiating the release of hostages by FARC, leading to protests outside his home.
- January – June 2008: Chavez begins talks with Colombia again, with aims to have hostages released to their families
- September – December 2008: A series of increased ties with Russia. In September, Chavez meets with Russian president. In December, the two nations begin joint military exercises and Russia sells weaponry to Venezuela.
- November 2009: Due to conflict with Colombia, Mercosur members revisit decision to allow Venezuelan entry.
- July 2012: Venezuela is granted entry into Mercosur after Paraguay is removed from trade bloc.
- March 2015: U.S. places sanctions on six officials in Venezuela.
- August 2017: U.S. president says he would not rule out military option in Venezuela

Turkey—Domestic Affairs

- (N) January 2004: Turkey bans the death penalty
- (T) March, July 2004: Terrorist attacks in Istanbul
- (N) 2005-2006: several writers and journalists jailed, including Hrat Dink and Orhan Pamuk.
- (N) May 2006: Judge Mustafa Ozbilgin shot and killed by someone alleged to be protesting his secular ruling on headscarves.
- (N) January 2007: Hrat Dink assassinated. The trial was set for July 2007.
- (T) June - July 2008: A series of terror attacks, including an attack on the U.S. consulate in June and another in Istanbul in July.

- (N) July 2008: The Justice and Development Party was put on trial for its religious leanings. It was at risk of being completely disbanded for violating the Turkish tradition of secularism. Because of a technicality, it is allowed to continue to exist.
- (N) December 2009: The Turkish Constitutional Court bans the Kurdish nationalist Democratic Society Party.
- (N) December 2009 – February 2010: A series of arrests of top military officials allegedly conspiring against Turkish leadership.
- (T) October 2010: Suicide bombing in Istanbul.
- (I) August 2011 – April 2012: Several more generals were arrested in anti-government conspiracies, including one prominent General Basbug.
- (I) June - July 2013: Demonstrations surged in Gezi Park after government plans to repurpose the park. The mass rallies were fueled by social media, and Prime Minister Tayyip Erdogan sent several warnings for protests to cease. In July, a court ruled against the changes to the park, but protests and clashes with police continued afterward.
- (I) December 2013 – March 2014: Tapes were released in December 2013 of Prime Minister Erdogan talking to his son, alluding to corrupt dealings. Protests ensued in the beginning of 2014. 350 police officers were dismissed or reassigned positions by Erdogan. In order to stop the spreading information on the issue, Erdogan shut down Twitter in March 2014. Erdogan would be running for president later in 2014.
- (I) March 2014: In 2013, General Basbug was sentenced to life in prison, but he was released on a technicality in March 2014.
- (E) September – October 2015: President Erdogan tightens his grip on the media, as more journalists are arrested. (included in series of earlier censorships)
- (I) July 2016: A military coup was attempted, and subsequently several media outlets were shut down.

Turkey—Election Related

- (N) May - July 2007: Parliament was set to elect a president in May but could not come to an agreement. The country's officials agreed to move parliamentary elections that were originally scheduled for November to July. The July elections for parliament were won by the Justice and Development Party (AKP), and they appointed Abdullah Gul as president.
- (N) September 2010: In a referendum vote, voters approved constitutional amendments that gave the ruling party more power over state institutions.
- (N) June 2011: Parliamentary elections.
- (I) August 2014: Turkey had its first direct presidential elections and Prime Minister Tayyip Erdogan of the AKP party was elected.
- (I) June 2015 – November 2015: Parliamentary elections were held in June, and the AKP party won a plurality of seats but not a majority. Parliament found itself at an impasse in electing a prime minister until August, when they decided to hold another snap election in November. That election resulted in AKP earning a majority of seats, and Ahmet Davutoglu was elected prime minister.
- (I) April 2017: A referendum was held to increase the executive power of the president. With a 51.5 percent vote, the motion passed.

Turkey—International Relations

- October – December 2004: Turkey's attempt to become a member-state of the EU is unsuccessful, as Cyprus is added instead.
- May 2006: Turkish and Greek planes collide.
- June 2006: A meeting in Luxemburg to discuss whether Turkey will join as a member-state.
- October 2006: The Kurdistan Worker's Party (PKK) calls for a ceasefire after ongoing conflict. Their request is rejected by the Turkish government.
- November 2006: Pope Benedict XVI visits Turkey.
- (T) Early 2007: a series of attacks ensue allegedly by members of the PKK.
- (T) September – December 2007: More attacks by members of PKK, including in Sirnak and on the border with Iraq in September and October, respectively. The Turkish government calls for the rebels to be overturned by the Iraqi government and threatens airstrikes if the request is not met. Turkey engages in airstrikes against Iraq in December.
- October 2009: Turkey and Armenia re-establish ties after longtime cold relations.
- September 2011: Turkish government challenges Israel's blockade of Gaza.

- June – December 2012: A series of conflicts with Syria occurs. A Turkish jet is shot down by Syrian forces in June. Turkish security officials force a Syrian jet to land in October. Syrian mortar fire kills five on the Turkish-Syrian border in October. Turkey authorizes military action on Syria in October and is backed by the U.S. in this endeavor in December.
- (E) July - September 2015: A series of terror attacks occur, in which both the PKK and ISIS are separately allegedly responsible. In some cases, a group claims responsibility, but in others, like an October attack on a peace rally in Ankara, it is unknown who is responsible. The Turkish response is primarily focused on the PKK (included as part of discussion of 2015 elections)
- October – December 2015: Russia violates Turkish airspace on separate occasions during these three months, leading to tense relations between the two nations.
- (T) January – June 2016: Another series of terror attacks occurs. President Tayyip Erdogan blames the Kurds, although it is unclear who is responsible in some cases.
- (T) August 2016: ISIS is found to be responsible for an attack on a wedding.
- December 2016: The Russian Ambassador to Turkey is assassinated.
- (T) January 2017: An investigation into a nightclub attack finds a Central Asian terror organization to be responsible.

Investigation of Constant Volume and Constant Flux Initial Conditions on Bidensity Particle-Laden Slurries on an Incline

Dominic Diaz, Jessica Bojorquez, Joshua Crasto, Margaret Koulikova, Tameez Latib, Aviva Prins, Andrew Shapiro, Clover Ye, David Arnold, Claudia Falcon, Michael R. Lindstrom, Andrea L. Bertozzi*

Department of Mathematics, University of California, Los Angeles, CA

https://doi.org/10.33697/ajur.2019.029

Students: dominicdiaz@g.ucla.edu, jessicarbojorquez@gmail.com, jcrasto@ucla.edu, m.koulikova@ucla.edu, tameezlatib@gmail.com, aviva@avivaprins.com, alshap1010@yahoo.com, clover1869@ucla.edu*
Mentors: darnold@math.ucla.edu, cfalcon@math.ucla.edu, mikel@math.ucla.edu, bertozzi@math.ucla.edu

ABSTRACT
Particle-laden slurries are pervasive in both natural and industrial settings, whenever particles are suspended or transported in a fluid. Previous literature has investigated the case of a single species of negatively buoyant particles suspended in a viscous fluid. On an incline, three distinct regimes emerge depending on the particle concentration and inclination angle: settled (where particles settle and there is a pure fluid front), well-mixed (where particle concentration is constant throughout), and ridged (where a particle-rich ridge leads the flow). Recently, the same three regimes were also found for constant volume two species bidensity slurries. We extend the literature on bidensity slurries by presenting results on constant volume and a new type of initial condition: constant flux, where slurry is pumped onto the incline at a constant rate. We present front positions of the slurries and compare them to theoretical predictions. In addition, height profiles (film thicknesses) are also presented for the constant flux case, showing the distinct behavior of the ridged regime. We find that for constant flux conditions the settled regime forms for small particle volume fractions and inclination angles while the ridged regime forms for large corresponding values. Intermediate values of these two parameters are shown to produce a well-mixed regime.

KEYWORDS
Thin Films; Particle-Laden Flow; Multiphase Fluids; Interfacial Flows; Particle Segregation

INTRODUCTION

A thin film of viscous fluid flowing down an incline has been observed experimentally and analyzed mathematically.[1] In nature, instead of being observed as pure fluids, fluids are more often observed as mixtures of various fluids and other particles. Expanding the work done by Huppert,[1] many studies have investigated thin, particle-laden slurries, which are mixtures of particles suspended in a fluid. Thin films of monodisperse particle-laden slurries (viscous fluids mixed with only a single type of particle) have been extensively studied both theoretically and experimentally.[2–8] The mathematical equations governing the flow of these slurries become increasingly complex as we add more species of particles to the mixture, but the solutions become more relevant to the fluids we observe in industrial and natural settings (such as in spiral particle separators, landslides, and mud).[9–13]

Bidensity particle-laden slurries, which are the focus of this study, are mixtures of two species of particles—with different densities and similar diameters—suspended in a viscous fluid. When an initially uniformly mixed slurry flows down an incline, the particles experience a fast initial equilibration period (this has been investigated for the monodisperse case,[14] but we assume similar results apply to the bidensity case we investigate here). During this period, particles in the mixture experience two significant and opposing effects whose relative strengths determine the long term behavior of the particles in the direction normal to the incline: sedimentation due to gravity (towards the incline surface)[15, 16] or shear-induced migration,[17, 18] which leads particles away from areas of high shear rate and high particle concentra-

tion (away from the incline surface). Depending on which effect dominates, there are three possible regimes that can arise: ridged, well-mixed, and settled. The ridged regime occurs when shear-induced migration dominates gravitational settling, and is identified by a high concentration of particles on the front edge of the fluid, forming a leading ridge. In the settled regime, where gravity dominates shear-induced migration, particles form a sediment at the bottom of the fluid as it flows down the track. Within this regime for a bidensity slurry, separation between different particles and fluid can be observed. The well-mixed regime, a transient state between the other two regimes,[4] is formed when neither of these effects dominate and particles stay evenly distributed throughout the fluid.

These three regimes have been extensively studied in the monodisperse (single particle species) case for a constant volume of fluid[3–5, 8] and in the bidensity case for a constant volume of fluid.[19] Murisic *et al.*[4] constructed a regime phase diagram for a specific fluid viscosity and particle diameter with varying particle volume fraction and angle of inclination. They find that the ridged regime tends to form for high inclination angle and particle concentration while the settled regime tends to form for small inclination angle and particle concentration. This result comes from the effect of shear-induced migration increasing with greater angle and/or particle concentration. The bidensity, constant volume case was then studied theoretically[20, 21] and experimentally[19]. In particular, Lee *et al.* observes the formation of the three regimes for various inclination angles and heavy-to-light particle ratios.[19]

In addition to observing regime formation of thin viscous slurries on an inclined surface, various studies have also investigated how the fluid's average front position evolves with time. For a constant volume of viscous fluid, Huppert[1] finds that the fluid's average front position evolves with a behaviour asymptotic to $t^{1/3}$ (where t is time). In both the monodisperse[5] and bidensity[21] case for a finite volume of fluid, it has been shown that the average front position is still asymptotic to $t^{1/3}$.

In the current study, we first extend the constant volume results presented in Lee *et al.*[19] and Wong *et al.*[21] by explicitly presenting experimentally found front velocities for bidensity particle-laden slurries. We then directly extend these results to a new type of initial condition: a constant flux condition, where slurry is pumped onto the top of the inclined surface at a constant rate. For this initial condition, we consider the results of Lee's model for particle distribution normal to the place of the track[20] and expect similar regime phenomena to arise. We present the experimentally found front positions and regime classifications for bidensity, constant flux slurries to examine the effect the initial condition has on the dynamics of the slurry. While much of the literature focuses on front position and regime classification, we additionally present height profiles of the bidensity, constant flux slurries.

METHODS AND PROCEDURES

Materials

The mixtures used in our experiments consisted of glass and ceramic beads suspended in a silicone oil. The particles, manufactured by Ceroglass, are described in **Table 1**. There is a slight disparity in the average diameter of the two particles although we assume that their diameters are the same for the purposes of this paper. For constant volume experiments, red ceramic beads were used to emphasize the separation of distinct fronts, while for constant flux experiments, red ceramic beads were used in some experiments and white ceramic beads were used in others. The viscous fluid we used was polydimethylsiloxane (see the last row of **Table 1** for properties).

Material	Density	Color	Other Properties
GSB-7 glass beads	2.5 g/cm^3	white	diameter: 0.18 - 0.25 mm
SLZ-2 ceramic beads	3.8 g/cm^3	red	diameter: 0.125 - 0.25 mm
polydimethylsiloxane (PDMS)	0.971 g/cm^3	clear	kinematic viscosity: 10 cm^2/s

Table 1. Materials used in our experiments. The density and diameter are the same for all experiments. Note that for some of the constant flux experiments, the color of the ceramic particles was white.

Conducting the experiments

In this study we performed a series of experiments on gravity driven bidensity slurries flowing on an incline. We varied four parameters for each experiment: inclination angle of the track α, the volume fraction ratio of lighter density particles (glass) to heavier density particles (ceramic) χ, total particle volume fraction ϕ, and the initial condition (either constant volume or constant flux). We define the volume fraction of glass and ceramic particles respectively as:

$$\phi_g = \frac{V_g}{V_g + V_c + V_f}, \qquad \phi_c = \frac{V_c}{V_g + V_c + V_f}. \qquad \textbf{Equation 1.}$$

Where V_g is the volume of glass particles, V_c is the volume of the ceramic particles, and V_f is the volume of fluid in the mixture. We additionally define the total particle volume fraction as the sum of the two particle volume fractions:

$$\phi = \phi_g + \phi_c. \qquad \textbf{Equation 2.}$$

We define the volume fraction ratio χ as the ratio of ϕ_g to the total volume fraction, $\phi_g + \phi_c$:

$$\chi = \frac{\phi_g}{\phi_g + \phi_c} = \frac{V_g}{V_g + V_c}. \qquad \textbf{Equation 3.}$$

The two initial conditions—constant volume or constant flux—are defined in terms of their nondimensional height by the following two equations, respectively:

$$h(x, t=0) = \begin{cases} 0 & \text{if } x < -l \\ 1 & \text{if } -l \le x \le 0 \\ 0 & \text{if } x > 0 \end{cases}, \quad \text{and} \quad h(x, t=0) = \begin{cases} 1 & \text{if } x \le 0 \\ 0 & \text{if } x > 0, \end{cases} \qquad \textbf{Equation 4.}$$

where x and t are nondimensional position and time, respectively. We define l as some nondimensional length, $x = 0$ as the location where the slurry starts to flow, and $t = 0$ as the time in which the slurry starts to flow. Schematic diagrams of these two initial conditions are presented in **Figure 1**.

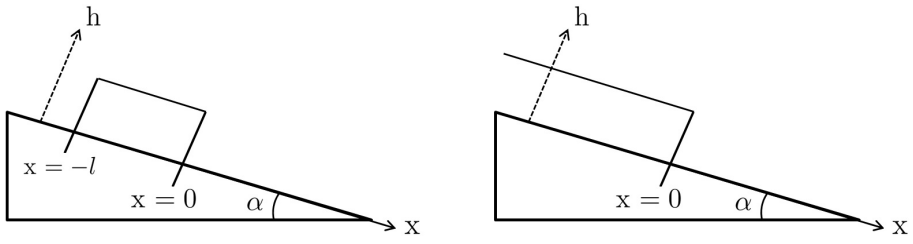

Figure 1. Schematic diagram of the constant volume (left) and constant flux (right) initial conditions.

To perform our experiments, we used an acrylic track (length 90 cm and width 14 cm) with an adjustable angle, α, (see **Figure 2**) that was adjusted to either 20° or 50° for each experiment. In the constant volume experiments, the region on the track behind the gate (see **Figure 2**, left) was filled with 80 mL of well-mixed slurry. The gate was then quickly lifted to allow the slurry to flow down the track. In the constant flux experiments, a weir was placed near the top of our track (see **Figure 2**, right). On the portion of the track above the weir, we constantly pumped well-mixed slurry onto the track. The purpose of the weir was to ensure that the slurry flowed onto the track evenly along the width of the track (y-axis). The volume of slurry entering the track over time was constant at around 3 cm^3/s for $\phi = 0.25$ experiments and around 0.75 cm^3/s for $\phi = 0.45$ experiments. Because of the weir the volumetric flux, or flow rate per unit surface, was constant at the top of the track. The length of the track (in the x-direction) is much longer than the width of the track (in the y-direction) but for the purposes of our analysis we ignore edge effects due to the walls of the track.

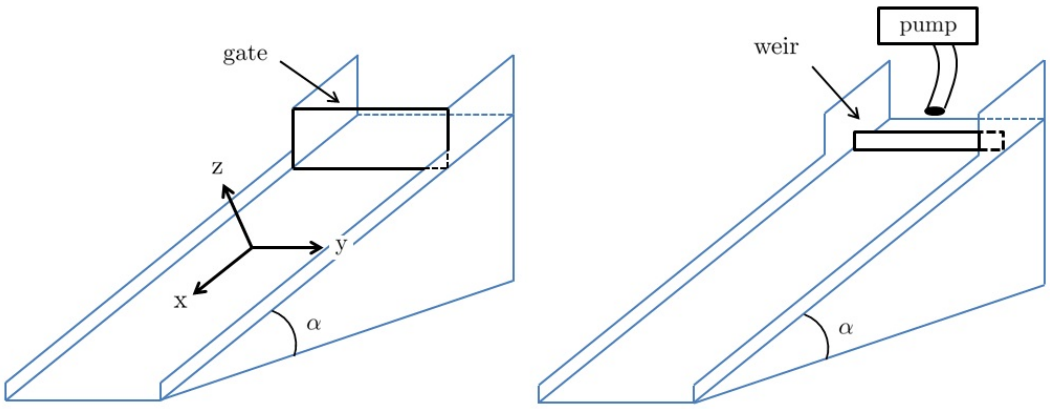

Figure 2. Schematic of our experimental setup. The left image depicts the setup for the constant volume experiments. The right image depicts the setup for the constant flux experiments. The coordinate system is kept constant for both initial conditions.

Data Analysis

We quantified the positions of the fronts and the slurry's film thickness (height profile) along the x-axis. Both methods utilized code written in MATLAB, which is summarized in **Supplement A**. In order to find the position of the individual fronts, a camera was set up above the track with the face of the lens parallel to the plane of the track, 0.5 to 1 m away. The front position was computed for individual frames of the resulting video after cropping out the background and the edges of the width of the track. We cropped out these edges to minimize the contamination of edge drag (which slows down the slurry close to the side walls [see **Figure 3**]) on our front position data since theoretical predictions do not account for wall effects. Fronts are identified using RGB values for each vertical strip of the frame. **Figure 4** shows individual frames of a settled and well-mixed experiment.

We also investigated the film thickness of the flow along the x-axis (we present pseudocode in Algorithm 2 of **Supplement A**). To do this, we first set up our camera next to the track such that the camera lens was pointed towards the track. We then shined a laser line on the middle of the track so that the line was parallel to the length of the track. The camera lens face was then made to be perpendicular to the incline so that the camera could pick up the laser line shining on the incline and its deflection due to the presence of some calibration object or the slurry on the incline. Using calibration images of the empty track and of the track with an object of known height resting on it, we were able to process the video of the experiment to obtain the film thickness. As the slurry flowed down the track, the laser line's position in each frame was deflected by the presence of the slurry. This deflection was computed using MATLAB, in mm, which resulted in figures such as **Figure 9**.

RESULTS AND DISCUSSION

Our results are divided into three sections, based on the initial condition and the type of data presented: front tracking and regime classification for constant volume experiments, front tracking and regime classification for constant flux experiments, and film thickness for constant flux experiments. For each experiment, the inclination angle α, volume ratio χ, and total particle volume fraction ϕ were varied. Based on previous research, we expect the ridged regime to form for large α and ϕ and the settled regime to form for small α and ϕ.

Constant volume: front tracking and regime classification

We conducted experiments with a constant volume of slurry moving down an incline positioned at inclination angle, α, with particle volume ratio, χ. Pictures of the experiments are shown in **Figure 3**. With the exception of the $\chi = 0.5$ experiments (which had ϕ values of 0.25 and 0.4), all constant volume experiments had a total volume fraction of $\phi = 0.45$; this allows us to present front speeds for slurries with three different ϕ values. We chose to use distinct ϕ values for the intermediate particle volume ratio as opposed to the more extreme volume ratios that are tested because

we wanted to compare the observed regimes for experiments with only the inclination angle or the volume fraction ratio being changed significantly. In terms of the regime that formed, the two angles produced different regimes for each χ value (see **Table 2** for the classifications of the constant volume experiments). If we look at the two $\chi = 0.389$ experiments, the smaller angle produced a settled slurry while the larger angle produced a ridged slurry. Angle was not the only parameter that affected the regime. If we compare the top left experiment with the top right experiment, we see the volume fraction ratio influenced the regime of the slurry. If we compare all three of the bottom experiments, we expect that the middle experiment would have also been ridged for a ϕ value of 0.45 but because the slightly lower ϕ value of 0.4 produced a well-mixed slurry, we can also conclude that the total particle volume fraction affects the regime. It appears that all three parameters—α, χ, and ϕ—affect the regime that is formed and this result agrees with the findings of Lee *et al.*[19]

Figure 4 provides the evolution of two sample flows. In **Figure 4a** (a settled slurry), three distinct fronts formed for the PDMS, glass beads, and ceramic beads. In **Figure 4b** (a well-mixed slurry), the fluid and the particle fronts remained together. Using the front tracking technique described in the *Methods and Procedures* section we produce the blue and green dots in **Figure 4** which correspond to individual particle front positions. The leftmost two images of **Figure 4a** do not track the particle fronts well (this occurs in the beginning of most of our settled experiments due to variation of particle front color as the particles begin to settle). This error does not affect our analysis since theory only predicts asymptotic behavior after the slurry has reached equilibrium (*i.e.* towards the end of the experiment) and thus front tracking early in the experiment was not as important as later on in the experiment. Notice that in **Figure 4a**, the fluid front moved faster than the particle fronts. With the angle and particle concentrations being so low, the particles settled to the bottom of the slurry (towards the incline surface) while the fluid flowed over the settled particles, moving faster. In **Figure 4b**, we do not observe this separation; the particles stayed well-mixed throughout the fluid.

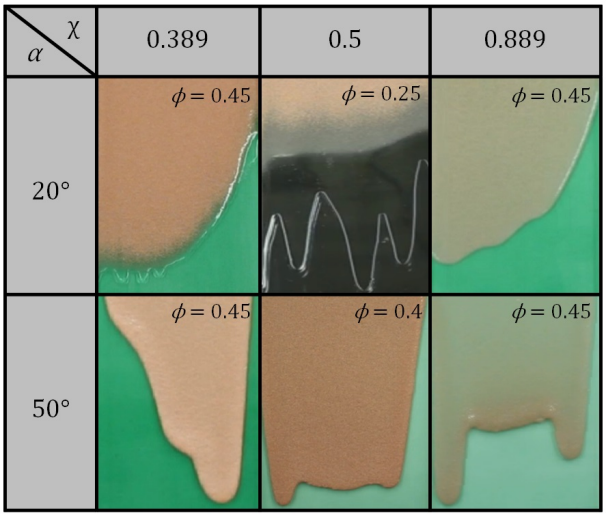

Figure 3. Experiments conducted with a constant volume of slurry. We performed six experiments in total, with three different χ values (0.389, 0.5, and 0.889) and with two different angles (20° and 50°). The total volume fraction, ϕ, for each experiment is also presented in the top right corner of each image. Note that the $(\chi, \alpha) = (0.5, 20°)$ experiment was conducted with a black background because it showed better contrast between each of the three fronts than a green background.

α \ χ	0.389	0.5	0.889
20°	settled ($\phi = 0.45$)	settled ($\phi = 0.25$)	well-mixed ($\phi = 0.45$)
50°	ridged ($\phi = 0.45$)	well-mixed ($\phi = 0.4$)	ridged ($\phi = 0.45$)

Table 2. The six constant flux experiments presented in **Figure 3** along with the observed regime and the total volume fraction of the fluid, ϕ.

According to theory, we expect the front position of the fluid to have behavior asymptotic to $t^{1/3}$, where t is time. This asymptotic behavior arises after the slurry has reached equilibrium so we fit the front position of the fluid to $x(t) = ct^{\beta} + k$ for constants c, k, and β when the slurry is approximately halfway down the incline. In **Table 3**, we present our fitted β values for each of our experiments presented in **Figure 3**. Notice that the settled experiments have fitted β values that are furthest away from our theoretically predicted value of 1/3. In these experiments, the fluid front separates from the particle front(s) and blends in with the incline making it difficult to track (see **Figure 4a**). There is strong agreement between theoretical predictions and our non-settled experimental results and we suspect that we would find better agreement for the settled experiments with either a different fluid color or a different front tracking method for settled experiments. One factor that may have had an impact on our fitted values is the presence of edge drag. Although we cropped our experimental videos to minimize its impact on our analysis, edge drag was present to varying degrees in every constant volume experiment depicted in **Figure 3** and could also have been a source of the slight deviations of our results from theoretical predictions. In **Figure 5a**, we present our experimental data against the best fit line for the $(\chi, \alpha) = (0.389, 50°)$ experiment. For most constant volume experiments, the data fits well with the fitted equations as seen in this figure. When we fit for β values with larger error, the experimental data does not align with the fitted equation as well as it does in **Figure 5a**. We generally find that the fitted experimental front positions agree, within error, with the theoretically predicted behavior.

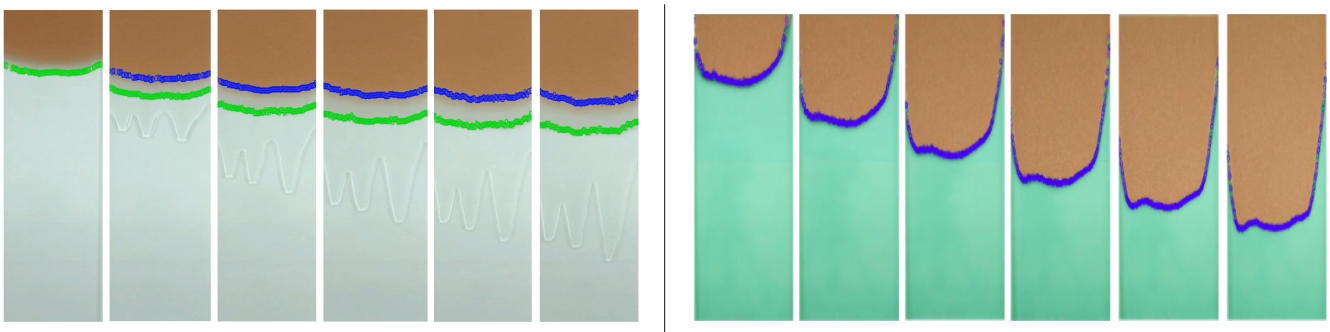

(a) $(\chi, \alpha) = (0.5, 20°)$ at 70 second intervals

(b) $(\chi, \alpha) = (0.5, 50°)$ at 12 second intervals

Figure 4. Processed video screenshots of the slurry flowing down the track. The light green and blue dots track the front position of the glass beads and ceramic beads, respectively. Throughout the course of our study, we experimented with various colored backgrounds that provided the best contrast between the fronts and the background color. We settled with a green background but present one of our early background color trials (a white background) in (a) for two reasons: (1) to show how the clear fluid blends in with the background making the fluid front difficult to track and (2) because this specific experiment produced the most symmetric and clear example of a settled slurry. Note that the first image in (a) only includes green dots since distinct fronts had not yet emerged in the experiment.

α \ χ	0.389	0.5	0.889
20°	0.19 ± 0.5	0.22 ± 0.05	0.32 ± 0.05
50°	0.31 ± 0.02	0.39 ± 0.5	0.38 ± 0.07

Table 3. Fitted β values for each of the experiments presented in **Figure 3** with their respective errors (95% confidence intervals). Theoretically, we expect our values to be around 1/3.

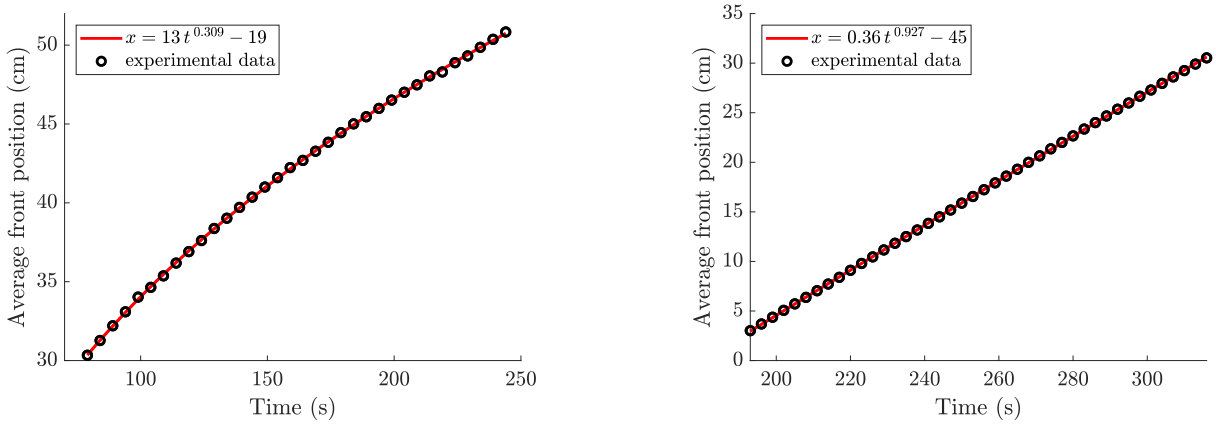

(a) constant volume fit **(b)** constant flux fit

Figure 5. Fitted equations plotted against experimental fluid front data for a constant volume and constant flux experiment, both of which are experiments in the ridged regime. (a) Corresponds to the $(\chi, \alpha) = (0.389, 50°)$ constant volume experiment while (b) corresponds to the $(\chi, \alpha) = (0.378, 50°)$ constant flux experiment.

Constant flux: front tracking and regime classification

We conducted eight constant flux experiments at different χ, α, and ϕ values, as shown in **Figure 6**. In each experiment we investigated the emergence of regimes, the front position, and film thickness (in the next section).

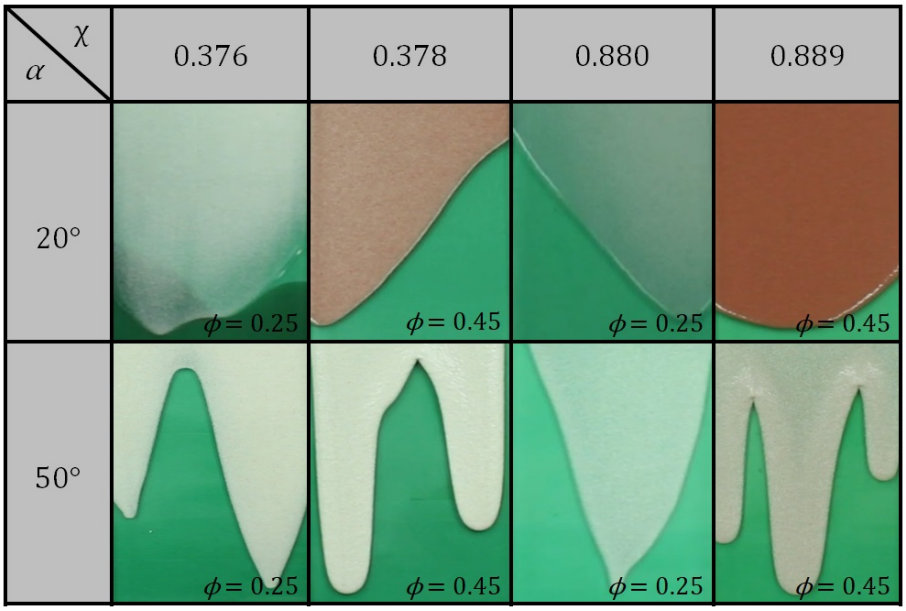

Figure 6. We performed eight constant flux experiments at four different χ values (0.376, 0.378, 0.880, and 0.889) and at two different inclination angles (20° and 50°). The ϕ value for each experiment is also presented in the bottom right corner. Each cell of the table is also classified by its regime in **Table 4**. Note that in only two of the experiments ($(\chi, \alpha) = (0.378, 20°)$ and $(\chi, \alpha) = (0.889, 20°)$) the ceramic particles are red and the glass particles are white while in the rest of the experiments both particle species are white.

Unlike constant volume experiments, we focus on two values of overall particle ratio ϕ: 0.25 and 0.45. For $\phi = 0.25$, the slurries are settled at $\alpha = 20°$, but at $\alpha = 50°$, the slurry is roughly well-mixed, possibly on the verge of a ridged regime. For $\phi = 0.45$ and $\alpha = 20°$, the slurries are well-mixed, possibly on the verge of a settled regime, while slurries at $\phi = 0.45$ and $\alpha = 50°$ are evidently ridged. While the volume fraction ratio χ is shown to have no effect on the regime (compare each of the four sets of experiments that only differ in their χ value), the angle of inclination α and

the total volume fraction ϕ do have an effect on the regime produced. To see the regime classification of each of the experiments in **Figure 6**, see **Table 4**. The transient well-mixed regime occurred frequently (half of our constant flux slurries were classified as well-mixed), indicating that some of the experiments may have ended prematurely. A longer track would allow our slurry to flow further and might lead to different regime classification in these experiments. We find that, similar to the constant volume experiments, large ϕ and α values produce a ridged regime while small corresponding values produce a settled regime for constant flux slurries. We also find that varying volume fraction ratio, χ, alone does not have a significant impact on regime formation of constant flux experiments; this contrasts with our findings that this parameter does have a significant impact on the regime formation of constant volume experiments.

α \ χ	0.376	0.378	0.880	0.889
20°	settled ($\phi = 0.25$)	well-mixed ($\phi = 0.45$)	settled ($\phi = 0.25$)	well-mixed ($\phi = 0.45$)
50°	well-mixed ($\phi = 0.25$)	ridged ($\phi = 0.45$)	well-mixed ($\phi = 0.25$)	ridged ($\phi = 0.45$)

Table 4. The eight constant flux experiments presented in **Figure 6** along with the observed regime and the total volume fraction of the fluid, ϕ.

In addition to the regime formation we investigated the fluid front position of constant flux bidensity slurries. For these experiments we again attempted to fit the front position of our fluid to an equation of the form $x(t) = ct^{\beta} + k$ for some constants c, k, and β where we now expect our β value to be 1. We present our fitted β values in **Table 5**, where we see that the β values centered around 1. We obtain loose agreement with theoretical predictions, with the settled experiment $(\chi, \alpha) = (0.376, 20°)$ producing the result furthest from our predictions. Again, this is likely due to the fluid front being difficult to track once it separates from the particle front(s). We suspect that using a non-clear fluid or a different fluid front tracking method would produce stronger agreement in this settled experiment. Similar to the constant flux experiments, edge drag may also have been a source of the slight deviations of our experimental results from theoretical predictions. To see an example fitted equation plotted against experimental data for a constant flux experiment, see **Figure 5b**. Notice that because we expect our front position to be linear (and we see linear behavior in the experimental data presented in **Figure 5b**), if we fit the front position data to some equation $x(t) = ct + k$, then c is the front speed of the slurry. For the $(\chi, \alpha) = (0.378, 50°)$ constant volume experiment (presented in **Figure 5b**), fitting to the linear equation produces a front speed of 0.22 ± 0.8 cm/s. As future work, we plan to use shock theory and numerical simulations to simulate the front velocity of the slurry and validate those numerical results against the experimentally found front velocities of the constant flux experiments presented in this paper.

α \ χ	0.376	0.378	0.880	0.889
20°	0.76 ± 0.3	0.90 ± 0.1	0.96 ± 0.1	0.91 ± 0.03
50°	1.1 ± 0.1	0.93 ± 0.09	1.18 ± 0.08	1.08 ± 0.09

Table 5. Fitted β values for each of the experiments presented in **Figure 6** with their respective errors (95% confidence intervals). We expected our values to be around 1.

One interesting phenomenon that we saw in our experiments is presented in **Figure 7**. We noticed a folding-over phenomenon in constant flux experiments for large inclination angles and total volume fractions but never in other experiments. It was also only observed between fingers in these experiments (fingers correspond to the individual streaks of fluid that run down the track) and became most prominent towards the bottom of the track. For example, in the $(\chi, \alpha) = (0.889, 50°)$ experiment, we observed the phenomenon starting to form in the corresponding image of **Figure 6** which, after some time, developed more prominently into what we present in the right image of **Figure 7**.

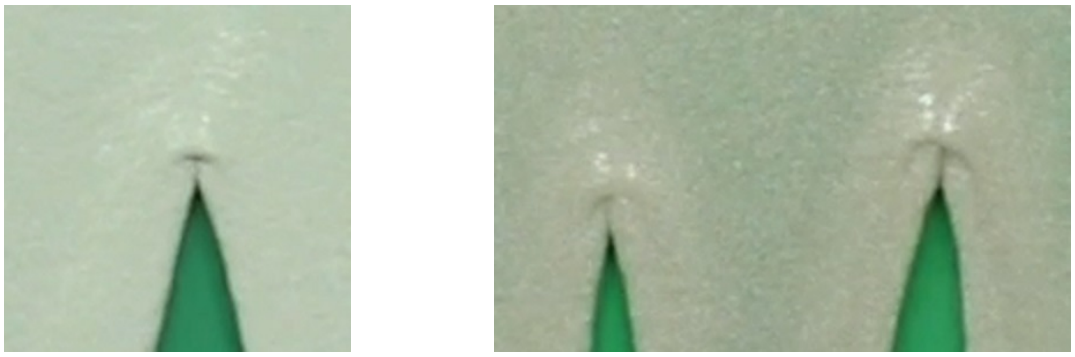

Figure 7. Two images of folding-over phenomenon occurring in constant flux experiments with large α and ϕ. Both images are zoomed in images from constant flux experiments with the left one corresponding to $(\chi, \alpha) = (0.378, 50°)$ and the right one corresponding to $(\chi, \alpha) = (0.889, 50°)$.

Constant flux: film thickness

To track the film thickness of the experiments presented in **Figure 6**, we implemented the film thickness tracking technique explained in the *Methods and Procedures* section. According to theory, we expect a distinct film thickness profile for each regime. We present the thickness of our fluid at four different times to show the evolution of the thickness for each of the three regimes in **Figures 8, 9,** and **10**. We estimate the error in the measured film thickness to be about 0.5 mm (the film thickness should be smooth because of surface tension but error is introduced because of the resolution of our images). The sequences of images in **Figures 8, 9,** and **10** are characteristic of the thickness results for the settled, well-mixed, and ridged regimes, respectively.

In most cases, we found that the settled and well-mixed film thicknesses were similar: the smallest thickness was found at the front of the fluid and it increased after the front until a certain point where it would approximately plateau. This behavior is most clearly seen in the rightmost graph of **Figures 8** and **9** although this behavior can also be seen in the other three graphs in the same figures. Considering the resolution of our images and surface tension, it is not surprising that we observe similar height profiles for the settled and well-mixed regimes. For the settled regime we expect to observe three distinct plateaus which correspond to the three fronts[21] while for the well-mixed regime we expect to observe a constant height wherever slurry is present due to the constant flux initial condition. The lack of three distinct plateaus in the settled regime is likely due to the resolution of our images while the lack of a single plateau in the well-mixed regime is likely due to surface tension. The ridged regime exhibits significantly different behavior than the other two: a tall leading ridge forms and is followed by an approximately constant plateau. This behavior agrees with the behavior of constant volume ridged slurries.

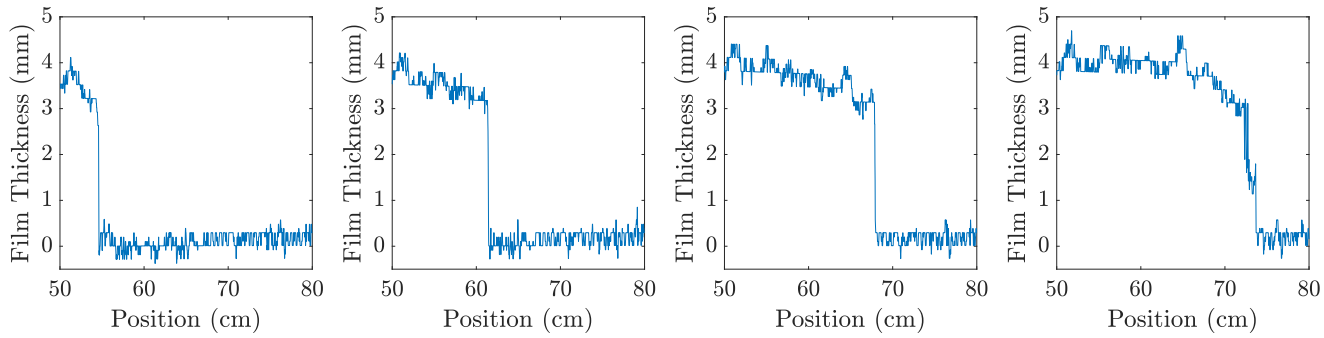

Figure 8. Film thickness of a constant flux slurry in the settled regime as it flows down an inclined track, with 30 seconds between consecutive graphs. These graphs correspond to the $(\chi, \alpha) = (0.880, 20°)$ experiment in **Figure 6**. The zero position is taken to be the location where the slurry starts to flow. Zero film thickness corresponds to positions on the track without slurry.

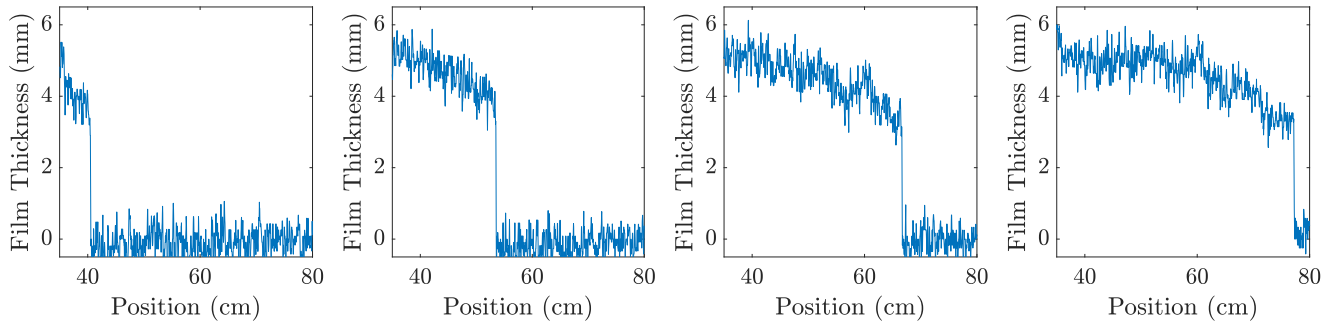

Figure 9. Film thickness of a constant flux slurry in the well-mixed regime as it flows down an inclined track, with 1 minute between consecutive graphs. These graphs correspond to the $(\chi, \alpha) = (0.378, 20°)$ experiment in **Figure 6**. The zero position is taken to be the location where the slurry starts to flow. Zero film thickness corresponds to positions on the track without slurry.

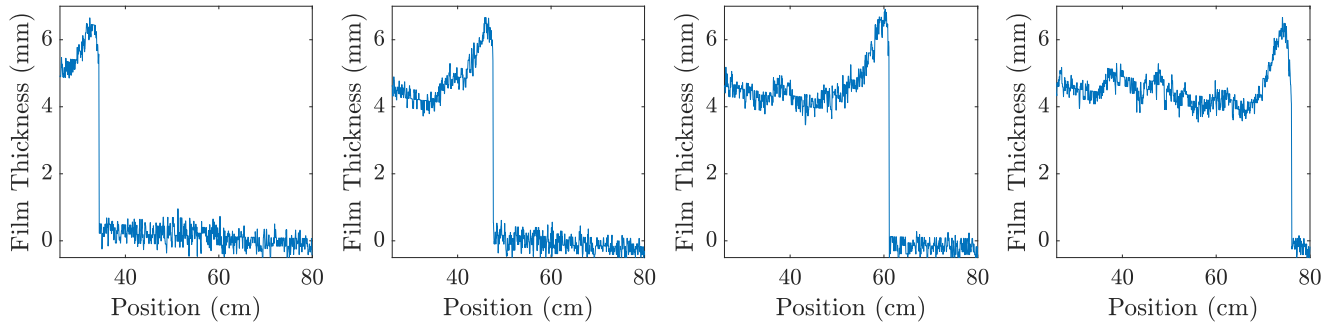

Figure 10. Film thickness of a constant flux slurry in the ridged regime as it flows down an inclined track, with 1 minute between consecutive graphs. These graphs correspond to the $(\chi, \alpha) = (0.889, 50°)$ experiment in **Figure 6**. The zero position is taken to be the location where the slurry starts to flow. Zero film thickness corresponds to positions on the track without slurry.

CONCLUSIONS

In this work we extended the existing literature on bidensity slurries flowing down an incline by analyzing both constant volume and constant flux initial conditions. We explicitly presented fitted fluid front positions and showed loose agreement with theoretical predictions ($\sim t^{1/3}$ for constant volume and $\sim t^1$ for constant flux). Regime results were also presented for both initial conditions and showed that regardless of the initial condition, large particle volume fractions and inclination angles led to a ridged slurry while small corresponding values led to a settled slurry. The ratio of lighter particles to total particles, χ, was shown to sometimes affect the regime of a constant volume slurry but had no effect on the regime of constant flux slurries, although a longer track would be required in future investigations to confirm this. Height profiles (film thicknesses) for constant flux initial conditions were similar for the settled and well-mixed regimes—a thin front increased into an approximate plateau—while the ridged regime exhibited distinct behavior—a tall leading ridge decreased into an approximate plateau.

ACKNOWLEDGMENTS

This work was funded by NSF grants DMS-1312543 and DMS-1659676. AB and CF were also funded by Simons Math + X Investigator Award number 510776. JB and AP were additionally funded by NSF grant CCF-1422795. MRL acknowledges the support of the Natural Sciences and Engineering Research Council of Canada (NSERC) [funding reference number PDF-502-479-2017]. Cette recherche a été financée par le Conseil de recherches en sciences naturelles et en génie du Canada (CRSNG) [numéro de référence PDF-502-479-2017].

REFERENCES

1. Huppert, H. E. (1982) Flow and instability of a viscous current down a slope, *Nature* 300, 427–429. *https://doi.org/10.1038/300427a0*
2. Cook, B. P., Bertozzi, A. L., and Hosio, A. E. (2008) Shock solutions for particle-laden thin films, *SIAM J Appl Math* 68(3), 760–783. *https://doi.org/10.1137/060677811*
3. Ward, T. , Wey, C. , Glidden, R., Hosoi, A. E., and Bertozzi, A. L. (2009) Experimental study of gravitation effects in the flow of a particle-laden thin film on an inclined plane, *Phys Fluids* 21(8), 083305. *https://doi.org/10.1063/1.3208076*
4. Murisic, N., Ho, J., Hu, V., Latterman, P., Koch, T., Lin, K., Mata, M., and Bertozzi, A. L. (2011) Particle-laden viscous thin-film flows on an incline: Experiments compared with a theory based on shear-induced migration and particle settling, *Phys D* 240(20), 1661–1673. *https://doi.org/10.1016/j.physd.2011.05.021*
5. Murisic, N., Pausader, B., Peschka, D., and Bertozzi, A. L. (2013) Dynamics of particle settling and resuspension in viscous liquid films, *J Fluid Mech* 717, 203–231. *https://doi.org/10.1017/jfm.2012.567*
6. Cook, B. P. (2008) Theory for particle settling and shear-induced migration in thin-film liquid flow, *Phys Rev E* 78(4), 045303. *https://doi.org/10.1103/PhysRevE.78.045303*
7. Wang, L., Mavromoustaki, A., Bertozzi, A. L., Urdaneta G., and Huang, K. (2015) Rarefaction-singular shock dynamics for conserved volume gravity driven particle-laden thin film, *Phys Fluids* 27(3), 033301. *https://doi.org/10.1063/1.4913851*
8. Zhou, J., Dupuy, A., Bertozzi, A. L., and Hosoi, A. E. (2005) Theory for shock dynamics in particle-laden thin films, *Phys Rev Lett* 94(11), 117803. *https://doi.org/10.1103/PhysRevLett.94.117803*
9. Lee, S., Stokes, Y., and Bertozzi, A. L. (2014) Behavior of a particle-laden flow in a spiral channel, *Phys Fluids* 26(4), 1661–1673. *https://doi.org/10.1063/1.4872035*
10. Arnold, D. J., Stokes, Y. M., and Green, J. E. F. (2015) Thin-film flow in helically-wound rectangular channels of arbitrary torsion and curvature, *J Fluid Mech* 764, 76–94. *https://doi.org/10.1017/jfm.2014.703*
11. Arnold, D. J., Stokes, Y. M., and Green, J. E. F. (2017) Thin-film flow in helically wound shallow channels of arbitrary cross-sectional shape, *Phys Fluids* 29(1), 013102. *https://doi.org/10.1063/1.4973670*
12. de Rooij, F. (2000) Sedimenting particle-laden flows in confined geometries, *http://131.111.17.133/lab/people/sd103/papers/Theses/FransDeRooij1999.pdf* (accessed Aug 2018).
13. Parsons, J. D., Whipple, K. X., and Simoni, A. (2001). Experimental study of the grain-flow, fluid-mud transition in debris flows, *J Geol*, 109(4), 427–447. *https://doi.org/10.1086/320798*
14. Wong, J. T., Lindstrom, M. and Bertozzi, A. L. (2019) Fast equilibration dynamics of viscous particle-laden flow in an inclined channel, *J Fluid Mech* 879, 28–53. *https://doi.org/10.1017/jfm.2019.685*
15. Richardson, J. F. and Zaki, W. N. (1954) The sedimentation of a suspension of uniform spheres under conditions of viscous flow, *Chem Eng Sci* 3(2), 65–73. *https://doi.org/10.1016/0009-2509(54)85015-9*
16. Schaflinger, U., Acrivos, A., and Zhang, K. (1990) Viscous resuspension of a sediment within a laminar and stratified flow, *Int J Multiph Flow* 16(4), 567–578. *https://doi.org/10.1016/0301-9322(90)90017-D*
17. Phillips, R. J., Armstrong, R. C., Brown, R. A., Graham, A. L., and Abbott, J. R. (1992) A constitutive equation for concentrated suspensions that accounts for shear-induced particle migration, *Phys Fluids A* 4(1), 30–40. *https://doi.org/10.1063/1.858498*
18. Leighton, D. and Acrivos, A. (1987) The shear-induced migration of particles in concentrated suspensions, *J Fluid Mech* 181, 415–439. *https://doi.org/10.1017/S0022112087002155*
19. Lee, S., Mavromoustaki, A., Urdaneta, G., Huang, K., and Bertozzi, A. L. (2014) Experimental investigation of bidensity slurries on an incline, *Granul Matter* 16(2), 269–274. *https://doi.org/10.1007/s10035-013-0480-2*
20. Lee, S., Wong, J., and Bertozzi, A. L. (2015) Equilibrium theory of bidensity particle-laden flows on an incline, in *Mathematical Modelling and Numerical Simulation of Oil Pollution Problems* (Ehrhardt, M., Ed.) 1st ed., 85–97, Springer, New York. *https://doi.org/10.1007/978-3-319-16459-5*$_4$

21. Wong, J. T., and Bertozzi, A. L. (2016) A conservation law model for bidensity suspensions on an incline, *Phys D* 330(1), 47–57. *https://doi.org/10.1016/j.physd.2016.05.002*

ABOUT THE STUDENT AUTHORS

All undergraduate authors either currently attend or have graduated from the University of California, Los Angeles. Dominic Diaz graduated in June 2019 with a B.S. in Applied Mathematics and Physics and is currently pursuing a Ph.D. in Applied Mathematics at Cornell University. Jessica Bojorquez graduated in June 2018 with a B.S. in Mathematics in Computation and is currently a software engineer for Raytheon in Los Angeles, CA. Josh Crasto graduated in June 2018 with a B.S. in Applied Mathematics and is currently a software engineer for Macquarie Bank in Houston, TX. Margaret Koulikova graduated in June 2019 with a B.S. in Applied Mathematics and Statistics and is currently pursuing a Masters in Financial Mathematics at the University of Chicago. Tameez Latib will graduate in June 2020 with a B.S. in Applied Mathematics and Computer Engineering. Aviva Prins graduated in June 2019 with a B.S. in Applied Mathematics and is currently pursuing a Ph.D. in Computer Science at University of Maryland, College Park. Andrew Shapiro graduated in Winter 2019 with a B.S. in Applied Mathematics and is currently pursuing a Ph.D. in Statistics at UCLA. Clover Ye graduated in June 2018 with a B.S. in Applied Mathematics and Psychology and is currently pursuing a Masters in Mathematics at New York University.

PRESS SUMMARY

Particle-laden slurries persist in various settings, whenever particles are mixed or transported within a fluid. Here we investigate the properties of slurries with two particle species of different density mixed within a viscous fluid on an incline. We investigate two initial conditions—constant volume (a fixed amount of mixture) and constant flux (mixture being continuously pumped onto the incline)—and how they affect the phenomena that arise while flowing down the incline. Specifically, we fit for the position of the front of the fluid, fit for the thickness of the fluid (for the constant flux condition), and classify the qualitative features of the flow based on the location of the highest concentration of particles. These findings show that for both initial conditions the qualitative features of the flow can vary drastically depending on the number of particles within the mixture and the incline angle.

APPENDIX: FRONT POSITION AND FILM THICKNESS CODES

We present a pseudocode for how we compute the front position of each individual fluid and particle front in Algorithm 1. In front tracking experiments, we placed the camera above the incline with the lens face parallel to the incline. Our track had a middle section for the slurry to flow down and a left section with equally-spaced measurement lines (see **Figure 11a**, a well-mixed slurry flowing down the incline). We present the cropped and rotated image of the slurry and measurement lines in **Figure 11b**. We present the same image with RGB values converted to HSV values and example clicks to find the maximum and minimum HSV values for each front in **Figure 11c**. For a settled slurry, the user should click 10-15 times for each distinct front.

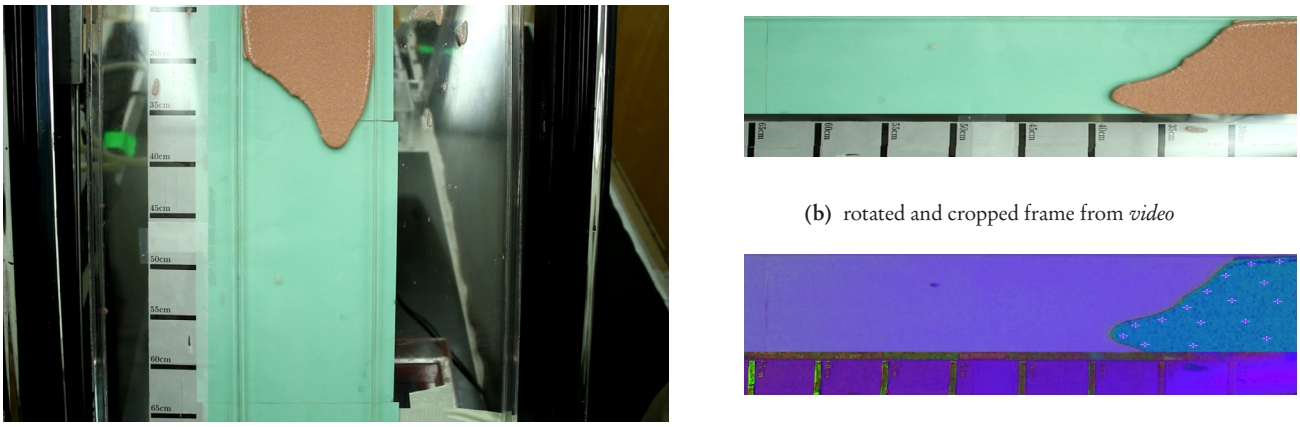

(a) unprocessed frame from *video*

(b) rotated and cropped frame from *video*

(c) HSV image with example clicking points

Figure 11. Images used in our front tracking code. (a) is an unprocessed image of the slurry flowing down the incline with measurement lines next to the slurry. (b) is a rotated and cropped version of (a). (c) is the same as (b) but with RGB values converted to HSV values and example clicks.

We present a pseudocode for how we compute the film thickness (height profile) of our slurries in Algorithm 2. To see example images that the code uses, see **Figure 12**. In these experiments, the camera must be in the same position for the *ref_image*, *cal_image*, and experimental *video*—next to the incline, with the camera lens face perpendicular to the incline so that the camera can pick up the laser line deflection due to the calibration object and the slurry.

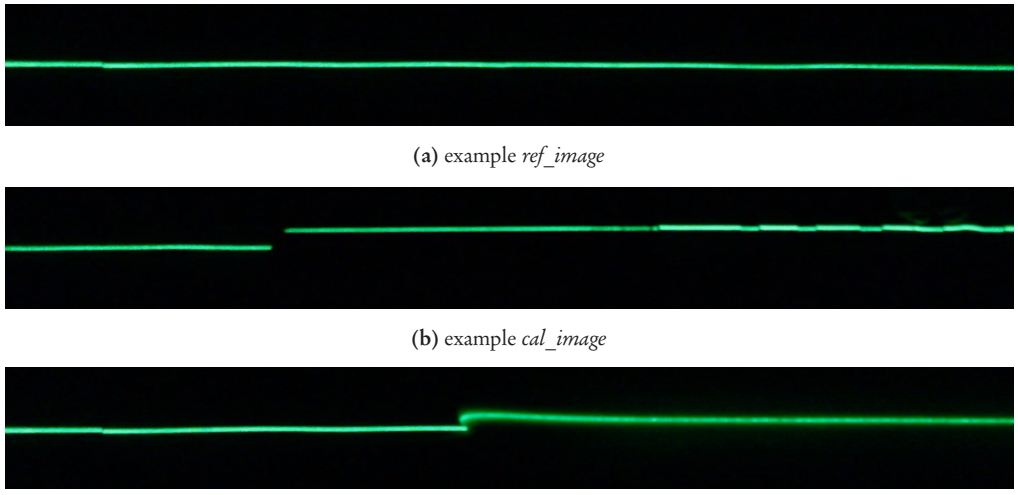

(a) example *ref_image*

(b) example *cal_image*

(c) example screenshot from experimental *video*

Figure 12. Images used in the height profile (film thickness) code. The three images are all taken from the same position and the slurry in (c) is flowing from right to left.

Algorithm 1 Front Position

function FRONT_POSITION(*video*,*n*,*m*)
  input: *video* video of the slurry moving down the track (**Figure 11a**)
    n number of frames to split the video into
    m number of fronts to process
  output: position of the front(s) over time

  function PROCESS_VIDEO(*video*,*n*,*m*)
    split the video into n equally-spaced frames
    for $i = 1, \ldots, n$ **do**
      rotate i^{th} frame such that the flow direction is pointing left
      crop i^{th} frame to only include the track and measurement lines (**Figure 11b**)
      save i^{th} frame as *frame*(i)
    output: *frame*(1), . . . , *frame*(n)

  function IDENTIFY_FRONT(*frame*(1), . . . , *frame*(n), n, m)
    for $i = 1, \ldots, m$ **do**
      click at about 10-15 points in the i^{th} front in *frame*(n) (**Figure 11c**)
      store the maximum and minimum HSV color value for i^{th} front
    for $i = 1, \ldots, n$ **do**
      let $p =$ the number of horizontal pixel rows in *frame*(i)
      for $j = 1, \ldots, m$ **do**
        for $k = 1, \ldots, p$ **do**
          find left-most pixel in the k^{th} pixel row of *frame*(i) within j^{th} HSV range
          save x-position (horizontal pixel position) of left-most pixel to $P_x(i, j, k)$
    average $P_x(i, j, k)$ over the third index and save averages into $\bar{P}_x(i, j)$
    output: $\bar{P}_x(i, j)$

  function CONVERSION_AND_PLOT(*frame*(n))
    prompt user to click on the measurement lines in *frame*(n)
    assign length measurement to each measurement line click (0 cm, 5 cm, . . .)
    interpolate between clicks such that each pixel is assigned a length value
    convert $\bar{P}_x(i, j)$ from pixels to centimeters using result from previous line
    output: $\bar{P}_x(i, j)$ in centimeters

Algorithm 2 Film Thickness

function FILM_THICKNESS(*video*, *ref_image*, *cal_image*, *time_start*, *time_end*, *time_step*)
  input: *video* video of the experiment (**Figure 12c**)
    ref_image image of laser beam on the clean track (**Figure 12a**)
    cal_image image of laser beam with calibration object (**Figure 12b**)
    time_start time when slurry front enters frame of video in seconds
    time_end time when slurry front leaves frame of video in seconds
    time_step time between frame samples in seconds
  output: film thickness in millimeters

  function CALIBRATION(*ref_image*, *cal_image*)
    extract undeflected laser line position from *ref_image* using pixel intensity
    linearly fit undeflected laser line position
    prompt the user to click the top of the calibration object in *cal_image*
    compute the pixel distance between the laser line fit and click
    equate calibration object thickness (in mm) and pixel distance for conversion factor
    output: *pixels_to_mm* pixels to mm conversion factor

  function HEIGHT(*video*, *ref_image*, *time_start*, *time_end*, *time_step*, *pixels_to_mm*)
    Split *video* into $n = \frac{(time\_end - time\_start)}{time\_step}$ frames
    for $i = 1, \ldots, n$ **do**
      rotate i^{th} frame and *ref_image* so that laser line is horizontal
      detect undeflected laser line position in *ref_image* using pixel intensity
      detect laser line position in i^{th} frame using pixel intensity
      compute laser line deflection in pixels between *ref_image* and i^{th} frame
      convert laser line deflection to mm using *pixels_to_mm*
      plot the laser line deflection in mm as the *film_thickness*
    output: *film_thickness* in millimeters

A Monte Carlo Simulation Study on the Power of Autocorrelation Tests for ARMA Models

Zachary Wenning, Emily Valenci*

Department of Statistics, Pennsylvania State University, University Park, PA

https://doi.org/10.33697/ajur.2019.030

Students: zrw5043@psu.edu, edv5042@psu.edu*
*Mentor: xxf13@psu.edu**

ABSTRACT

It is often the case when assessing the goodness of fit for an ARMA time series model that a portmanteau test of the residuals is conducted to assess residual serial correlation of the fitted ARMA model. Of the many portmanteau tests available for this purpose, one of the most famous and widely used is a variant of the original Box-Pierce test, the Ljung-Box test. Despite the popularity of this test, however, there are several other more modern portmanteau tests available to assess residual serial autocorrelation of the fitted ARMA model. These include two portmanteau tests proposed by Monti and Peña and Rodríguez. This paper focuses on the results of a power analysis comparing these three different portmanteau tests against different fits of ARMA - derived time series, as well as the behavior of the three different test-statistics examined when applied to a real-world data set. We confirm that for situations in which the moving average component of a fitted ARMA model is underestimated or when the sample size is small, the portmanteau test proposed by Monti is a viable alternative to the Ljung-Box test. We show new evidence that the Peña and Rodríguez test may also be a viable option for testing for residual autocorrelation in cases where the sample size is small.

KEYWORDS

Time Series; Monte Carlo; ARMA Models; Power; Simulation; Autocorrelation Tests; Portmanteau Tests; Monti; Ljung-Box; Peña and Rodríguez

INTRODUCTION

In many situations in statistics, data used for statistical modeling is required to obey the assumption of independence, as is often the case in variants of regression analysis and analysis of variance. However, there are endless examples of real-world scenarios where such an assumption is invalid and the data display autocorrelation with respect to time, such as in financial and agricultural data. This is often the case in time series, which are defined by data being collected periodically over time, and we may denote one as Y_t for $t = 1, ..., T$ where T is the total number of observations of the time series.[1] In the case where the data is quite simple in structure and seasonal variations are not present, it suffices to model autocorrelated data with an autoregressive-moving average model (denoted as ARMA(p, q) where p and q are the orders of the autoregressive and moving average components of the fitted ARMA model respectively) which can be written as:[2]

$$Y_t = \sum_{j=1}^{p} \phi_j Y_{t-j} + \sum_{k=1}^{q} \theta_k e_{t-k} + e_t \qquad \textbf{Equation 1.}$$

Where e_t denotes the errors of the fitted ARMA model and $\phi_1, ..., \phi_p$ and $\theta_1, ..., \theta_q$ are the corresponding parameters which are estimated using Conditional Least Squares, Method of Moments, or Maximum Likelihood methods.[1, 2]

When fitting the above data, we require that 1) the error terms e_t be independent and identically distributed Gaussian white noise terms (e.g., normally distributed with mean 0 and variance σ^2), and 2) weak stationarity of the time series Y_t.[2] It is this first assumption which we will be assessing in our power analysis.

Note that, in theory, the goodness of fit for a particular ARMA model fit to a time series Y_t can be assessed by the validity of the first assumption. If the ARMA model is a sufficient fit for the time series, then it will take into account all serial autocorrelation present in the data, including autocorrelation of the data to its own past values and any current and past values of the stochastic term e_t.[1]

Much of this paper aims to confirm the findings of Safi and Al-Reqep's research on the power of portmanteau tests.[3] In this paper, we additionally seek to provide evidence that the Peña and Rodríguez test for residual autocorrelation is suitable for small sample sizes. We will now present three autocorrelation tests which assess this lack of fit.

METHODS AND PROCEDURES

Autocorrelation Tests for ARMA Models.

Autocorrelation is tested for using portmanteau tests as they are powerful for detecting deviations from independence. Each of the following portmanteau tests described in this paper test the lack of fit of an ARMA model by measuring the residual autocorrelation present after fitting the model to the time series data. Furthermore, the null and alternative hypothesis for each of the following tests can be written as follows:[4, 6, 7]

H_0 : The errors of the fitted ARMA model are independently distributed

H_A : The errors of the fitted ARMA model are not independent; they display serial autocorrelation

Arguably the most popular of the three different portmanteau tests examined for this power analysis is the Ljung-Box test. The test statistic for the Ljung-Box test is:[4]

$$Q = n(n+2)\sum_{k=1}^{h}\frac{r_k^2}{n-k} \qquad \textbf{Equation 2.}$$

Here, *n* denotes the sample size, *h* is the number of lags being tested, and r_k is the residual autocorrelation at lag *k*. Ljung and Box showed that for residuals derived from a fitted ARMA(p, q) model, *Q* is asymptotically distributed as χ^2 with h - p - q degrees of freedom.[4]

A similar test was proposed by Monti, and is quite similar to the Ljung-Box test statistic, although the residual autocorrelation at lag *k* is replaced by the residual partial autocorrelation at lag *k*. The test statistic for the portmanteau test proposed by Monti can be denoted as:[6]

$$M = n(n+2)\sum_{k=1}^{h}\frac{\pi_k^2}{n-k} \qquad \textbf{Equation 3.}$$

Here, *n* denotes the sample size, *h* is the number of lags being tested, and π_k is the residual partial autocorrelation at lag *k*. Monti showed that for residuals derived from a fitted ARMA(p, q) model, *M* is asymptotically distributed as χ^2 with h - p - q degrees of freedom.[6]

The last test being examined in this paper is one which was proposed in Peña and Rodríguez. The test statistic for this portmanteau test, which follows the same null and alternative hypotheses specified above, can be written as:[7]

$$D_m = n[1 - |\mathbf{R}_m|^{1/m}] \quad \textbf{Equation 4.}$$

Where n is the sample size. Here, $\mathbf{R}_m$ refers to the residual correlation matrix of dimension m, which can be written as:

$$\mathbf{R}_m = \begin{vmatrix} 1 & r_1 & \cdots & r_m \\ r_1 & 1 & \cdots & r_{m-1} \\ \vdots & \vdots & \ddots & \vdots \\ r_m & r_{m-1} & \cdots & 1 \end{vmatrix} \quad \textbf{Equation 5.}$$

Where r_m is the residual autocorrelation at lag m. Peña and Rodríguez showed that for relatively large sample sizes, D_m is approximately distributed as Gamma with mean $(m+1)/2-(p+q)$ and variance $(2m+1)(m+1)/3m-2(p+q)$.[7]

Keeping these three different tests in mind, we will now briefly define power for a binary hypothesis test, and how an estimate for the power of each of the above tests can be derived via Monte Carlo simulation. Then, we will move on to the execution and results of the power analysis.

Power for a Binary Hypothesis Test.

Recall the hypotheses being tested by the above portmanteau tests (see *Introduction*), and let λ denote the power of the above test against the alternative hypothesis H_A. Then we can define the power of the above hypothesis test as:

$$\lambda = P(Reject\ H_0 | H_A\ is\ true) \quad \textbf{Equation 6.}$$

One problem that this paper seeks to address is the derivation of an estimate for λ for each of the above portmanteau tests. A reasonable method of achieving such an estimate is to model the probability of the portmanteau test rejecting the null hypothesis H_0 given the alternative hypothesis H_A is true by a Bernoulli distribution (and thus, the simulation of such trials as a Bernoulli process).

Hence, if one simulates n time series derived from an ARMA(p, q) process and models the simulated time series using an ARMA(p*, q*) model (such that the ARMA(p*, q*) model is an *underfit* of the ARMA(p, q) process), then the power of each of the above portmanteau tests can be estimated by calculating the proportion of times that the test correctly rejects the null hypothesis H_0 for the underfitted model.[1] Let X_i equal 1 if the i^{th} application of the portmanteau test correctly classifies the ARMA(p*, q*) model as an underfit, and 0 otherwise. Then a reasonable estimate for λ would be:

$$\hat{\lambda} = \sum_{i=1}^{n} \frac{X_i}{n} \quad \textbf{Equation 7.}$$

Hence, the sampled X_i are independently and identically distributed random variables such that:

$$X_i = \begin{cases} 1 & w/\ probability\ \lambda \\ 0 & w/\ probability\ 1-\lambda \end{cases} \quad \textbf{Equation 8.}$$

Note that the above estimation is valid only for modeling the derived ARMA(p, q) process with an underfitting model. Therefore, we must know that the alternative hypothesis is true, else we would not obtain a valid estimate of the portmanteau test's power. This is because a model which is a proper fit (or even a model which suffers from overfitting) for the derived ARMA(p, q) process would theoretically be able to sufficiently model all serial autocorrelation present in the data, causing the p-value of the corresponding portmanteau test to inflate and thereby making it less likely that we would reject H_0.[1] Therefore, this condition is required to be satisfied if we are to obtain an accurate estimate of λ.

Execution of Power Analysis in R.

The execution of the power analysis in R consisted of using a custom built R function which allowed for the simulation of an ARMA(p, q) process with specified length and model fit.

The methods employed in the power analysis were as follows. The Ljung-Box, Monti, and Peña and Rodríguez portmanteau tests were conducted on either White Noise, AR(1), or MA(1) fits. These models were fitted against an ARMA(p, q) derived process with specified length and parameters which were generated randomly according to a uniform distribution $U(-1, 1)$ for each combination of N and k. These are shown in the corresponding tables below in *Results*. For this simulation study, only AR(2), MA(2) and ARMA(1, 1) derived processes were considered. Sample sizes N = 30, 100, 300 were used in this simulation as the goal was to investigate small to moderate sample sizes. Number of lags k = 5, 10, 15 were investigated as Safi and Al-Reqep showed that high number of lags resulted in a decrease in power.[3] Furthermore, 10,000 replications were used for each simulated process in order to achieve an estimate for the power of the corresponding portmanteau test accurate to four significant digits and also for the purpose of improving upon the accuracy from Safi and Al-Reqep's study.[3] Such power estimates were calculated using the theoretical approach outlined above in *Methods and Procedures* and generally align with the methods from Safi and Al-Reqep's simulation study.[3] All models were fitted to the corresponding derived ARMA(p, q) process using a Conditional Sum of Squares - Maximum Likelihood approach. This method is very similar to the power analysis conducted by Fisher, Monti, and Peña and Rodríguez.[1, 6, 7]

RESULTS

Power Analysis.

Below are the results of the power analysis for the derived AR(2), MA(2), and ARMA(1, 1) processes. Note that in Tables 1, 2, and 3 (displayed below), N denotes the length of the derived process, k denotes the number of lags used to calculate the test statistics of the three portmanteau tests, ϕ_1, ϕ_2, θ_1, and θ_2 denote the parameters of the derived ARMA(p, q) process, and $\hat{\lambda}_{D_m}, \hat{\lambda}_M$, and $\hat{\lambda}_Q$ denote the corresponding estimates for the power of the Peña and Rodríguez, Monti, and Ljung-Box tests.

Model Fit	N	k	ϕ_1	ϕ_2	θ_1	θ_2	$\hat{\lambda}_{D_m}$	$\hat{\lambda}_M$	$\hat{\lambda}_Q$
White Noise	30	5	.1860	N/A	.8632	N/A	**.9471**	.9446	.7096
AR(1)	30	5	.1860	N/A	.8632	N/A	**.6437**	.6140	.3955
MA(1)	30	5	.1860	N/A	.8632	N/A	**.1116**	.1032	.1079
White Noise	100	10	-.6639	N/A	.1716	N/A	**.9936**	.9811	.9873
AR(1)	100	10	-.6639	N/A	.1716	N/A	.0613	.0686	**.0688**
MA(1)	100	10	-.6639	N/A	.1716	N/A	**.7051**	.5755	.6488
White Noise	300	15	-.1472	N/A	.3672	N/A	**.8286**	.6452	.6015
AR(1)	300	15	-.1472	N/A	.3672	N/A	**.1499**	.1119	.1183
MA(1)	300	15	-.1472	N/A	.3672	N/A	.0644	.0662	**.0689**

Table 1. Power Analysis Results for ARMA(1,1) Derived Process

Model Fit	N	k	ϕ_1	ϕ_2	θ_1	θ_2	$\hat{\lambda}_{D_m}$	$\hat{\lambda}_M$	$\hat{\lambda}_Q$
White Noise	30	5	N/A	N/A	.8632	-.4690	.3046	**.4092**	.2278
AR(1)	30	5	N/A	N/A	.8632	-.4690	.3826	**.3897**	.2776
MA(1)	30	5	N/A	N/A	.8632	-.4690	**.1994**	.1907	.1217
White Noise	100	10	N/A	N/A	.1716	.2125	**.4154**	.3355	.3811
AR(1)	100	10	N/A	N/A	.1716	.2125	**.2000**	.1677	.1740
MA(1)	100	10	N/A	N/A	.1716	.2125	**.2746**	.2125	.2070
White Noise	300	15	N/A	N/A	.3672	-.1208	**1.0000**	.9997	.9899
AR(1)	300	15	N/A	N/A	.3672	-.1208	**.9225**	.7865	.7157
MA(1)	300	15	N/A	N/A	.3672	-.1208	**.3115**	.2101	.2100

Table 2. Power Analysis Results for MA(2) Derived Process

Model Fit	N	k	ϕ_1	ϕ_2	θ_1	θ_2	$\hat{\lambda}_{D_m}$	$\hat{\lambda}_M$	$\hat{\lambda}_Q$
White Noise	30	5	.1860	-.6302	N/A	N/A	.7572	.7782	**.7890**
AR(1)	30	5	.1860	-.6302	N/A	N/A	**.8718**	.8334	.8344
MA(1)	30	5	.1860	-.6302	N/A	N/A	**.7713**	.7326	.6032
White Noise	100	10	-.6639	-.5996	N/A	N/A	**1.0000**	**1.0000**	.9999
AR(1)	100	10	-.6639	-.5996	N/A	N/A	**.9998**	.9976	.9979
MA(1)	100	10	-.6639	-.5996	N/A	N/A	**.9319**	.8811	.8949
White Noise	300	15	-.1472	-.3845	N/A	N/A	**1.0000**	.9992	.9991
AR(1)	300	15	-.1472	-.3845	N/A	N/A	**.9999**	.9985	.9984
MA(1)	300	15	-.1472	-.3845	N/A	N/A	**.9994**	.9950	.9934

Table 3. Power Analysis Results for AR(2) Derived Process

We can see from the above that the portmanteau test proposed by Monti had an estimated power better than or similar to that of the Ljung-Box test on several occasions, the most notable of these being when either the moving average component of the derived ARMA(p, q) process was underestimated or when the sample size and lag used for testing was sufficiently small (e.g., N = 30 and k = 5, respectively). These results agree with those obtained by Monti.[6]

Furthermore, in 7 out of the 9 cases in which the derived ARMA(p, q) process had a large sample size and lag used for testing was high (e.g., N = 300 and k = 15), the results of the power analysis for the portmanteau test suggested by Monti continued to outperform that of the Ljung-Box test.

The results of the power analysis for the Ljung-Box test meanwhile, were quite mixed. Although the Ljung-Box test tended to have an estimated power greater than than that of Monti's portmanteau test for occasions when the number of lags used for testing and the sample size of the derived ARMA(p, q) process was moderately large (e.g., N = 100 and k = 10), the Ljung-Box test was almost always outperformed by Peña and Rodríguez's portmanteau test, regardless of sample size, number of lags used for testing, or type of derived process. Indeed, in 24 of the 27 simulations ran for the power analysis, the portmanteau test suggested by Peña and Rodríguez had an estimated power greater than that of the Ljung-Box test.

However, the results seen in the performance of the portmanteau test suggested by Peña and Rodríguez compared to that of the Ljung-Box test are not surprising for the sample sizes which were greater than or equal to 100, and further support the results originally obtained by Peña and Rodríguez.[7] What should be noted though, is that in 6 of the 9 cases tested in which the derived ARMA(p, q) process had a small sample size and the number of lags used for testing was also small (e.g., N = 30 and k = 5), the portmanteau test proposed by Peña and Rodríguez outperformed the other two portmanteau tests (e.g., had greater estimated power).

Applied example: Sheep.

In order to show the results of the power analysis in an applied context, we performed a time series analysis of a real data set. The data set, *Sheep*, is of the total annual sheep population (1000s) in England and Wales from 1867 to 1939 ($N = 73$).[8] Firstly, an initial visual inspection of the time series was performed in order to address the requirement of weak stationarity prior to fitting any ARMA models to the data.

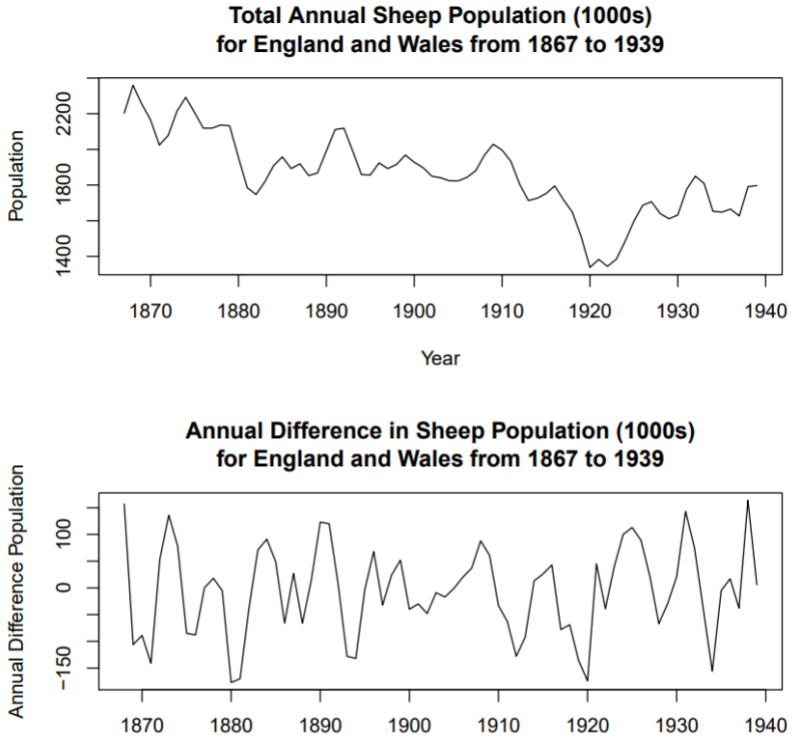

Figure 1. *Sheep* data visualization. The top graph shows a time series plot of the data which exhibits a negative linear trend and the bottom graph shows the differenced time series which appears to be stationary.

The time series plot of the data shows a general decreasing linear mean trend. Hence, the data was stationarized in order to satisfy the assumptions of fitting an ARMA(p, q) model to the time series. It is clear from the second plot that we successfully stationarized the sheep data by taking the first difference of the time series. We can now safely examine the autocorrelation function (ACF) and partial autocorrelation function (PACF) in order to conduct ARMA(p, q) modeling of the differenced data.

Judging from the plots of the ACF and PACF in Figure 2, an AR(2) model was found to be the most likely candidate for modeling the differenced time series as a higher order AR model would likely be an overfit of the data. From the power analysis, it was found that for moderately large sample sizes (e.g., $N \geq 100$), the Peña and Rodríguez test often has greater statistical power compared to the Monti and Ljung-Box tests. Therefore, we expected that the portmanteau test proposed by Peña and Rodríguez would be the most conservative in testing for residual autocorrelation of fitted ARMA models to the differenced *Sheep* data (likely followed by the Ljung-Box test and Monti's portmanteau test).

Table 4 shows the estimated coefficients for each of the ARMA models fit to the differenced *Sheep* time series data. The Akaike Information Criterion (AIC) is included to give an idea of the goodness of fit for each model relative to that of the others.[5] A smaller AIC value indicates a better fit. It can be noted that the ARMA(2,1) model has the lowest AIC out of all of the models considered and therefore is the model (out of the subset of ARMA fits considered) which best fits the differenced *Sheep* time series. Note that the white noise model has the highest AIC of all the ARMA models considered and therefore is the model which has the worst relative fit to the data.

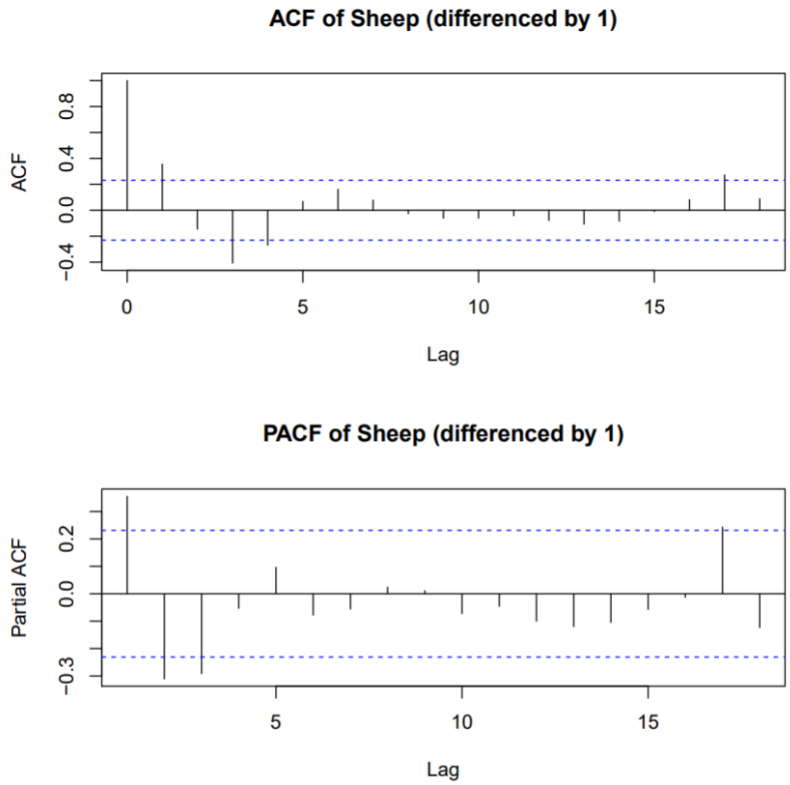

Figure 2. Residual Autocorrelation Analysis of Differenced *Sheep* Time Series Data.

Model Fit	$\hat{\phi}_1$	$\hat{\phi}_2$	$\hat{\theta}_1$	*AIC*
AR(1)	.3734	N/A	N/A	832.71
MA(1)	N/A	N/A	.4798	828.83
AR(2)	.5348	-.3873	N/A	824.82
ARMA(1,1)	.0671	N/A	.4267	830.75
ARMA(2,1)	.9150	-.5454	-.4553	822.70
White Noise	N/A	N/A	N/A	841.12

Table 4. Results of *Sheep* data model fits.

For this example, we considered three types of models: "good" models (models of adequate fit, which we will define as those below the 50th percentile of AIC scores i.e. ARMA(2,1), AR(2), and MA(1)), "not so good" models (models of obvious underfit, which we will define as those above the 50th percentile of AIC scores i.e. ARMA(1,1) and AR(1)), and White Noise models (e.g., models of a Gaussian stochastic process).

Model Fit	$p^*_{D_m}$	p^*_M	p^*_Q	Overall Conclusion
AR(1)	.0123	.0637	.0168	Inconclusive
MA(1)	.0630	.1769	.1776	No Residual Autocorrelation Detected
AR(2)	.1548	.4670	.5120	No Residual Autocorrelation Detected
ARMA(1,1)	.0193	.1244	.1313	Inconclusive
ARMA(2,1)	.4560	.6759	.7042	No Residual Autocorrelation Detected
White Noise	.0004	.0040	.0001	Residual Autocorrelation Detected

Table 5. Results of Portmanteau Tests of Sheep Data Models.

Table 5 shows the p-values corresponding to each of the portmanteau tests considered against each of the ARMA models applied to the differenced *Sheep* time series data. It was found that for the AR(1) model, at a significance level of 5% and specified number of lags set to 10, Peña and Rodríguez's portmanteau test and the Ljung-Box test both detected sig-

nificant residual autocorrelation in the fitted model while the portmanteau test suggested by Monti failed to detect any significant residual autocorrelation.

Furthermore, it was found that for the MA(1), AR(2), and ARMA(2,1) models, at a significance level of 5% and specified number of lags set to 10, all of the portmanteau tests failed to detect any significant residual autocorrelation for these fitted models. The ARMA(2,1) model was found to be one of the "good" models for the fitted data, so as expected, none of the portmanteau tests found any significant residual autocorrelation for this model.

Additionally, for the ARMA(1,1) model, at a significance level of 5% and specified number of lags set to 10, the portmanteau test suggested by Peña and Rodríguez resulted in the rejection of the null hypothesis and therefore detected significant residual autocorrelation in the fitted ARMA model, while the rest of the portmanteau tests failed to detect any significant residual autocorrelation.

Lastly, the white noise model, at a significance level of 5% and specified number of lags set to 10, was found to have significant residual autocorrelation present by all three portmanteau tests. This was expected as the results from Table 3 showed all of the portmanteau tests have high estimated power for testing underfitting white noise models.

DISCUSSION

From the power analysis, it was found that Monti's portmanteau test had an estimated power better than or similar to that of the Ljung-Box test when either the moving average component of the derived ARMA(p, q) process was underestimated or when the sample size (and lag used for testing) were sufficiently small. These results support those originally obtained by Monti and those by Safi and Al-Reqep.[3, 6] Even for higher sample sizes and increased lag, Monti's portmanteau test continued to fare better than that of the Ljung-Box test.

Meanwhile, the estimated power for the Ljung-Box test compared to that of Peña and Rodríguez's portmanteau test was quite poor, and had an estimated power greater than Peña and Rodríguez's portmanteau test in only 3 of the 27 simulations conducted. For large sample sizes, Peña and Rodríguez found similar results,[7] but our power analysis demonstrated that Peña and Rodríguez's portmanteau test still had sufficiently high estimated power for a majority of the cases where the sample size (and number of lags used for testing) was small. This expands upon the findings of Safi and Al-Reqep as their paper does not discuss Peña and Rodríguez's original test statistic as a viable option in this situation.[3]

These results are quite surprising, as Peña and Rodríguez showed that the approximate convergence of their D_m test statistic to the Gamma distribution with mean $(m+1)/2-(p+q)$ and variance $(2m+1)(m+1)/3m-2(p+q)$ is quite slow and often lacking in power for small sample sizes.[7] These results challenge that idea, as although Peña and Rodríguez's portmanteau test was shown to suffer from reduced power on a few occasions in which the sample size was small, the estimated power of Peña and Rodríguez's portmanteau test was still close to that of the portmanteau test suggested by Monti (which in turned fared better than the Ljung-Box test for 6 of the 9 simulations in which the sample size and lag used for testing was small).

CONCLUSIONS

In summary, our results confirm that the portmanteau test proposed by Monti is a viable alternative to the Ljung-Box test for when either the moving average component of the fitted ARMA model is underestimated or when sample size is small. However, for time series with small to moderate sample sizes, the portmanteau test proposed by Peña and Rodríguez may be considered, as this portmanteau test performed well for all sample sizes examined.

Furthermore, the time series analysis of the *Sheep* data supports the results found in our initial power analysis of the portmanteau tests considered in this paper, and this is evident in the results of the goodness of fit tests performed on the ARMA(p, q) models fit to the data. We can see that for when a possible moving average component was underestimated, Monti's portmanteau test was more conservative, and overall, gave results similar to that of the Ljung-Box

test, while Peña and Rodríguez's portmanteau test was the most conservative with regards to all of the non white-noise model fits (see Table 5 above). Moreover, we provide evidence that the original test statistic proposed by Peña and Rodríguez may be suitable for sample sizes as small as 30, contradicting the initial findings of Peña and Rodríguez as well as Safi and Al-Reqep.[3, 7]

Future work regarding this subject matter should investigate further applications of the portmanteau tests considered in this study. Furthermore, the theory of these portmanteau tests extends to testing for conditional heteroscedasticity in raw time series data (e.g., checking for the presence of GARCH effects in an otherwise stochastic time series process). There seems to be very little statistical literature regarding applying Monti's and Peña and Rodríguez's portmanteau tests to this task.

ACKNOWLEDGEMENTS

We thank Dr. Fang of the Pennsylvania State University for his utmost support during this project, as well as for his critiques and willingness to sponsor us for this project. His guidance has been invaluable.

REFERENCES

1. Fisher, T. J. (2011) Testing Adequacy of ARMA Models Using a Weighted Portmanteau Test on the Residual Autocorrelations, *SAS Global Forum 2011 - Statistics and Data Analysis. support.sas.com/resources/papers/proceedings11/327-2011.pdf*
2. Moran, P. A., and Whittle, P. (1951) Hypothesis Testing in Time Series Analysis, *Journal of the Royal Statistical Society*, Series A (General), Vol. 114, No. 4, pp. 579.
3. Safi, S. K., and Al-Reqep, A. A. (2014) Comparative Study of Portmanteau Tests for the Residuals Autocorrelation in ARMA Models. *Science Journal of Applied Mathematics and Statistics* Vol. 2, No. 1, pp. 1–13. *doi.org/10.11648/j.sjams.20140201.11*
4. Ljung, G. M., and Box, G. E. P. (1978) On a measure of lack of fit in time series models, *Biometrika*, Vol. 65, No. 2, pp. 297–303. *https://doi.org/10.1093/biomet/65.2.297*
5. Akaike, H. (1974) A new look at the statistical model identification, *IEEE Transactions on Automatic Control*, Vol. 19, No. 6, pp. 716–723. *doi.org/10.1109/TAC.1974.1100705*
6. Monti, A. C. (1994) A Proposal for a Residual Autocorrelation Test in Linear Models, *Biometrika*, Vol. 81, No. 4, pp. 776–790. *https://doi.org/10.1093/biomet/81.4.776*
7. Peña, D., and Rodríguez, J. (2002) A Powerful Portmanteau Test of Lack of Fit for Time Series, *JASA*, Vol. 97, No. 458, pp. 601–610. *https://doi.org/10.1198/016214502760047122*
8. Kendall, M. G., and Ord, J. K. (1990) Annual Sheep Population (1000s) in England & Wales 1867–1939, DataMarket. *datamarket.com/data/set/22px/annual-sheep-population-1000s-in-england-wales-1867-1939#!ds=22px&display=line* (accessed May 2019)

ABOUT THE STUDENT AUTHORS

Zachary Wenning and Emily Valenci are recent undergrad graduates from the Pennsylvania State University. Both graduated with Bachelor of Science degrees in Statistics under the Biostatistics option. Zachary Wenning is currently a Junior Analytics Consultant, and is a graduate student of the Pennsylvania State University's World Campus pursuing a Master of Applied Statistics degree. Emily Valenci is a Data Analyst and Statistical Researcher.

PRESS SUMMARY

When modeling autocorrelated data such as time series, it is often required to check how well the model describes the data. One such way to do this is to apply statistical tests called portmanteau tests. Our paper compares the statistical power, or the proportion of times a statistical test correctly rejects a null assumption, for three different portmanteau tests. We show that there is noticeable improvement in statistical power for two more modern portmanteau tests compared to the commonly used Ljung-Box test.

Evaluating the Effects of Bisphenols F and S with Respect to Bisphenol A on Primordial Germ Cell Migration in Zebrafish (*Danio rerio*) Embryos Using Immunofluorescence Microscopy

Siti Sarah Safura[*#], George Roba[#], & Edward Freeman*

Department of Biology, St. John Fisher College, NY

https://doi.org/10.33697/ajur.2019.031

[#]*both of these authors contributed equally to this work*

Students: sss03429@sjfc.edu and gr00103@sjfc.edu*
Mentor: efreeman@sjfc.edu

ABSTRACT
Primordial Germ Cell (PGC) migration occurs in early embryonic development and is highly conserved across taxa. PGC migration occurs within the first 24 hours post fertilization (hpf) in zebrafish, making the organism an efficient model for observing the migration pathway. Proper PGC migration is necessary for normal gonad development and, in some species, sex determination. Disruption of this process leads to defects in gonad formation and abnormal sex determination and differentiation. Studies show that endocrine-disrupting chemicals such as bisphenol A (BPA) disrupt PGC migration in zebrafish. BPA is an estrogenic compound that has been linked to a variety of human diseases, including various cancers, diabetes, reproductive disorders, obesity, and cardiovascular diseases. It is one of the most widely used synthetic compounds worldwide, as it is used to make polycarbonate plastics. Many studies provide evidence of the harmful effects of BPA on living organisms. In response, manufacturers have started to use replacements such as bisphenol F (BPF) and bisphenol S (BPS). However, due to their structural similarity, it is likely that BPF and BPS are just as harmful to organisms as BPA. In this study, we use antibody staining and immunofluorescence microscopy to confirm that BPA exposure results in abnormal PGC migration in zebrafish embryos, as previously studied, and to illustrate that BPF and BPS exposure results in similar PGC migration defects.

KEYWORDS
Zebrafish; Zebrafish Embryos; Primordial Germ Cells; PGC Migration; Gonad Development; Endocrine-Disrupting Chemicals; Bisphenol A; Bisphenol S; Bisphenol F; Sex Determination

INTRODUCTION

Primordial germ cell migration and sex determination in zebrafish

Primordial germ cells (PGCs) are precursor cells that eventually develop into gametes in sexually-reproducing organisms. PGC migration is a process common among vertebrates and invertebrates, including the common model organisms *Xenopus, Drosophila*, and *Danio rerio*. A study comparing mechanisms of PGC migration in *Mus musculus*, *Danio rerio,* and *Drosophila melanogaster* found that although there is variation among the species, it appears that some molecular mechanisms are conserved for PGC migration and maintenance.[1] A number of genes involved in PGC migration are conserved across phyla, indicating that the process is similar in different organisms including those indicated above.[2] Early in vertebrate development, PGCs migrate from the primary ectoderm to the gonadal ridge where they later develop into gametes. PGC migration is directed by chemical cues secreted by somatic cells. The process is tightly regulated as the pathway that PGCs use to travel to the gonad goes through different tissues.[3] Migration occurs between embryonic weeks 4 and 6 in humans,[4] between embryonic days 8 and 10 in mice,[5] and within 24 hpf (hours post fertilization) in zebrafish.[6] As zebrafish do not have specific sex chromosomes, sex determination in zebrafish is likely the result of gonadal gene expression, environmental factors, and the presence of PGCs at the gonadal ridge. Therefore, PGC migration and their presence at the gonadal ridge are an important factor in sex determination and eventual differentiation in zebrafish. Defects in the PGC migration pathway have been shown to have adverse effects in zebrafish, including improper gonad formation and infertility.[7,8] Vasa, an RNA binding protein, is used as a marker for germ cells due to its role in germ cell determination and function.[3] By analyzing PGCs in zebrafish fixed at 24 hpf, we can see a baseline of where germ cells are normally localized and compare this to when embryos are treated with a particular bisphenol.

Bisphenols in the environment

Bisphenols are synthetic plasticizers that are used in the production of polycarbonate plastics. Bisphenol A (BPA) is a known endocrine-disrupting chemical (EDC) whose estrogenic effects were first observed in 1936.[9] In the 1950s, it was found that BPA could be used to make polycarbonate plastics and it became one of the most widely used synthetic compounds worldwide, despite its estrogenic effects.[9] Bisphenols have been linked to a variety of human diseases, including various cancers, diabetes, reproductive disorders, obesity, and cardiovascular diseases.[9] The greatest source of human exposure to BPA is leaching of the chemical from everyday household items, including food and beverage containers, thermal receipt paper, and medical devices.[9,10] Although BPA is biodegradable, trace amounts of BPA are found even in treated wastewater and background concentrations exist in the aquatic environment.[11]

Effects of endocrine-disrupting chemicals (EDCs) on organisms

Organisms are much more vulnerable to the adverse effects of EDCs in-utero and during the early stages of development, as early developmental processes are tightly regulated by many factors including chemical signaling. Exposure to BPA (an estrogen mimic) during development has been found to lead to reproductive disorders, birth defects, and brain malformations in mammals such as mice and humans.[9,10] Human fetal testis tissue, particularly Leydig cells, have been reported to be a major target of BPA.[9] Concentrations as low as 10 nM were shown to reduce human fetal Leydig cell function, supporting that BPA has estrogenic effects on organ systems and that embryonic exposure is problematic.[9] Zebrafish share many developmental processes with humans and can therefore provide insight into the potential effects of EDCs in humans. Prior studies have demonstrated that exposure to BPA at doses as low as 0.001 μM negatively impact zebrafish reproductive health.[12] In 2017, researchers found that higher levels of BPA exposure in zebrafish can cause a reduction in egg production and reduce chances of fertilization.[12] Because BPA exhibits a non-monotonic dose-response curve, trace BPA concentrations in aquatic environments can still have adverse effects on aquatic organisms.[9]

Due to potential health concerns, Canada (2009), USA (2010), and the European Union (2011) prohibited the use of BPA in the manufacture of polycarbonate feeding bottles for infants.[10] That being said, the Food and Drug Administration (FDA) has only restricted the use of BPA in baby bottles, sippy cups, and packaging for infant formula. Therefore, consumer concern has pushed companies to replace BPA in other products--it is often replaced with other bisphenols, such as bisphenol F (BPF) and bisphenol S (BPS). Bisphenols share structural similarities, indicating that they may have similar estrogenic effects in organisms **(Figure 1).**

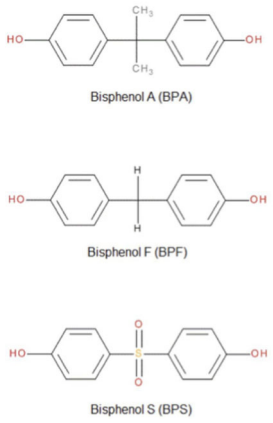

Figure 1. Structures of bisphenols A, F, and S.

All three bisphenols in this study (BPA, BPF, and BPS) are shown to have neurological, metabolic, endocrine, and reproductive effects on organisms. A 2018 study showed that exposure to BPA disrupts differentiation of human-derived neural progenitor cells.[13] In regards to BPS, exposure to the chemical during development causes precocious neurogenesis in the zebrafish hypothalamus and is associated with hyperactive behavior in zebrafish.[14] Another study found that exposure to BPF during development affects gonadotropin-releasing hormone neurons in zebrafish through an estrogen-mediated pathway.[15] BPA, BPF and BPS were all found to affect the transcription levels of genes for neurotransmitter-metabolizing enzymes in female rats when exposed during development.[16] In regards to metabolism, studies show that all three bisphenols are associated with obesity in some context. In a 2019 study, perinatal exposure to BPA in male rats showed that BPA acts as an obesogen as it induced obesity and increased food intake.[17] There is evidence that BPA exposure during critical periods of development can cause epigenetic changes that are related to the onset of obesity.[18] The estrogenic potency of BPF and BPS are both in the same order of

magnitude as BPA and all three bisphenols show the same amount of inhibitory hormonal signaling in adipocytes.[19] Another study found that both BPS and BPA enhance adipocyte differentiation, and that BPS (a common BPA replacement) is an even stronger adipogen than BPA.[20] BPF is also associated with higher risk of obesity in children and adolescents.[21] These bisphenols are known to have endocrine effects as well: a 2017 study found that all three transactivate estrogen receptors (ERs) in zebrafish.[22] BPS also alters estradiol-induced non-genomic signaling in rat pituitary cells; this disrupted signaling may result in cell death.[23] A 2016 study using both in-vivo and in-vitro studies showed that BPA, BPS, and BPF all upregulate Aromatase B, a key enzyme in estrogen synthesis, in the brains of developing zebrafish.[10] In a study analyzing the effects of BPA, BPF, and BPS on gene expression in fetal Leydig cells, all three were found to reduce the expression of key genes in testosterone synthesis, further illustrating the estrogenic mimicry of these chemicals.[9] Another study showed that when adult zebrafish were exposed to 0.002, 0.02, and 0.2 μM BPS, maternal exposure to BPS greater than 0.02 μM caused delayed egg hatching and developmental delays in offspring.[24] Lastly, a 2013 study showed that exposure to BPA during the first 24 hpf results in abnormal PGC migration in zebrafish embryos.[3] The current study illustrates that exposure to BPS and BPF also results in abnormal PGC migration in zebrafish.

Bisphenol A and Danio rerio primordial germ cell migration

Fish are particularly sensitive to the presence of EDCs, due to the environmental and epigenetic cues influencing sex determination and differentiation.[25] Exposure of zebrafish embryos to 17-alpha-ethinylestradiol (EE_2) showed that estrogen receptors play a role in PGC migration.[26] Bisphenols are especially of concern, as their wide commercial use causes them to be ubiquitous in the environment and they operate as sex hormone mimics that can alter essential developmental processes.[11, 14, 27] A 2013 study looked at the effects of BPA on PGC migration in zebrafish and found that BPA exposure during the first 24 hpf at concentrations of 17.5 μM and 35 μM caused an increased number of PGCs compared to controls and caused PGCs to migrate to ectopic locations.[3] Failure of PGCs to reach the gonadal ridge leads to defects in sex determination and gonadal differentiation.

Different geographical regions have various amounts of BPA in the environment. Areas near waste treatment plants have varying amounts of BPA, from not detectable to 1.6 μM in some, to maximum amounts of 36.8 μM and 45.1 μM in others, while tap water was found to have a maximum concentration of 5.7 μM.[28,29,30] That being said, because BPA exhibits a non-monotonic dose-response curve, the relationship between dosage and effect may be nonlinear.[9] In this study, we exposed embryos to published concentrations of BPA (17.5 μM and 35 μM) that are known to cause abnormal PGC migration in zebrafish during the first 24 hpf[3] to act as a positive control, and to ensure that fluorescent immunocytochemistry is an effective method for visualizing PGC migration in zebrafish. We exposed embryos to an intermediate dose of BPF and BPS to evaluate whether or not these replacement bisphenols have similar effects on PGC migration as BPA. 25 μM was chosen as the intermediate dosage between two known BPA doses that disrupt PGC migration in zebrafish (17.5 μM and 35 μM).[3] For both BPF and BPS-treated embryos, we expected to see migration patterns similar to those of BPA at similar doses.

METHODS AND PROCEDURES

Fish maintenance

Zebrafish were purchased from local pet stores throughout Rochester, NY. Zebrafish were introduced to the housing system and allowed to acclimate to the water and room conditions for two weeks. Experimentation was reviewed and approved by the Institutional Animal Care and Use Committee at St. John Fisher College (IACUC Protocol #61). Females and males were kept together in tanks that had a constant flow of system water. System water was maintained at 27-29 °C with a salinity between 1400-1600 microsiemens, which was checked every other day. The pH level was kept between 6.9-7.4 and was measured twice per week. The fish were kept on a 14 hour light/10 hour dark schedule and fed twice daily. The fish were fed with live brine shrimp (Utah Red Shrimp from Artemac L.L.C) and either Zebrafish select diet (Aquaneering) or flake food (Ocean Star International freshwater aquarium flake food).

Breeding and embryo collection

Zebrafish embryo collection chambers were created using pipette boxes, with yarn attached to the holes in the top of the box, simulating aquatic plants. The holes allowed embryos to fall into the chamber so they were not consumed by adults. Collection chambers were added to tanks the night prior to collection. After giving the zebrafish one hour for mating, collection chambers were removed from the tanks. Embryos were sorted and dead or unhealthy embryos were then removed.

Endocrine-disrupting chemical exposure

Within the first hour after fertilization, 3-5 embryos were added to each well of a 24-well plate. Embryos were split into five different treatment groups throughout six different experiments. All embryos were incubated with 998 μL of system water and 2 μL of either ethanol or an EDC. Vehicle control embryos were exposed to 2 μL of ethanol. BPA, BPF, and BPS groups were exposed to 2 μL of each chemical, respectively. Final concentrations were low dose BPA-treated (17.5 μM in ethanol), high dose

BPA-treated (35 μM in ethanol), BPF-treated (25 μM in ethanol), and BPS-treated (25 μM in ethanol). All stock solutions were made in ethanol and stored in the dark to protect from light degradation. The embryos were allowed to grow for 24 hours at 28 °C. After 24 hours, if more than two embryos were dead in any well, the embryos in that well were not used for analysis of PGC migration.

Fluorescent microscopy

After EDC or vehicle treatment for the first 24 hpf, embryos were then transferred to 1 mL centrifuge tubes. Bisphenol solutions were removed and replaced with 4% paraformaldehyde (PFA). Embryos were then kept in a refrigerator at 4 °C. Embryos were washed the following day with 100% methanol and placed in 100% methanol at -20°C for long term storage. Before staining, embryos were dechorionated using surgical tweezers and a Leica dissecting microscope (#S8APO). The staining procedure began with three 30 minute 500 μL washes in a phosphate-buffered saline (PBS)/1% triton X-100 solution at room temperature. Next, embryos received two one-hour washes and two 5 minute washes, each using 500 μL of blocking buffer containing PBS/1% triton X-100 with 10% goat serum. Embryos were then placed in a solution containing 2 μL of primary antibody (rabbit anti-vasa, Abcam #ab209710) added to 298 μL of blocking buffer (1:150 dilution). Primary antibody incubations were done overnight with gentle rotation on an orbital shaker at 4 °C. Following the primary antibody incubations, embryos underwent three one-hour washes in 500 μL of blocking buffer at room temperature. Next, embryos received six 10 minute washes with PBS/1% triton X-100 at room temperature. Finally, 3 μL of secondary antibody (goat-anti-rabbit IgG-FITC, Santa Cruz # sc-2012) were added to 297 μL of blocking buffer (1:100 dilution) for incubation with the embryos. Secondary antibody incubations were done overnight with gentle rotation on an orbital shaker at 4 °C. Following the secondary antibody incubations, embryos underwent three 10 minute washes with 500 μL of PBS/1% triton X-100 at room temperature. Embryos were then placed onto concave slides with minimal buffer and visualized using a Leica fluorescent microscope while avoiding light exposure to prevent fading of FITC. Embryos were visualized with a 10X objective and photographs were taken using the Q-Capture Pro 7 program **(Figure 2).**

Data and Statistical Analysis

After visualization, the embryos were categorized into either normal (clustered) or abnormal (dispersed) groups for statistical analysis **(Table 1).** Through the use of Social Science Statistics software, Fisher's Exact tests were ran on experimental groups to see if they were significantly different from control, as well as to see if there was a significant difference between bisphenols **(Table 2)**.

RESULTS

Control embryos visualized under the microscope showed a clustered localization pattern, as expected **(Figure 2, A and B**). For the purposes of this study, "dispersed localization" was defined as any localization of PGCs significantly different from control. These embryos demonstrated a non-clustered pattern with visible spacing between cells. Embryos were categorized into either normal (clustered at the gonadal ridge) or abnormal (dispersed). After visualization, specific distances were not quantified. Fluorescent microscopy with BPF and BPS-treated embryos showed a similar PGC staining pattern as BPA-treated embryos, which served as a positive control **(Figure 2).** The majority of bisphenol-treated embryos showed dispersed PGC localization when compared to control **(Table 1)**. Percentages of dispersed localization are also represented graphically **(Figure 3).** BPA, which is known to cause dispersed PGC migration, served as our positive control and was also compared to BPS and BPF-treated groups **(Table 2).**

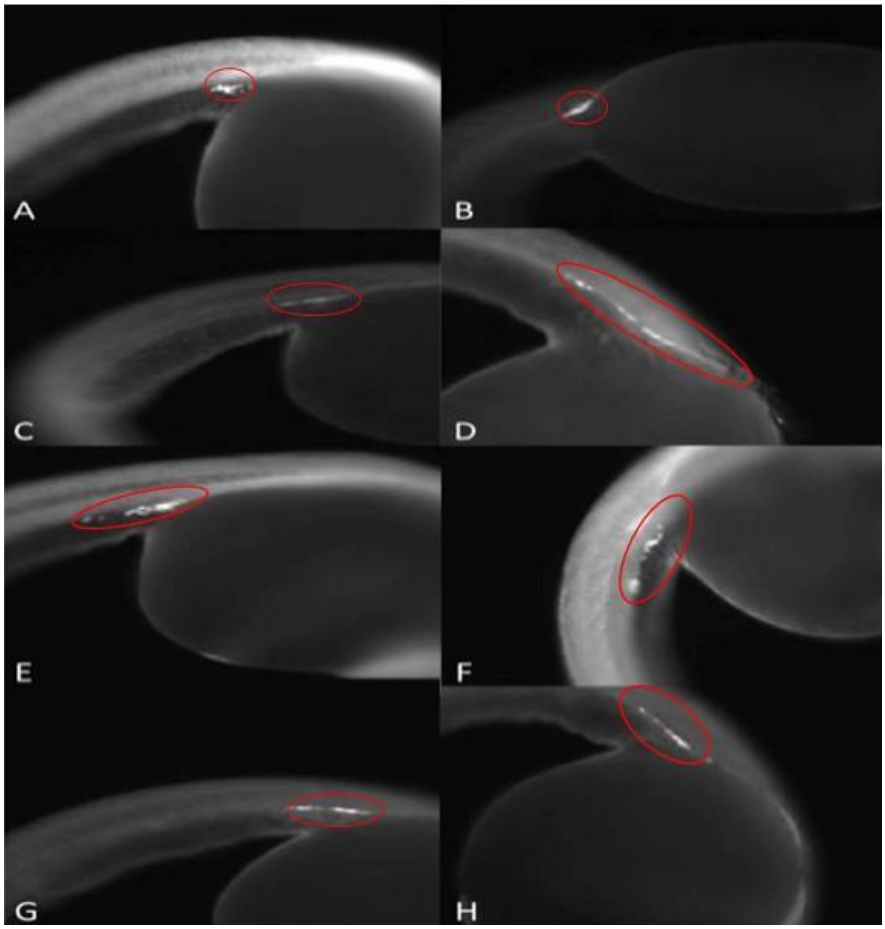

Figure 2. BPA, F, and S representative staining patterns. A and B) Control embryos, C) 17μM BPA-treated, D) 35 μM BPA-treated, E and F) 25 μM BPF-treated, G and H) 25 μM BPS-treated.

Treatment	Number of embryos	Dispersed migration (%)
Vehicle Control	31	2/31 (6%)
Positive Control: 17.5 μM BPA	38	31/38 (81.5%)
Positive Control: 35 μM BPA	31	31/31 (100%)
25 μM BPF	32	26/32 (81%)
25 μM BPS	32	29/32 (91%)

Table 1. Treatments, number of embryos per treatment, and percentage of embryos with dispersed migration. Data are representative of six experiments using fluorescent immunocytochemistry.

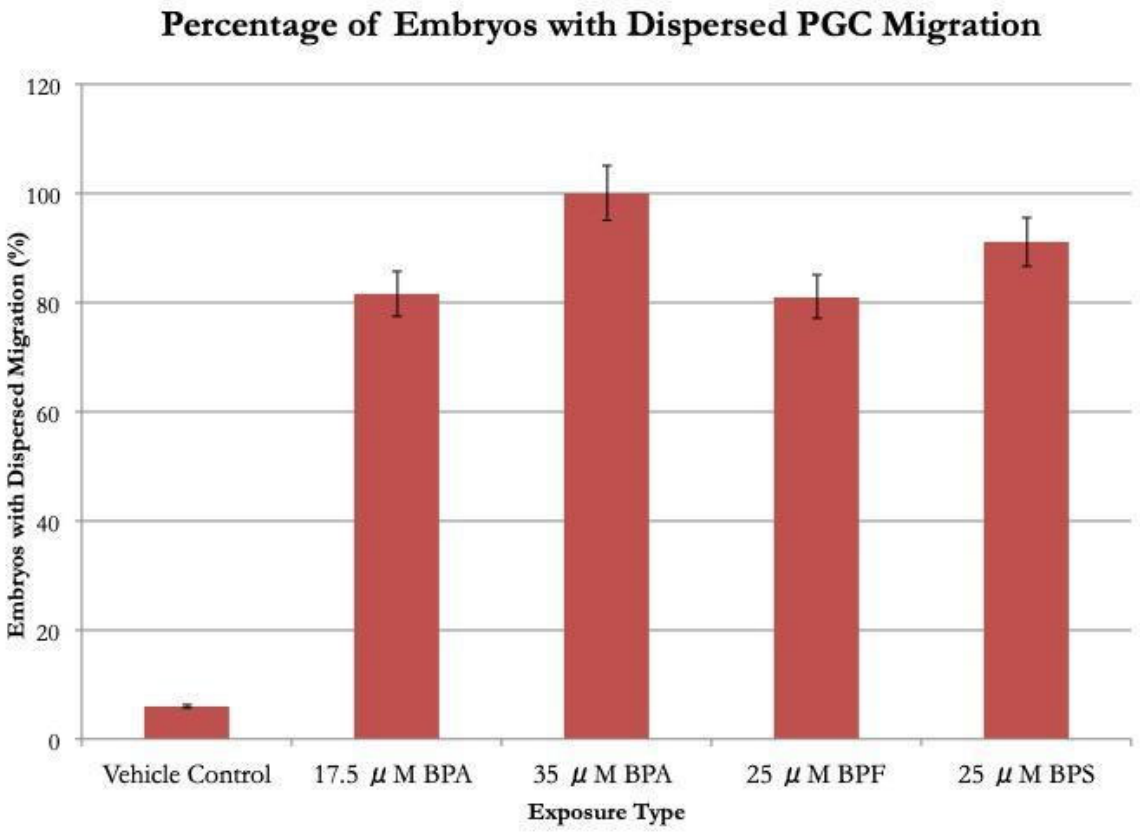

Figure 3. Percentage of embryos with dispersed migration in each experimental group.

	Vehicle Control	17.5 μM BPA	35 μM BPA	25 μM BPF	25 μM BPS
25 μM BPF	SS	NS	NS	--	NS
25 μMBPS	SS	NS	NS	NS	--
17.5 μM BPA	SS	--	NS	NS	NS
35 μM BPA	SS	NS	--	NS	NS

Table 2. Statistical significance of differences between groups. Fisher's Exact tests were done between treatment groups. "NS" indicates the difference is not statistically significant. "SS" indicates the difference is statistically significant. A dash indicates that the test was not done. All tests were done using p-value < 0.01.

Data and statistical analysis showed that the differences between all bisphenol-exposed groups and vehicle control were statistically significant **(Table 2)**. No statistically significant difference was found when comparing bisphenol-exposed groups to each other, illustrating that BPA, BPS, and BPF all have similar effects on PGC migration in zebrafish embryos.

DISCUSSION

The existence of EDCs in the environment is the result of human activity, as EDCs are not produced naturally. The ecological implications of releasing bisphenols into the environment are not yet fully understood. Bisphenols A, F, and S are known to disrupt a variety of processes in many organisms. A 2014 study found that embryonic BPS exposure at 0.004, 0.04, and 0.4 μM

caused zebrafish sex ratios to be skewed towards females.[31] Another study found that germline-deficient zebrafish developed as phenotypic males without germ cells and were therefore unable to reproduce.[7] Based on this information, it is possible that wild populations would see skewed sex ratios and infertility from bisphenol exposure, hurting the species' chances of survival—especially in the presence of other selective pressures. A 2013 study found that doses of BPA 1-4 magnitudes of order lower than a commonly used lowest observed adverse effect level (LOAEL) tested in traditional toxicology assessments of 50 mg/kg/day can have adverse effects on animals.[32] It is logical to predict that due to their structural similarities, BPA replacements BPF and BPS may have similar low dose effects. Not only does this have ecological implications, but it likely affects human health as well, since manufacturers continue to use bisphenols. Further research on the effects and mechanisms of these EDCs would contribute to the literature that can be used to persuade lawmakers to enforce the use of safer alternatives, to reduce environmental and consumer exposure, and to create more effective waste management policies.

The mechanism of EDC action that disrupts PGC migration is not understood and could involve many different parameters within either the PGCs, the somatic cells of the gonad, or both. It is likely that aromatase plays a key role in the mechanism of action of bisphenols, as this is the key enzyme in estrogen synthesis. In a 2014 study, simultaneous exposure to BPA and fadrozole (an aromatase inhibitor) showed inhibition of BPA-induced effects.[14] This may indicate that BPA requires aromatase in order to cause abnormalities. Furthermore, a 2016 study that looked at the effects of inhibiting aromatase alone found that the manipulation of the aromatase system during the critical period of sexual differentiation is responsible for a complete and irreversible alteration of the process of gonadal differentiation in zebrafish.[33] Therefore, aromatase plays an essential role in sexual differentiation in zebrafish and may be a target of bisphenols in inducing PGC migration defects.

CONCLUSIONS

We report that bisphenols F and S cause abnormal PGC migration patterns in zebrafish, similar to those of BPA. After conducting antibody staining and fluorescent microscopy on BPF and BPS-treated embryos, it appears that neither BPF nor BPS are suitable replacements for BPA, as they all disrupt PGC migration at similar exposure levels. BPA, BPF, and BPS are all compounds with adjoined phenolic rings, differing in the identity of the functional group connecting the two rings (**Figure 1)**. It is likely that the phenolic rings, common among the three different compounds, have a similar biochemical function. However, the exact mechanism by which bisphenols cause these effects is unknown. It is important to note that bisphenols are not the only endocrine-disrupting chemicals that affect PGC migration. Embryonic exposure to estrogenic EDCs nonylphenol and endosulfan also disrupted normal PGC migration.[34] It is likely that the chemical cues secreted from somatic cells, that direct PGC migration, are interrupted by nonylphenol and endosulfan.[34] Bisphenol exposure may also interrupt this signaling, causing abnormal migration.

Insight on the mechanism of BPA and its analogues would be useful in learning how to provide safe alternatives to these plasticizers. Goals for expanding on our results include examining other bisphenols to study how their functional groups relate to PGC migration. Bisphenol G is of particular interest due to its additional functional groups attached to the two trademark phenolic rings found in most bisphenols. Bisphenol BP is also of interest because it has two extra phenolic rings. Knowing if small differences in chemical structure cause significant differences in effects on organisms could also help find safer alternatives to BPA. The use of fadrozole, an aromatase inhibitor, has been utilized to prevent the activity of BPA in various systems and its use in preventing altered PGC migration could also be explored. Finally, decreasing to nanomolar exposure concentrations would help to determine the point of effect drop-off.

It is also important to consider that in the environment, exposure to EDCs is variable. It is unlikely that organisms are exposed to a constant amount of a single EDC for a fixed amount of time; therefore, it is likely that organisms have a time period in which they can recover from exposure.[32] Few studies evaluate the ability of zebrafish to recover from EDC-induced effects, therefore more research could be done to see if the effects of certain estrogenic EDCs are reversible.

ACKNOWLEDGMENTS

Authors thank Jennifer Gantress, Lab Manager, for purchasing supplies and St. John Fisher College for providing budgetary support.

REFERENCES

1. Richardson, B.E. and Lehmann, R. (2010) Mechanisms guiding primordial germ cell migration: strategies from different organisms, *Nat Rev Mol Cell Biol* 11(1), 37-49. *https://doi.org/10.1038/nrm2815*
2. Saito, T., Goto-Kazeto, R., Kawakami, Y., Nomura, K., Tanaka, H., Adachi, S., Arai, K., and Yamaha, E. (2011) The mechanism for primordial germ cell migration is conserved between Japanese eel and zebrafish, *PLoS ONE,* 6(9), e24460. *https://doi.org/10.1371/journal.pone.0024460*
3. Akbulut, C., Kizil, A., and Yon, N.D. (2013) Effects of low doses of bisphenol A on primordial germ cells in zebrafish (*Danio rerio)* embryos and larvae, *Kafkas Universitesi Veteriner Fakultesi Dergisi,* 19(4), 647-653. *https://doi.org/10.9775/kvfd.2013.8600*
4. Fujimoto, T., Miyayama, Y., and Fuyuta, M. (1977) The origin, migration and fine morphology of human primordial germ cells, *Anat Rec,* 188(3), 315-329. *https://doi.org/10.1002/ar.1091880305*
5. Wear, H.M., McPike, M., and Watanabe, K. (2016) From primordial germ cells to primordial follicles: a review and visual representation of early ovarian development in mice, *J Ovarian Res*, 9: 36. *https://doi.org/10.1186/s13048-016-0246-7*
6. Paksa, A. and Raz, E. (2015) Zebrafish germ cells: motility and guided migration, *Curr Opin Cell Biol,* 36, 80-85. *https://doi.org/10.1016/j.ceb.2015.07.007*
7. Siegfried, K.R. and Nüsslein-Volhard, C. (2008) Germ line control of female sex determination in zebrafish, *Dev Biol*, 324(2), 277-287. *https://doi.org/10.1016/j.ydbio.2008.09.025*
8. Wong, T.T. and Collodi, P. (2013) Inducible sterilization of zebrafish by disruption of primordial germ cell migration, *PLoS ONE,* 8(6): e68455. *https://doi.org/10.1371/journal.pone.0068455*
9. Eladak, S., Grisin, T., Moison, D., Guerquin, M.J., N'Tumba-Byn, T., Pozzi-Gaudin, S., Benachi, A., Livera, G., Rouiller-Fabre, V., and Habert, R. (2015) A new chapter in the bisphenol A story: bisphenol S and bisphenol F are not safe alternatives to this compound, *Fertil Steril*, 103(1), 11-21. *https://doi.org/10.1016/j.fertnstert.2014.11.005*
10. Cano-Nicolau, J., Vaillant, C., Pellegrini, E., Charlier, T.D., Kah, O., and Coumailleau, P. (2016) Estrogenic effects of several BPA analogs in the developing zebrafish brain, *Front Neurosci*, 10, 112. *https://doi.org/10.3389/fnins.2016.00112*
11. Tsai, W. T. (2006) Human health risk on environmental exposure to bisphenol-A: a review, *J Environ Sci Health C Environ Carcinog Ecotoxicol Rev,* 24(2), 225-255. *https://doi.org/10.1080/10590500600936482*
12. Chen, J., Saili, K.S., Liu, Y., Li, L., Zhao, Y., Bai, C., Tanguay, R.L., Dong, Q., and Huang, C. (2017) Developmental bisphenol A exposure impairs sperm function and reproduction in zebrafish, *Chemosphere,*169, 262-270. *https://doi.org/10.1016/j.chemosphere.2016.11.089*
13. Fujiwara, Y., Miyazaki, W., Koibuchi, N., and Katoh, T. (2018) The effects of low-dose bisphenol A and bisphenol F on neural differentiation of a fetal brain-derived neural progenitor cell line, *Frontiers in Endocrinology*, 9, 1-9. *https://doi.org/10.3389/fendo.2018.00024*
14. Kinch, C.D., Ibhazehiebo, K., Jeong, J.H., Habibi, H.R., and Kurrasch, D.M. (2014) Low-dose exposure to bisphenol A and replacement bisphenol S induces precocious hypothalamic neurogenesis in embryonic zebrafish, *Proc Natl Acad Sci USA*, 112(5), 1475-1480. *https://doi.org/10.1073/pnas.1417731112*
15. Weiler, K. and Ramakrishnan, S. (2019) Bisphenol F causes disruption of gonadotropin-releasing hormone neural development in zebrafish via an estrogenic mechanism, *NeuroToxicology,* 71, 31-38. *https://doi.org/10.1016/j.neuro.2018.12.001*
16. Castro, B., Sanchez, P., Torres, J.M., and Ortega, E. (2015) Bisphenol A, bisphenol F, and bisphenol S affect differently 5α-reductase expression and dopamine-serotonin systems in the prefrontal cortex of juvenile female rats, *Environ Res*, 142, 281-287. *https://doi.org/10.1016/j.envres.2015.07.001*
17. Stoker, C., Andreoli, M.F., Kass, L., Bosquiazzo, V.L., Rossetti, M.F., Canesini, G., Luque E.H., and Ramos, J.G. (2019) Perinatal exposure to bisphenol A (BPA) impairs neuroendocrine mechanisms regulating food intake and kisspetin system in adult male rates. Evidence of metabolic disruptor hypothesis, *Mol Cell Endocrinol,* 499. *https://doi.org/10.1016/j.mce.2019.110614*
18. vom Saal, F.S., Nagel, S.C., Coe, B.L., Angle, B.M., and Taylor, J.A. (2012) The estrogenic endocrine disrupting chemical bisphenol A (BPA) and obesity, *Mol Cell Endocrinol*, 354(1-2), 74-84. *https://doi.org/10.1016/j.mce.2012.01.001*
19. Rochester, J.R. and Bolden, A.L. (2015) Bisphenol S and F: A systematic review and comparison of the hormonal activity of bisphenol A substitutes, *Environ Health Perspect*, 123(7), 643-650. *https://doi.org/10.1289/ehp.1408989*
20. Ahmed, S. and Atlas, E. (2016) Bisphenol S and bisphenol A induced adipogenesis of murine preadipocytes occurs through direct peroxisome proliferator-activated receptor gamma activation, *Int J Obes*, 40, 1566-1573. *https://doi.org/10.1038/ijo.2016.95*
21. Liu, B., Lehmler, H., Sun, Y., Xu, G., Sun, Q., Snetselaar, L.G., Wallace, R.B., and Bao, W. (2019) Association of bisphenol A and its substitutes, bisphenol F and bisphenol S, with obesity in United States children and adolescents*, Diabetes Metab J,* 43(1), 59-75. *https://doi.org/10.4093/dmj.2018.0045*
22. Le Fol, V., Aït-Aïssa, S., Sonavane, M., Porcher, J., Balaguer, P., Cravedi, J., Zalko, D., and Brion, F. (2017) In vitro and in vivo estrogenic activity of BPA, BPF, and BPS in zebrafish-specific assays, *Ecotox Environ Safe,* 142, 150-156. *https://doi.org/10.1016/j.ecoenv.2017.04.009*

23. Viñas, R. and Watson, C.S. (2013) Bisphenol S disrupts estradiol-induced nongenomic signaling in a rat pituitary cell line: effects on cell functions, *Environ Health Perspect,* 121(3), 352-358. *https://doi.org/10.1289/ehp.1205826*
24. Ji, K., Hong, S., Kho, Y., and Choi, K. (2013) Effects of bisphenol S exposure on endocrine functions and reproduction of zebrafish, *Environ Sci Technol*, 47(15), 8973-8800. *https://doi.org/10.1021/es400329t*
25. Nagabhushana, A. and Mishra, R.K. (2016) Finding clues to the riddle of sex determination in zebrafish, *J Biosci*, 41, 145-155. *https://www.ncbi.nlm.nih.gov/pubmed/26949096*
26. Hu, J., Sun, S., Guo, M., and Song, H. (2014) Use of antagonists and morpholinos in loss-of-function analyses: estrogen receptor ESR2a mediates the effects of 17alpha-ethinylestradiol on primordial germ cell distribution in zebrafish, *Reprod Biol Endocrinol*, 12:40. *https://doi.org/10.1186/1477-7827-12-40*
27. Tse, W.K.F., Yeung, B.H.Y., Wan, H.T., and Wong, C.K.C. (2013) Early embryogenesis in zebrafish is affected by bisphenol A exposure, *Biol Open,* 2(5), 466-471. *https://doi.org/10.1242/bio.20134283*
28. Corrales, J., Kristofco, L.A., Steele, W.B., Yates, B.S., Breed, C.S., Williams, E.S., and Brooks, B.W. (2015) Global assessment of bisphenol A in the environment: review and analysis of its occurrence and bioaccumulation, *Dose-Response ,*13, 1-29. *https://doi.org/10.1177/1559325815598308*
29. Fukazawa, H., Watanabe, M., Shiraishi, F., Shiraishi, H., Shiozawa, T., Matsushita, H., and Terao, Y. (2002) Formation of chlorinated derivatives of bisphenol A in waste paper recycling plants and their estrogenic activities, *J Health Sciences* 48, 242–249. *https://doi.org/10.1248/jhs.48.242*
30. Urase, T. and Miyashita, K. (2003) Factors affecting the concentration of bisphenol A in leachates from solid waste disposal sites and its fate in treatment processes, *J Mater Cycles Waste Manag*, 77–82. *http://dx.doi.org/10.1007/s101630300012*
31. Naderi, M., Wong, M., and Gholami, F. (2014) Developmental exposure of zebrafish (*Danio rerio*) to bisphenol-S impairs subsequent reproduction potential and hormonal balance in adults, *Aquat Toxicol*, 148, 195-203. *https://doi.org/10.1016/j.aquatox.2014.01.009*
32. Vandenberg, L.N., Ehrlich, S., Belcher, S.M., Ben-Jonathan, N., Dolinoy, D.C., Hugo, E.R., Hunt, P.A., Newbold, R.R., Rubin, B.S., Saili, K.S., Soto, A.M., Wang, H., and vom Saal, F.S. (2013) Low dose effects of bisphenol A, *Endocrine Disruptors,* 1:1, e26490. *https://doi.org/10.4161/endo.26490*
33. Luzio, A., Monteiro, S.M., Rocha, E., Fontaínhas-Fernandes, A.A., and Coimbra, A.M. (2016) Development and recovery of histopathological alterations in the gonads of zebrafish (*Danio rerio*) after single and combined exposure to endocrine disruptors (17α-ethinylestradiol and fadrozole), *Aquat Toxicol,* 175, 90-105. *https://doi.org/*10.1016/j.aquatox.2016.03.014
34. Willey, J.B. and Krone, P.H. (2001) Effects of endosulfan and nonylphenol on the primordial germ cell population in pre-larval zebrafish embryos, *Aquat Toxicol*, 54,(1-2), 113-123. *https://www.ncbi.nlm.nih.gov/pubmed/11451430*

ABOUT STUDENT AUTHORS

Siti Sarah Safura graduated with a BS in Biology with minors in Chemistry and Women & Gender Studies from St. John Fisher College in 2017 and an MS in Medical Humanities from the University of Rochester in 2018. She is currently pursuing a career in medicine. George Roba graduated with a BS in Biology, a BA in Psychology, and a minor in Spanish for the Health Care Professional from St. John Fisher College in 2018. He has recently completed training as a paramedic and is pursuing a career in healthcare.

PRESS SUMMARY

This project was done to analyze the effects of BPF and BPS on primordial germ cell (PGC) migration in zebrafish embryos. Zebrafish are a commonly used model organism and are an excellent model for analyzing the effects of EDCs. Proper PGC migration is necessary in vertebrates, including humans, for proper gonad formation. BPA has been shown to cause abnormal PGC migration in zebrafish embryos. BPS and BPF are commercial plasticizers often used as replacements for BPA. Numerous reports have demonstrated the negative effects of BPA exposure on organisms including zebrafish, mice, and humans. However, work describing the impacts of BPF and BPS are still emerging. Because all three bisphenols share structural similarities, it is possible that they have similar effects on PGC migration. This study illustrates that at similar doses to BPA, BPF and BPS cause abnormal PGC migration in zebrafish embryos.

Exposure and Loss of Environmental Enrichment Mediates Ethanol Consumption in Adolescent Female Rats

Natalie Lipari[a]*, Max Baron[b], & Joshua A. Peck[a]

[a]*Psychology Department, State University of New York at Cortland, Cortland, NY*
[b]*Psychology Department, University of Michigan, Ann Harbor, MI*

https://doi.org/10.33697/ajur.2019.032

Students: natalie.lipari@cortland.edu, maxbaron@umich.edu*
Mentors: joshua.peck@cortland.edu

ABSTRACT
Alcohol use among adolescent females has significantly increased in the United States with young women drinking alcohol at the same rate as young men. One potential treatment strategy that could help sustain alcohol abstinence is Environmental Enrichment (EE). Environmental enrichment is a process concerning the stimulation of the brain by one's physical and social surrounding, which promotes non-drug reinforcement alternatives (e.g. voluntary exercise) supporting drug abstinence. Thus, the primary focus of this study was to investigate the effect of EE on ethanol (ETOH) abstinence in adolescent female rats. All adolescent female rats, starting on postnatal day 30, had 24-h access to 2%, then 4%, and then 6% ethanol concentrations. At the end of the four weeks, the environmental conditions were switched (EE→NEE and NEE→EE) and the 6% ethanol measure was repeated. We found that EE significantly reduced ethanol consumption for adolescent female rats compared to controls. Further, the removal of EE opportunities resulted in a significant increase in ethanol consumption. Collectively, the results suggest that access to enriched life conditions are important in facilitating alcohol abstinence in adolescent female rats.

KEYWORDS
Adolescent Females; Alcohol Consumption; Environmental Enrichment; Alcohol Use Disorder; Treatment Strategy; Alcohol Abstinence; Ethanol; Adolescent Female Rats

INTRODUCTION

Alcohol use among young women has significantly increased in the United States within recent years. Young women are now drinking alcohol at similar rates as young men, suggesting that differences in consumption of alcohol for males and females has dramatically narrowed.[1] For example, thirty-seven percent of ninth grade girls—averaging at about 14 years old—report drinking in the past month, surpassing the percentage rate reported for ninth grade boys.[2] Unfortunately, the increased use of alcohol in young women can set the stage for development of an alcohol use disorder (AUD) later in life.[3,4] According to the National Institute of Health, AUD is a chronic relapsing brain disease characterized by compulsive alcohol use, loss of control over alcohol intake, and a negative emotional state when not using.[2] Given the recent upward trend of AUDs among adolescent females, it is important that substance abuse animal research examine possible treatment strategies that may be effective for treating adolescent female alcohol abuse.

One promising treatment strategy that has shown to support drug abstinence is environmental enrichment. Environmental Enrichment (EE) can be defined as the non-contingent delivery of alternative non-drug rewards such as food, social interaction, novelty objects and voluntary physical activity either in the presence of drug (concurrent) or in the absence of drug (non-concurrent).[5-12] Access to nondrug alternatives can impede or prevent acquisition and decrease drug-maintained responding.[13,14] For example, given the choice between drug and other types of rewards (*e.g.*, toys or social interaction) they will typically prefer the alternative rewards over drug .[5,6,13-17] Further, the removal of such non-drug alternatives may also result in increased drug taking.[18,19]

To date, research has provided promising evidence that EE may indeed support drug abstinence in male animal populations. Access to EE can prevent the acquisition of drug taking and decrease drug responding in male rats.[6,13] For example, male animal studies have shown that EE reduces cocaine and heroin's reinforcing effects when concurrently available with the drug.[10,14,15] However, there is a paucity of research concerning EE as a possible treatment strategy for substance abuse in female animal populations. To our knowledge, there have been no studies examining EE as a possible treatment method for alcohol consumption in adolescent female rats. Therefore, the current study examined a novel approach by implementing an EE treatment strategy that may help support alcohol abstinence in adolescent female rats.

Our primary focus was to investigate the effects of exposure and loss of EE on ethanol (ETOH) consumption in adolescent female rats. During phase one, adolescent female rats were either placed in the EE or in standard non-enriched cages (NEE) with both groups having access to ETOH. For both groups, adolescent female rats were given 2% ETOH for one week, then increased to 4% for another week and finished with 6% over the span of two weeks. At the end of the fourth week, we switched the groups (phase two) where female rats that were originally in the EE were now placed into the NEE and rats that were first in the NEE were given access to the enriched environment. We hypothesized that both groups of adolescent female rats would show significantly less ETOH consumption while in the EE condition, than in the NEE condition. If these results were to be observed then this would lend support for the implementation of EE as a strategy to facilitate alcohol abstinence in adolescent female rats.

METHODS AND PROCEDURES

Subjects

Twenty Sprague-Dawley adolescent female rats weighing between 300 and 350 g were used as subjects for both phases of the experiment. Estrous levels in free cycling females were not assessed. Each rat was housed in a climate-controlled environment ranging from 70.0-72.0 degrees Fahrenheit with constant access to water and Lab Rat Chow was provided during all phases of the experiment. Each rat was individually housed under a reversed 12-hour light: dark cycle (lights on at 19:00 h). This study complied with the guidelines of the National Institute of Health guide for the care and use of laboratory animals and was conducted in accordance with the SUNY Cortland's Institutional Animal Care and Use Committee ethics protocol (IACUC Protocol #43).

Environmental Enrichment

Every female adolescent rat was provided a standard cage, $25 \times 20 \times 15$ cm^3 for the NEE and $60 \times 38 \times 20$ cm^3 for the EE (depending upon experimental phase). The EE contained running wheels, a 10-cm diameter tunnel, ladders, treats, and two additional objects that were rotated daily, such as a jingly ball, paper roll, and a dog chew toy. The components and procedure of rotating objects daily within enrichment cages, are similar to those used in other enrichment studies that have shown effects of the treatment.[8,20-22]

Procedure

The procedure consisted of two four week phases. During phase 1, starting on postnatal day 30, adolescent female rats were assigned to either the EE (n = 10) or NEE (n = 10) with a 14-oz drinking bottle containing an ascending series of ethanol concentrations placed on their home cages 24 hours per day (continuous access). Twenty female rats were exposed to different concentrations of ETOH by a fade-in procedure **(Table 1)**. This procedure gradually introduces the rats to the ETOH solutions that provide a measure of volitional intake under restrictive conditions.[21] This fade-in series started with 2% ETOH for the first seven days, followed by 4% for the next seven days and then 6% for 14 days. Bottles were weighed to the nearest 0.1g at the same time daily. At the end of the fourth week, we switched the groups (phase 2) where female rats that were in the EE were now placed into the NEE (EE-NEE) and rats that were in the NEE were given access to the enriched environment (NEE-EE). During phase 2, all rats had continued access to 6% for 14 days.

Experimental Groups: (EE →NEE *vs.* NEE → EE)	**Week 1**	**Week 2**	**Weeks 3 & 4**
Phase 1:			
Ethanol Exposure	2%	4%	6%
Duration	7 Days	7 Days	14 Days
Phase 2: Switched			
Ethanol Exposure	6%	6%	N/A
Duration	7 Days	7 Days	

Table 1. Ascending series of ETOH concentrations administered during phases 1 and 2.

Statistical Analysis

The dependent variable consisted of the amount of ethanol consumption (6%) by the female rats across both phases. The independent variables were environmental history (NEE or EE) and groups (EE→NEE *vs.* NEE→EE). A two-way ANOVA with group (between-subjects) and environmental history (repeated measures) was conducted comparing the mean 6% ETOH consumption amounts in the EE and NEE conditions for both EE→NEE and NEE→EE groups. Differences were considered significant at the $p<0.05$ level. Standard error bars are indicated in Figure 1. All statistical analyses were conducted using IBM Statistical Package for Social Sciences (SPSS) 26 software.

RESULTS

A two-way ANOVA with group (between-subjects) and environmental history (repeated measures) as factors was conducted comparing the mean 6% ETOH consumption amounts in the EE and NEE conditions for both EE→NEE and NEE→EE groups. The 6% ETOH consumption over 14 days for the EE→NEE female adolescent rats during the NEE condition yielded a mean of 17.73 ± 2.16 grams (g), while the 6% ETOH consumption over 14 days for the EE→NEE group during the EE condition led to a mean of 5.40 ± 0.93(g) . The 6% ETOH consumption over 14 days for the NEE→EE rats during the NEE condition yielded a mean of 19.71 ± 2.45(g), while the 6% ETOH consumption over 14 days for this same group led to a mean of 7.54 ± 1.23(g). **(Figure 1)**. For both EE→NEE and NEE→EE groups, there was a significant effect of environmental history [F (1, 39) =16.59, p < .01]. However, there were no significant effects for group [F = 3.59, p > .05] or group by environmental history interaction [F = 0.89, p > .05].

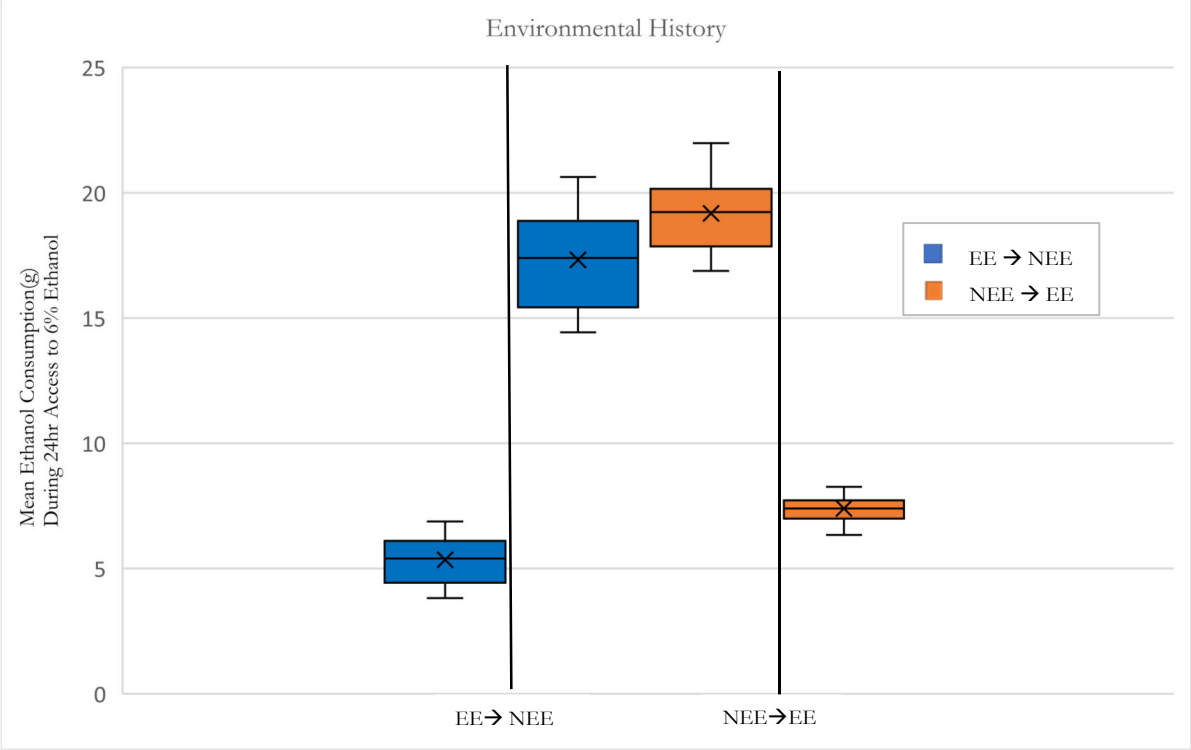

Figure 1: Mean (±SEM) of 6% ETOH consumed during both phases for the EE→NEE and NEE→EE groups. N = 10 for each group

DISCUSSION

The current study examined a possible treatment method for supporting alcohol abstinence in adolescent female rats. We found that EE exposure led to significantly less consumption of ethanol for both female groups, while loss of EE led to a significant increase in ethanol intake. The results suggest that having access to EE opportunities while alcohol is readily available may be an effective treatment strategy for promoting decreased ethanol consumption in adolescent female rats. A possible explanation for this finding is that the introduction of rewarding stimulation experienced in the enriched environment might have reduced the reinforcing effects of the ethanol through a behavioral contrast mechanism. Behavioral contrast refers to a change in the rate of reinforcement on one component of a concurrent schedule produces an opposite change in the rate of response on another component creating an inverse relationship.[23-25] For example, a change to a high reinforcement rate in one schedule component typically results in a lower response rate in the other schedule component. A relevant example for the current experiment is when environmental enrichment studies provide concurrent access to alternative reinforcement (e.g. toys and treats) while the drug is

made readily available for consumption and a decrease in drug use is observed.[12-16] Likewise, in the current experiment, EE was provided concurrently with ethanol availability that led to a decrease in ethanol consumption by adolescent female rats. Notable to mention is that we observed the treatment effect of EE while rats were isolated and given concurrent access to ethanol. Previous research has demonstrated that social interaction is an important component of EE on decreasing drug consumption. For example, studies have shown that when rats are housed in groups within the EE condition, they show significantly decreased drug consumption.[12] Indeed, previous research has demonstrated that social isolation is a stressful condition for rodents and therefore, may lead to an increase in drug consumption.[19,26] However, the current study's results suggest that EE is still a viable treatment option for reducing ethanol consumption even when placed in the stressed-induced condition of social isolation.

An important aspect of the current study was to examine the changes in adolescent female ethanol consumption after loss of EE stimulation. Previous research has shown that the removal of non-drug alternatives results in the behavioral resurgence of drug responding or an increase in drug taking.[18,19] Furthermore, in humans, researchers have suggested a link between the removal of alternative, reinforcing events and increases in drug intake or instances of behavioral resurgence after periods of abstinence.[25] For example, researchers examined data from a Health and Retirement study in order to explore the relationship between involuntary job loss and smoking intensity, as well as, relapse in abstinent smokers. They found that involuntary job loss contributed significantly to elevated levels of smoking in individuals who already smoked. Furthermore, risk of relapse doubled after job loss in ex-smokers.[27] Similarly, we found that loss of access to non-drug alternatives (EE) led to a significant increase in ethanol consumption for adolescent female rats. Thus, the common feature that both the current and previous studies all demonstrate is that when stimulation or reward is derived from a source other than the drug itself (enrichment), there is a reduction in the reinforcing effects of the drug(s), thereby supporting abstinence. Further, when non-drug alternative rewards are no longer being delivered, a behavioral resurgence of drug use could be the result.

One possible neural mechanism whereby EE may produce its effect on ethanol consumption in adolescent female rats is by disrupting neural circuits in areas involved in ethanol taking. For example, researchers have found that EE housing reduced the incentive value of novelty and the reinforcing properties of ETOH that are mediated by the mesocorticolimbic dopaminergic reward system.[28] The disruption of neural circuitry by EE is supported by other studies that found EE rats previously trained to self-administer cocaine and after cue-induced relapse tests for cocaine had activated cFos protein in the mesocorticolimbic system to a lesser extent than in NEE animals.[7,8,29,30] Brain alterations in neural pathways associated with alcohol abuse suggests that EE may play a disruptive role in the neural mechanisms associated with alcohol consumption. Further, this may help explain how the concurrent introduction of rewarding stimulation (EE), may have the effect of reducing the reinforcing effects of ethanol through the contrast mechanism described above.

Previous male animal studies that delivered alternative non-drug rewards such as, food, novelty objects, and voluntary physical activity in the presence of drug found that access to nondrug alternatives led to a decrease in drug-maintained responding.[5,7-9] Similarly, the current study found that when adolescent female rats were provided access to EE alternatives there was a reduction in ethanol consumption. Therefore, EE may also be an effective treatment strategy for substance abuse when implemented in female populations.

One limitation to the present study is that we did not assess estrous levels in freely cycling adolescent female rats, while in the EE or NEE conditions. Increased estrogen levels have been shown to be related to increased alcohol use in females.[31,32] However speculative, it may be that EE disrupts the estrogenic effects that contribute to female's increased sensitivity to the rewarding effects of alcohol. In part, this possible explanation could account for significantly less ETOH consumption rates by female rats during the EE condition compared to the NEE condition. Therefore, future studies should examine the possible role that EE may play in mediating the estrogenic effects on alcohol use in adolescent female rats. Another limitation to the present study involves the restricted age cohort of investigating the possible EE preventative effects on ETOH in adolescent female rats. Future studies should examine the heterogeneity of treatment effects concerning EE on ETOH use by observing other female age cohorts.

CONCLUSIONS

The primary focus of this study was to investigate a potential treatment strategy that would support ETOH abstinence in adolescent female rats. We found that exposure to EE led to significantly less consumption of ETOH for both female groups, while loss of EE led to a significant increase in ethanol volitional intake. The present results support previous research findings (largely with animal male populations) using EE by demonstrating that when having concurrent access to alternative reinforcement (e.g., wheel running) it leads to a reduction in the reinforcing effects of the drug, thereby facilitating abstinence. The current findings may have important implications concerning treatment strategies for alcohol abuse in adolescent females.

ACKNOWLEDGEMENTS
The authors thank the State University of New York at Cortland for their generous funding that made this work possible.

REFERENCES

1. Substance Abuse and Mental Health Services Administration, SAMSHA. National Survey on Drug Use and Health, *https://datafiles.samhsa.gov/study-series/national-survey-drug-use-and-health-nsduh-nid13517* (accessed Feb 2018)
2. National Institute on Alcohol Abuse and Alcoholism. Alcohol facts and statistics, *http://www.niaaa.nih.gov/alcohol-health/overview-alcohol-consumption/alcohol-facts-and-statistics* (accessed Feb 2018)
3. Keyes, K.M., Hatzenbuehler, M.L., Grant, B.F., and Hasin, D.S. (2012) Stress and Alcohol: Epidemiologic Evidence, *Alcohol Res: Current Rev* 34, 4. *https://doi.org/10.1007/s00213-011-2236-1*
4. White, A., Castle, I.P., Chen, C.M., Shirley, M., Roach, D., Hingson, R. (2015) Converging 640 Patterns of Alcohol Use and Related Outcomes Among Females and Males in the United 641 States, 2002 to 2012, *Alcohol Clinical and Experimental Res.,* 39, 1712-1726. *doi: 10.1111/acer.12815*
5. Carroll ME. (1993) The economic context of drug and non-drug reinforcers affects acquisition and maintenance of drug reinforced behavior and withdrawal effects, *Drug Alcohol Depend* 33, 201–210. *https://doi.org/10.1016/0376-8716(93)90061-T*
6. Carroll ME, Lac ST, Nygaard SL. (1989) A concurrently available nondrug reinforcer prevents the acquisition or decreases the maintenance of cocaine reinforced behavior, *Psychopharmacol (Berlin)* 97, 23–29. *doi.org/10.1007/BF004434077*
7. Zlebnik NE, Anker JJ, Gliddon LA, Carroll ME. (2010) Reduction of extinction and reinstatement of cocaine seeking by wheel running in female rats, *Psychopharmacol* 209, 113–125. *https://doi.org/10.1007/s00213-010-1776-0*
8. Chauvet C, Lardeux V, Goldberg SR, Jaber M, Solinas M. (2009) Environmental enrichment reduces cocaine seeking and reinstatement induced by cues and stress but not by cocaine, *Neuropsychopharmacol* 34, 2767–2778. *https://doi.org/10.1038/npp.2009.127*
9. Thiel KJ, Sanabria F, Pentkowski NS, Neisewander JL. (2009) Anticraving effects of environmental enrichment, *Int. J. Neuropsychopharmacol* 12, 1151–1156. *https://doi.org/10.1017/S1461145709990472*
10. Peck, J. A., Galaj, E., Eshak, S., Newman, K. L., & Ranaldi, R. (2015) Environmental enrichment induces early heroin abstinence in an animal conflict model, *Pharmacol Biochem and Behav* 138, 20-25. *https://doi.org/10.1016/j.pbb.2015.09.009*
11. Ewing, Scott, Ranaldi, Robert. (2018) Environmental enrichment facilitates cocaine abstinence in an animal conflict model, *Pharmacol Biochem and Behav* 166, 35-41. *https://doi.org/10.1016/j.pbb.2018.01.006*
12. Solinas M, Thiriet N, Chauvet C, Jaber, M. (2010) Prevention and treatment of drug addiction by environmental enrichment, *ScienceDirect 92* (4). *https://doi.org/10.1016/j.pneurobio.2010.08.002*
13. Lynch WJ, Piehl KB, Acosta G, Peterson AB, Hemby SE. (2010) Aerobic exercise attenuates reinstatement of cocaine-seeking behavior and associated neuroadaptations in the prefrontal cortex, *Biol Psychiatry* 68, 774–777. *https://doi.org/10.1016/j.biopsych.2010.06.022*
14. Smith MA, Schmidt KT, Iordanou JC, Mustroph ML. (2008) Aerobic exercise decreases the positive-reinforcing effects of cocaine, *Drug Alcohol Depend* 98,129–135. *https://doi.org/10.1016/j.drugalcdep.2008.05.006*
15. Zlebnik NE, Anker JJ, Carroll ME. (2012) Exercise to reduce the escalation of cocaine self-administration in adolescent and adult rats, *Psychopharmacol (Berlin)* 224, 387–400. *https://doi.org/10.1007/s00213-012-2760-7*
16. Cosgrove KP, Hunter RG, Carroll ME. (2002) Wheel-running attenuates intravenous cocaine self-administration in rats: sex differences, *Pharmacol Biochem Behav* 73, 663–671. *https://doi.org/10.1016/S0091-3057(02)00853-5*
17. Grimm JW, Osincup D, Wells B, Manaois M, Fyall A. (2008) Environmental enrichment attenuates cue-induced reinstatement of sucrose seeking in rats, *Behav Pharmacol* 19, 777–785. *doi.org/10.1097/FBP.0b013e32831c3b18*
18. Podlesnik CA, Jimenez-Gomez C, Shahan TA. (2006) Resurgence of alcohol seeking produced by discontinuing non-drug reinforcement as an animal model of drug relapse, *Behav Pharmacol* 17, 369–374. *doi.org/10.1097/01.fbp.0000224385.09486.ba*
19. Nader, Joelle, Claudia, Chauvet, Rawas El Rana, Favot, Laure, Jaber, Mohamed, Thiriet, Nathalie, Solinas, Marcello. (2012) Loss of Environmental Enrichment Increase Vulnerability to Cocaine Addiction, *Neuropsychopharmacol 1579-1587. https://doi.org/10.1038/npp.2012.2*
20. Peck, A. Joshua, Galaj, Ewa, Eshak, Stephanie, Newman, L. Kristena, Ranaldi, Robert. (2015) Environmental enrichment induces early heroin abstinence in an animal conflict model, *Pharmacol, Biochem Behav 138, 20-25. https://doi.org/10.1016/j.pbb.2015.09.009*
21. Ranaldi R, Kest K, Zellner M, Hachimine-Semperbrom P. (2011) Environmental enrichment, administered after establishment of cocaine self-administration, reduces lever pressing in extinction and during a cocaine context renewal test, *Behav Pharmacol* 22, 347–353. *doi.org/10.1097/FBP.0b013e3283487365*
22. Berger, D.F., Lombardo, J.P., Peck, J.A., Faraone, S.V., Middleton, F.A. and Youngetob, S.L. (2010) The effects of strain and prenatal nicotine exposure on ethanol consumption by adolescent male and female rats, *Behav Brain Res* 210(2), 147-154. *https://doi.org/10.1016/j.bbr.2010.01.047*
23. Reynolds, GS. (1961) Contrast, generalization, and the process of discrimination, *J Exp Anal Behav* 4, 289–294. *doi.org/10.1901/jeab.1961.4-289*

24. Williams, B.A. (2002) Behavioral contrast redux, *Animal learning & behav* 30(1), 1-20. *https://doi.org/10.3758/BF03192905*
25. Troisi JR II (2013) Perhaps more consideration of Pavlovian–operant interaction may improve the clinical efficacy of behaviorally based drug treatment programs. *Psychol Rec* 63:863–894. *https://doi.org/10.11133/j.tpr.2013.63.4.010*
26. Raz, Sivan., Berger, BD. (2010) Social isolation increases morphine intake: behavioral and psychopharmacological aspects. *Behav Pharmacol 21*(1) 39-46. *doi: 10.1097/FBP.0b013e32833470bd*
27. Falba T, Teng H, Sindelar JL, Gallo WT. (2005) The effect of involuntary job loss on smoking intensity and relapse, *Addiction* 100, 1330-1339. *https://doi.org/10.1111/j.1360-0443.2005.01150.x*
28. de Carvalho, C.R., Pandolfo, P., Pamplona, F.A. and Takahashi, R.N. (2010) Environmental enrichment reduces the impact of novelty and motivational properties of ethanol in spontaneously hypertensive rats, *Behav Brain Res 208*(1), 231-236. *https://doi.org/10.1016/j.bbr.2009.11.043*
29. Chauvet, C., Lardeux, V., Jaber, M. and Solinas, M. (2011) Brain regions associated with the reversal of cocaine conditioned place preference by environmental enrichment, *Neurosci 184*, 88-96. *https://doi.org/10.1016/j.neuroscience.2011.03.068*
30. Thiel, K.J., Pentkowski, N.S., Peartree, N.A., Painter, M.R. and Neisewander, J.L. (2010) Environmental living conditions introduced during forced abstinence alter cocaine-seeking behavior and Fos protein expression, *Neurosci 171*(4), 1187-1196. *https://doi.org/10.1016/j.neuroscience.2010.10.001*
31. Lenz, B, Müller, C. P., Stoessel, C., Sperling, W., Biermann, T., Hillemacher, T., Bleich, S., Kornhuber, J. (2012) Sex hormone activity in alcohol addiction: integrating organizational and activational effects, *Progress in Neurobio 96,* 136-163. *https://doi.org/10.1016/j.pneurobio.2011.11.001*
32. Hudson, A., Stamp. J. A. (2011) Ovarian hormones and propensity to drug relapse: a review, *Neurosci and Biobehav Rev* 35, 427-436. *https://doi.org/10.1016/j.neubiorev.2010.05.001*

ABOUT STUDENT AUTHORS

Natalie Lipari will graduate in 2020 with a Bachelor of Science degree in Psychology and plans to continue her research focus in the area of substance abuse as she pursues her Ph.D. in Behavioral Neuroscience. Max Baron will graduate in 2021 from the University of Michigan with a Bachelor of Science degree in Biopsychology, Cognition and Neuroscience. He plans to continue research in the area of Behavioral Neuroscience upon graduate school acceptance.

PRESS SUMMARY

Recent research has shown that female adolescent alcohol abuse is on the rise in the United States. In fact, the number of adolescent females (ages 12-17) with an alcohol use disorder (AUD) actually surpassed the number of adolescent males with an AUD. The consequences of underage drinking can be devastating and may result in truancy, motor vehicle injuries, sexual assault cases, and even death. Thus, with the rise of adolescent female alcohol consumption and increased risk of AUD, it is essential to determine a treatment method that supports long-term alcohol abstinence in females. One potential treatment is the implementation of environmental enrichment (EE). Environmental enrichment is a process concerning the stimulation of the brain by one's physical and social surrounding that promotes non-drug reinforcement alternatives supporting drug abstinence. Further, accumulating evidence indicates that exposure to an EE during the earlier stages of life reduces the effects of abused drugs and decreases the vulnerability to develop a substance abuse disorder. To our knowledge, there have been no studies that have examined EE as a possible treatment strategy to support alcohol abstinence in adolescent female rats. Therefore, the current research sought to examine this novel approach by implementing EE as a viable treatment option to support abstinence in female alcohol abuse. The results suggest that access to enriched life conditions are important in facilitating alcohol abstinence in adolescent female rats.

Print Edition ISSN 1536-4585
Online Edition ISSN 2375-8732